Morphodynamics and Morphological Development of Shelf Mud Depocenters

Dissertation

zur Erlangung des Doktorgrades der Naturwissenschaften

an der Fakultät für Mathematik, Informatik und Naturwissenschaften

Fachbereich Geowissenschaften

der Universität Hamburg

vorgelegt von Lucas Porz

aus Bonn, Deutschland

Hamburg, 2021

Als Dissertation angenommen am Fachbereich Geowissenschaften

Tag des Vollzugs der Promotion:	30.11.2021
Gutachter/Gutachterinnen:	Prof. Dr. Corinna Schrum Dr. Wenyan Zhang
Vorsitzender des Fachpromotionsausschusses Geowissenschaften:	Prof. Dr. Hermann Held
Dekan der Fakultät MIN:	Prof. Dr. Heinrich Graener

Abstract

Mud depocenters are accumulations of fine-grained sediment with meter-scale thickness that occur on many modern continental shelves. While a depocenter's sedimentary record can provide useful data on past environmental conditions, its morphology can also be highly dynamic, and processes driving mud depocenter development are not yet fully understood. This thesis elucidates the physical mechanisms behind shelf mud accumulation. An extensive literature survey represents the first comprehensive compilation of known physical processes controlling mud depocenter development. Detailed case studies on two mud depocenters in the southwestern Baltic Sea give new insights into their morphodynamics by combining oceanographic and geological data with numerical modeling.

Five physical processes are deemed key for shelf mud dynamics: 1. Wave- and current-supported sediment gravity flows, in which a highly-concentrated bottom layer is kept in suspension by waves and/or currents and moves down the gentle shelf slope as a result of gravitational force, 2. Hydrodynamic fronts, which either plow the inner shelf through generation of strong coast-parallel jets at the seafloor, or provide lateral and vertical barriers to cross-shelf sediment transport on seasonal and longer timescales through stable density gradients in regions of freshwater influence, 3. Internal waves at the interfaces of stratified coastal oceans, which keep the outer shelf free of mud through resuspension and transport during shoaling or breaking, 4. Bedload deposition of mud forming laminated bedding under energetic flow conditions, 5. Chronic bottom trawling, in which heavy fishing gear is dragged along the seafloor, resuspending and mixing large amounts of sediment in the process. Notably, many of these processes are episodic and short-lived in nature. This is a stark contrast to most geological methods of analysis such as stratigraphy, which imply a morphodynamic equilibrium condition for the interpretation of any geological record. This work suggests that shelf mud sedimentation is a much more dynamic process than previously thought, and care must be taken when comparing in-situ observations of sediment transport to both the recent and ancient sedimentary record.

The nearly tide-less and semi-enclosed situation of the Baltic Sea lends itself to the study of morphodynamics and sediment transport processes. While the hydrodynamics of the Baltic Sea have been extensively surveyed for many decades, little is known about the dynamics of the muddy depocenters in its sub-basins. I apply a source-to-sink approach to two

muddy depocenters in the southwestern Baltic Sea, the Arkona and Bornholm Basins. Mass budget estimates are compiled for sources and sinks of fine-grained sediment in the study area. Potential sources considered are coastal erosion, riverine loads, and biogenic production of solids. Coastal erosion at the German and Polish Baltic Sea coasts is shown to be the major supplier of fines, making up roughly half of all sources. Supply from riverine loads and biogenic production are an order of magnitude smaller. The sinks are given by deposition in the sub-basins and outflow towards the North Sea within the surface waters. Comparison of sources and sinks reveals an imbalance, wherein at least 900 kt/yr of sink material is not accounted for, amounting to between one half and one fifth of all other source considered. A potential source mechanism to close this gap exists in the form of sediment-laden, saline inflows from the North Sea. These wind-driven events, termed Major Baltic inflows (MBIs), occur episodically and with varying intensities, with large events occurring about once per year on average. During an MBI, inflowing water travels as a dense bottom current, transporting a large amount of salt into the Baltic Sea. A three-dimensional numerical coastal ocean and sediment transport model is set up and used to simulate two monitored MBIs. Comparison to the monitoring data shows that the hydrodynamics of these MBIs are well reproduced by the model. Model experiments are carried out by placing a pool of erodible sediment in the Kattegat Strait, to be resuspended and advected into the Baltic Sea along with the inflowing water during the MBIs. Based on the outcome, a scaling relationship relating salt flux to sediment flux is computed, allowing an upscaling of the model results in time. According to those scaling relationships, a few hundred kt/yr of fine-grained sediment can be advected into the Baltic Sea by MBIs during the last 150 years, on average. Large inflows advect more sediment per Gt of salt individually than smaller inflows, but smaller inflows are responsible for the bulk of the total flux due to their more frequent occurrence. Comparison with measured suspended matter concentrations in the Kattegat indicates that fluxes computed by the model are plausible, though may possibly be underestimated. Nevertheless, the results show that MBIs are capable of advecting a significant amount of suspended matter into the Baltic Sea.

In order to explore the process-product relationship between bottom currents and morphology, a high-resolution model experiment with emphasis on the Bornholm Basin and Bornholm Channel is conducted. During an MBI, bottom currents are directed downslope at the channel entrances, where large density gradients and steep bathymetric slopes lead to gravity-driven flows with minor influence of Coriolis forcing. As the bottom current enters Bornholm Basin, it transitions into a geostrophic contour current at about 70 m depth. There, the inflowing dense water mass reaches neutral buoyancy in the Bornholm Basin, having continuously entrained less saline water during its passage through the Baltic Sea. These dynamics match the results of previous geological studies, which related bottom-current controlled submarine geometries, so-called contourites, in the Baltic Sea to MBIs. Symmetric mud deposition on channel flanks results from downslope currents, and asymmetric deposition results from geostrophic currents. In the Arkona Basin, no such contouritic features are found. Based on model results, it is hypothesized that a high variability of bottom current directions in the Arkona Basin has an overall diffusive effect on lateral sediment distribution, explaining the basin’s flat appearance. The results presented within this thesis allow, for the first time, a mechanistic connection between hydrodynamics and morphodynamics of mud depocenters in the southwestern Baltic Sea.

Zusammenfassung

Schlammdepozentren sind Ablagerungen feinkörnigen Sediments mit Mächtigkeiten von einigen Metern, die auf vielen heutigen Kontinentalschelfen vorkommen. Während die Sedimentabfolgen eines Depozentrums nützliche Daten über vergangene Umweltbedingungen liefern können, kann die Morphologie eines Schlammdepozentrums auch sehr dynamisch sein, und die treibenden Prozesse hinter der Entwicklung von Schlammdepozentren sind noch nicht vollständig erforscht. In dieser Arbeit werden die Mechanismen der Schlammsedimentation auf dem Schelf ergründet. Eine umfangreiche Literaturrecherche stellt die erste umfassende Zusammenstellung derjenigen physikalischen Prozesse dar, welche die Entwicklung von Schlammdepozentren steuern. Detaillierte Fallstudien an zwei Schlammdepozentren in der südwestlichen Ostsee geben neue Einblicke in ihre Morphodynamik, indem ozeanographische und geologische Daten, sowie numerische Modellierung kombiniert werden.

In der Vergangenheit wurden fünf physikalische Prozesse als entscheidend für die Dynamik von Schlamm auf dem Schelf angesehen: 1. Wellen- und strömungsgestützte Suspensionsströme, bei denen eine hochkonzentrierte Bodenschicht durch Wellen und/oder Strömungen in Suspension gehalten wird und sich aufgrund der Schwerkraft den sanften Schelfhang hinabbewegt, 2. Hydrodynamische Fronten, welche entweder den inneren Schelf durch die Erzeugung starker, küstenparalleler Bodenströmungen aufwirbeln, oder als beständige Dichtegradienten auf saisonalen und längeren Zeitskalen laterale und vertikale Barrieren für den Sedimenttransport bilden, 3. Interne Wellen an den Sprungschichten geschichteter Küstenmeere, die den äußeren Schelf durch Wiederaufschlämmung bei Auflaufen oder Brechen von Schlamm frei halten, 4. Geschiebetransport ausgeflockter Feinsedimente, welche bei der Ablagerung laminierte Lagen bilden, 5. Grundschleppnetzfischerei, bei der schweres Gerät den Meeresboden durchpflügt und dabei große Mengen an Sediment wiederaufschlämmt. Bemerkenswert ist, dass viele dieser Prozesse episodisch und von kurzer Dauer sind. Dies steht in einem ausgesprochenen Gegensatz zu den meisten geologischen Analysemethoden wie z.B. der Stratigraphie, die ein morphodynamisches Gleichgewicht bei der Interpretation der Sedimentabfolgen voraussetzen. Diese Arbeit zeigt, dass die Schlammablagerung auf dem Schelf ein sehr viel dynamischerer Prozess ist, als bisher angenommen. Eine Gegenüberstellung von in-situ-

Beobachtungen des Sedimenttransports mit rezenten und fossilen Sedimentabfolgen bedarf daher besonderer Vorsicht.

Die nahezu tidenfreie und halbgeschlossene Lage der Ostsee bietet sich für die Untersuchung von Morphodynamik und Sedimenttransportprozessen besonders an. Während die Hydrodynamik der Ostsee seit vielen Jahrzehnten ausgiebig untersucht wird, ist über die Dynamik der Schlammdepozentren in ihren Becken noch wenig bekannt. In dieser Arbeit wird ein Source-to-Sink-Ansatz auf zwei Schlammdepozentren im Arkona- und Bornholmbecken in der südwestlichen Ostsee angewendet. Dazu werden Massenbudgetschätzungen für alle Quellen und Senken von feinkörnigem Sediment im Untersuchungsgebiet erstellt. Als potentielle Quellen werden Küstenerosion, Flussfrachten und biogene Produktion von Feststoffen berücksichtigt. Die Erosion der deutschen und polnischen Ostseeküsten erweist sich als Hauptlieferant von Feinsedimenten und macht etwa die Hälfte aller Quellen aus. Die Zufuhr durch Flussfrachten und biogene Produktion ist um eine Größenordnung geringer. Die Senken sind durch Ablagerung in den Depozentren und durch Ausstrom Richtung Nordsee in der oberen Wasserschicht gegeben. Bei der Gegenüberstellung von Quellen und Senken zeigt sich ein Ungleichgewicht, wobei die Senken die Quellen um mindestens 900 kt/Jahr übersteigen, was zwischen der Hälfte und einem Fünftel aller anderen berücksichtigten Quellen entspricht. Sedimentbeladene, salzhaltige Einströme aus der Nordsee sind ein potenzieller Mechanismus, der diese Lücke schließen kann. Diese windgetriebenen Ereignisse werden als Major Baltic Inflows (MBI) bezeichnet. Sie treten episodisch und mit unterschiedlichen Intensitäten auf, wobei größere MBIs im Durchschnitt etwa einmal pro Jahr auftreten. Während eines MBIs bewegt sich das einströmende Wasser als dichtegetriebene Bodenströmung hangabwärts und transportiert dabei große Mengen an Salz in die Ostsee. Zur Simulation zweier messtechnisch beobachteter MBIs wird ein dreidimensionales numerisches Küstenmeer- und Sedimenttransportmodell aufgesetzt. Ein Vergleich mit den Messdaten zeigt, dass die Hydrodynamik dieser MBIs durch das Modell gut abgebildet wird. In Modellexperimenten durchgeführt wird ein Vorrat aus erodierbarem Feinsediment am Boden des Kattegats platziert. Dieses wird während des MBIs aufgeschlämmt und mit dem einströmenden Wasser in die Ostsee eingetragen. Basierend auf den Ergebnissen wird ein Skalierungsverhältnis zwischen Salzfluss und Sedimentfluss berechnet, was ein Hochskalieren der Modellergebnisse in der Zeit ermöglicht. Gemäß dieser Beziehung wurden während der vergangenen 150 Jahre im Durchschnitt einige hundert

Kilotonnen feinkörnigen Sediments pro Jahr durch MBIs in die Ostsee eingebracht. Dabei verfrachten große Einströme individuell mehr Sediment pro Gigatonne Salz als kleinere Einströme, jedoch sind kleinere Einströme aufgrund ihres häufigeren Auftretens für den Großteil des Gesamtflusses verantwortlich. Der Vergleich mit gemessenen Schwebstoffkonzentrationen im Kattegat zeigt, dass die im Modell berechneten Sedimentflüsse plausibel sind, möglicherweise jedoch unterschätzt werden. Dennoch zeigen die Ergebnisse, dass MBIs in der Lage sind, eine signifikante Menge an Schwebstoffen in die Ostsee zu transportieren.

Um den Zusammenhang zwischen Bodenströmungen und Morphologie zu untersuchen, wird ein hochauflösendes Modellexperiment mit Schwerpunkt auf dem Bornholmbecken und dem Bornholmkanal durchgeführt. Während eines MBIs werden die Bodenströmungen an den Kanaleingängen hangabwärts gelenkt, wobei hohe Dichtegradienten und steile Bathymetrie zu schweregetriebenen Strömungen unter geringem Einfluss der Corioliskraft führen. Nachdem die Bodenströmung in das Bornholmbecken eintritt, geht sie in einer Tiefe von etwa 70 Metern in eine geostrophische Konturströmung über. In dieser Tiefe erreicht die einströmende, dichte Wassermasse im Bornholmbecken neutralen Auftrieb, nachdem sie auf ihrem Weg durch die Ostsee kontinuierlich weniger salzhaltiges Wasser mitgerissen hat. Diese Dynamik stimmt mit den Ergebnissen früherer geologischer Studien überein, welche die submarinen Ablagerungen der Ostsee, die unter Einfluss von Bodenströmungen entstanden sind, sogenannte Konturite, mit MBIs in Verbindung brachten. Demnach werden symmetrische Ablagerung von Schlamm an den Kanalflanken durch Abwärtsströmungen erzeugt, und asymmetrische Ablagerung durch geostrophische Konturströmungen. Im Arkonabecken sind keine derartigen konturitischen Merkmale zu finden. Basierend auf den Modellergebnissen wird die Hypothese aufgestellt, dass eine hohe Variabilität der Bodenströmungsrichtungen im Arkonabecken einen diffusiven Effekt auf die laterale Sedimentverteilung hat, was die Ebenheit der Beckenfüllung erklärt. Die in dieser Arbeit dargestellten Ergebnisse erlauben somit erstmals eine mechanistische Verbindung zwischen Hydrodynamik und Morphodynamik von Schlammdepozentren in der südwestlichen Ostsee

List of publications

1. Porz, L., Zhang, W., Hanebuth, T.J., Schrum, C., 2021. Physical processes controlling mud depocenter development on continental shelves – Geological, oceanographic, and modeling concepts. Marine Geology 432. 10.1016/j.margeo.2020.106402

2. Porz, L., Zhang, W., Schrum, C., 2021. Density-driven bottom currents control development of muddy basins in the southwestern Baltic Sea. Marine Geology 438. 10.1016/j.margeo.2021.106523

3. Porz, L., Zhang, W., Schrum, C., 2021. On the development of two mud depocenters in the southwestern Baltic Sea. (to be submitted)

Contents

1. Contextualization

1.1 Introduction

Timescales of subaqueous sedimentation span at least 14 orders of magnitude (Miall, 2015) – from burst-sweep cycles related to near-bed turbulence lasting a few seconds to the evolution of major sedimentary basins prevailing for millions of years under tectonic control (Figure 1). According to the timescales considered, two types of approaches have developed in the search of those processes that drive seafloor morphodynamics.

On one side are in-situ observations and laboratory experiments, which give valuable information about short-term deposition and erosion processes. In addition to day-to-day processes such as tidal pumping and hemi-pelagic sedimentation, the short-lived and episodic events exhibiting high sediment fluxes such as internal waves, storms, or riverine floods are of particular interest during observations (e.g. Wright and Friedrichs, 2006; Cheriton et al., 2014; Zhang et al., 2016; Zhang et al., 2019). The concept of episodicity is closely tied to our understanding of sediment transport processes, because a certain bottom shear stress threshold must be exceeded in order for particles to be resuspended from the seafloor. This is the reason why temporally averaged current patterns are, in principal, not able to explain bed-scale sedimentation (Dott, 1983).

On the other side of the sedimentation-timescale spectrum lies the interpretation of the geological record using stratigraphic methods. It is thereby implied that at timescales of more than about one thousand years, the impacts of individual events average out, such that the overall sedimentation regime is in a dynamic equilibrium controlled by sediment supply

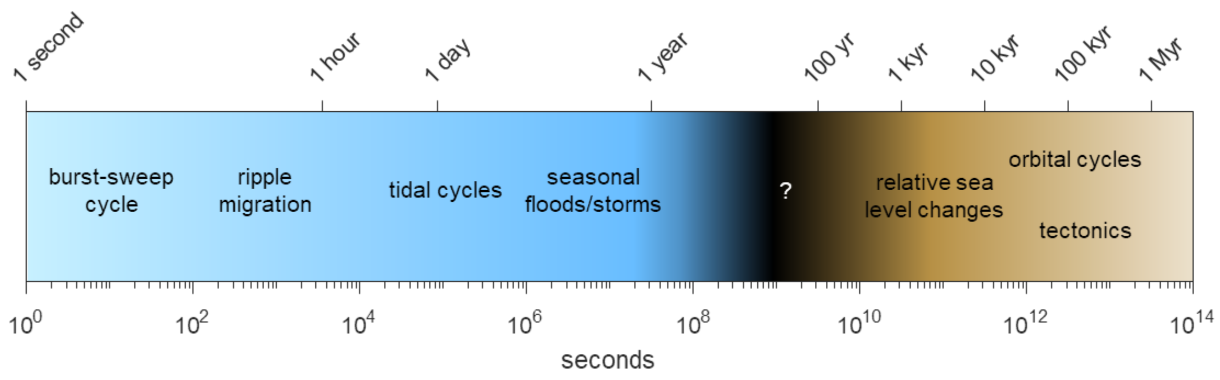

Figure 1. Timescales of sedimentation and some associated processes as observed in-situ (left side) and deduced from the geological record (right side). The dark area represents a "blind spot" in observations, where driving processes are not easily discerned.

and accommodation space (Thorne and Swift, 1991; Catuneanu, 2019). Whatever is retained in the geological record then represents the statistical external forcing given by climate, tectonism, and orbital cycles. The stratigraphic approach comes with caveats owing to the fact that only a small fragment of time is recorded in the sediment column (Ager, 1973; Paola et al., 2018), which is a direct result of the aforementioned episodic nature of sedimentation. This circumstance is indirectly recorded in many continental shelf sediments as an inverse relationship between apparent sedimentation rate and sediment age (depth), where younger deposits seem to have much higher sedimentation rates than older (deeper) deposits (Sadler, 1981). This effect does not result from a lower sediment supply in the past, but from the drastic decrease of preservation potential over time (Sommerfield, 2006).

A dichotomy remains between the observed episodicity of sediment fluxes in the modern environment and the consistency of sedimentation implied in the application of geological methods. Dott (1996), for example, warned the geological community of misinterpretations of the sedimentary record through mistaking event deposits for stratigraphic sequences. Furthermore, a newly deposited bed must be considered ephemeral rather than part of the sedimentary record, so long as it can be eroded by subsequent events. Any attempt to compare in-situ observations with the recent sedimentary record must therefore be subjected to the inquiry whether observed processes are representative of the entire system, and whether beds deposited during the observation will become buried or resuspended and redeposited elsewhere. As a result, it usually remains unknown what the integrated effect of short-term processes is on the long-term. This challenge is further exacerbated by the presence of benthic biota, which muddles the individual event beds through bioturbation, and by anthropogenic activity on the sea floor such as bottom trawling, which can alter depositional signatures lastingly (Wheatcroft and Drake, 2003; Bentley and Nittrouer, 2003; Oberle et al., 2016).

There exists a range in timescales between the two extremes of event-driven episodicity and geological equilibrium, spanning roughly decades to millennia, at which internal dynamics and external forcing overlap, and neither geological nor in-situ measurements alone are able to explain patterns and rates of sedimentation (Woodroffe and Murray-Wallace, 2012). It is on these timescales on which mud depocenters have developed. These accumulations of silt- and/or clay-sized particles, and usually some amount of sand and organic matter, arose to thicknesses of several meters on many modern continental shelves during the Holocene in the form of riverine mud belts, mud patches, or subaqueous deltas, among others (Hanebuth et al., 2015). Mud's fine-grained composition makes it susceptible to winnowing during phases of high bottom shear stress, while its cohesive nature increases the resistance to erosion once left undisturbed for a sufficient period. Mud depocenters can therefore be highly dynamic, and at the same time can contain useful records of past environmental conditions.

During the past decades, advances in computing technology and the development of process-based numerical models have proven useful tools in the study of shelf morphodynamics (e.g. Warner et al., 2008; Pinto et al., 2012; Sherwood et al., 2018; Deltares, 2020). However, the ability to predict multi-decadal mud fluxes using such models remains limited not only by computational power, but also by insufficient parametrizations of cohesive sediment transport processes (Fringer et al., 2019; Diaz et al., 2020). Recently, the concept of source-to-sink analysis has been proposed as a means of bridging temporal gaps by connecting areas of material production with sites of transfer and locations of storage in a budgetary manner (Walsh et al., 2016). Notably, this approach goes beyond traditional stratigraphic analyses by quantifying potential sources in addition to the basin fill. The inherently higher uncertainty of the sources compared to the sinks remains a major challenge of the source-to-sink approach (Helland-Hansen et al., 2016). Nevertheless, studies based on the source-to-sink mentality have been successfully applied to muddy shelf environments (e.g. Farnsworth and Warrick, 2007; Liu et al., 2016; Kuehl et al., 2016; Cong et al., 2021).

The aim of this thesis is to elucidate the physical processes involved in shelf mud sedimentation, while also addressing the dichotomy of episodic vs. long-term processes. A method is sought to bridge the gap in timescales by means of source-to-sink analysis using sediment budgets and high-resolution numerical modeling. The southwestern Baltic Sea, which hosts several muddy depocenters, serves as a study area. It represents a type of natural laboratory for the examination of individual processes. Specifically, the following research questions will be answered:

1. What drives shelf mud accumulation on different timescales?
2. What are the sources and sinks of fine-grained sediment in the southwestern Baltic Sea?

3. Can dense inflows from the North Sea import a significant amount of fine-grained sediment into the Baltic Sea?
4. How do bottom currents shape the mud depocenters in the southwestern Baltic Sea?

The thesis comprises five parts, including three research papers. This introductory chapter proceeds with a brief overview of the Baltic Sea's recent geological history and the current knowledge of mud dynamics in the southwestern Baltic Sea. The first paper is a literature review of mud depocenter development on continental shelves (Porz et al., 2021a). In an attempt to reconcile various viewpoints on mud accumulation, the review summarizes processes that have been deemed key for shelf mud accumulation in the literature, and the role of episodic events in shelf mud accumulation. The second paper applies a variant of source-to-sink analysis to the southwestern Baltic Sea using a combination of sediment budget analysis and numerical modeling in order to discern the processes involved in the supply of mud to the study area (Porz et al., 2021b). In particular, the role of Major Baltic Inflows (MBIs) and their capacity to advect sediment into the Baltic Sea is investigated. The third paper (Porz et al., 2021c) explores the process-product relationship between episodic bottom currents and mud deposition in the Bornholm Basin, and contrasts this with mud deposition in the Arkona Basin, which shows no obvious indication of bottom current control. The goal is to examine the long hypothesized mechanistic connection between dense inflows and morphology, culminating in a conceptual model for the development of the Arkona and Bornholm Basins during the last few thousand years. The thesis concludes with an overall discussion of the results in a broader context and outlook towards further research.

1.2 The mud depocenters of the southwestern Baltic Sea

Following the retreat of the ice sheets after the last glacial maximum ca. 20,000 yrs BP, the Baltic Sea area was subject to complex morphological changes determined largely by relative sea level related to draining of melt water, global sea level rise, isostatic uplift in Scandinavia and subsidence along the southern coasts. During this time, four major stages are recorded in the Baltic Sea sediments (Andrén et al., 2011): the freshwater Baltic Ice Lake, the partly brackish Yoldia Sea, the freshwater Ancylus Lake, and the brackish Littorina Sea. This thesis focuses on the Littorina stage, which initiated ca. 8000 yrs BP. Since this transgression, relative sea level in the southwestern Baltic has slowed to its current rate and sedimentation conditions have remained relatively stable until today. The transition from freshwater to brackish-marine conditions was accompanied by deposition of silty, organic-rich mud in the sub-basins. The base of this mud constitutes a prominent acoustic reflector (Virtasalo et al., 2016), allowing mud thickness estimates to be derived from seismo-acoustic data (Bonacker, 1996; Lemke, 1998).

The southwestern Baltic Sea has a long history of oceanographic and, to a lesser extent, morphological research. This fact makes it a natural laboratory for studying morphodynamic processes. Early work by Seibold (1965) recognized the role of water exchange with the North Sea through the Great Belt on recent sedimentation in the Baltic Sea, and proposed a general eastward transport direction as a result of dense water inflows. He also noticed that the extent of mud accumulation seems to be limited to depths below the mean position of the summer halocline in each basin. In the Bornholm Basin, sedimentation is thought to be related to bottom current control (Sivkov and Sviridov, 1994; Emelyanov et al., 1995; Sivkov et al., 2002; Jensen et al., 2017), producing depositional structures known as contourites. Originally, this term was used to describe the large-scale deposit geometries forced by thermohaline contour-following currents on the continental slope (Heezen et al., 1966). After similar features were found in shelf settings, Faugères and Stow (1993) suggested the use of the umbrella term "bottom current deposit". It has since been proposed to broaden the definition of the term "contourite" to any deposit reworked by bottom currents (Stow et al., 2002; Rebesco, 2005; Rebesco et al., 2014). Lithologic facies models have been conceived for the identification of contourites from sediment cores (Gonthier et al., 1984; Stow and Faugères, 2008). The contouritic facies generally consists of a bioturbated, bi-gradational sequence (coarsening-up/fining-up) believed to result from cyclic changes in bottom current strength and/or sediment supply. This facies certainly does not apply to the laminated muddy deposits in the in the Baltic Sea, which have previously been classified as contourites (Sivkov et al., 2002; Jensen et al., 2017), but are not listed in the review of contourite depositional systems of Rebesco et al. (2014). Nevertheless, the term “contourite” shall be used in this thesis to describe the bottom-current reworked deposits in the Baltic Sea.

For some decades now, a growing network of permanent observational stations (e.g. BSH, 2020; ICES, 2021) has provided useful information on the large-scale circulation in the Baltic Sea, including inflow events. By contrast, measurements of near-bottom suspended matter in the southwestern Baltic Sea remain scarce, which constitutes one of the major motivations of the case studies presented in this thesis. Only two direct measurements of bottom SPM during MBIs have been reported: One of SPM in transit from the Arkona to the Bornholm Basin (Sivkov et al., 1995), and one SPM transect from the Kattegat to the Arkona Basin during a small inflow (Lund-Hansen and Christiansen, 2008). However, neither of these studies allow a conclusive connection between hydrodynamics and sediment transport to be made.

Detailed observations of SPM transport in the Pomeranian Bight have been reported, where the Oder River discharges into the southwestern Baltic Sea as the major riverine sediment source (e.g. Leipe et al., 2000; Witt et al., 2001; Christiansen et al., 2002; Emeis et al., 2002). Similar observations have been conducted in the Mecklenburg Bight (Jähmlich et al., 2002; Ziervogel and Forster, 2005). All of these reports focused on the so-called fluff layer, which describes the young and extremely mobile layer of particulate matter that accumulates on the sediment surface under quiescent conditions. The fluff layer is composed of macroflocs which contain a high amount of organic matter (up to 45%, Christiansen et al., 2002), most of which is labile and prone to remineralization. However, organic matter contents within the fluff layer do reduce to a few percent towards the Arkona Basin, which is a similar range as found in the mud depocenter itself. Though little is known about the behavior of fluff layers during the sedimentation process, they seem to be the primary conduit of fine-grained sediment from the coast to the depocenters.

A prerequisite of any three-dimensional numerical matter transport model is a high quality of its hydrodynamic host model. Today, numerical models are able to reproduce hydrodynamic processes with reliable accuracy, including those during MBIs (e.g. Hofmeister et al., 2011; Gräwe et al., 2015; Stanev et al., 2018). The same cannot be said for sediment transport, where no modeling efforts have been able to be validated. Nevertheless, various sediment transport models have been applied in the Baltic Sea with different objectives. Edelvang et al. (2002) modeled sedimentation from outflow of the Oder River and indicate that 2/3 of this river load moves toward the Arkona Basin, and 1/3 toward the Bornholm Basin. A combined numerical modeling and sedimentological study by Bobertz and Harff (2004) found that the surface grain size distribution in the southwestern Baltic Sea corresponds to mean sediment transport pathways, with general transport pathways being directed from coastal sources toward the basin depocenters. Their results are a strong indication that surface sediments in the southwestern Baltic Sea are controlled by recent hydrodynamic setting. In the modeling experiments of Kuhrts et al. (2004), no resuspension of fine material takes place in the Arkona and Bornholm Basins. On the other hand, a modeling study by Zhurbas et al. (2018) found that a resuspension threshold of the fluff layer is occasionally exceeded everywhere in the Baltic Sea. Roughness maps were generated by Bobertz et al. (2009) by combining grain size maps (Figure 2) with habitat mapping in order to account for the roughness induced by the presence of macrobenthos, though this effect was shown to be limited (Seifert et al., 2009). The model of Almroth-Rosell et al. (2011) reproduced the areas of erosion, transport and accumulation reasonably, but some marked differences were also revealed when compared to grain size distribution maps.

Many of these model uncertainties and inconsistencies are likely related to differences in sediment transport parametrizations, which remain poorly constrained. The problem of representing the dynamics of the fluff layer was expanded on by Ziervogel and Bohling (2003) using Mecklenburg Bight sediments. They found significant discrepancies for mud between measured erosion thresholds and those given by theoretical formulas from grain size: While the erosion threshold for the fluff layer was six times lower than the calculated value, the underlying cohesive bed layer was not resuspended at all during their experiments. Their results also suggest that sediment transport in the Mecklenburg Bight is controlled by storm events, because bottom shear stresses do not exceed the critical values for resuspension under calm conditions. A recent sensitivity study of particulate matter transport modeling by Osinski et al. (2020) concluded that even if settling and resuspension parameters are sufficiently constrained, considerable uncertainties in particle fluxes would remain due to uncertainties in the atmospheric forcing fields during strong wind events. Nevertheless, their ensembles showed overall similarity in the depositional areas.

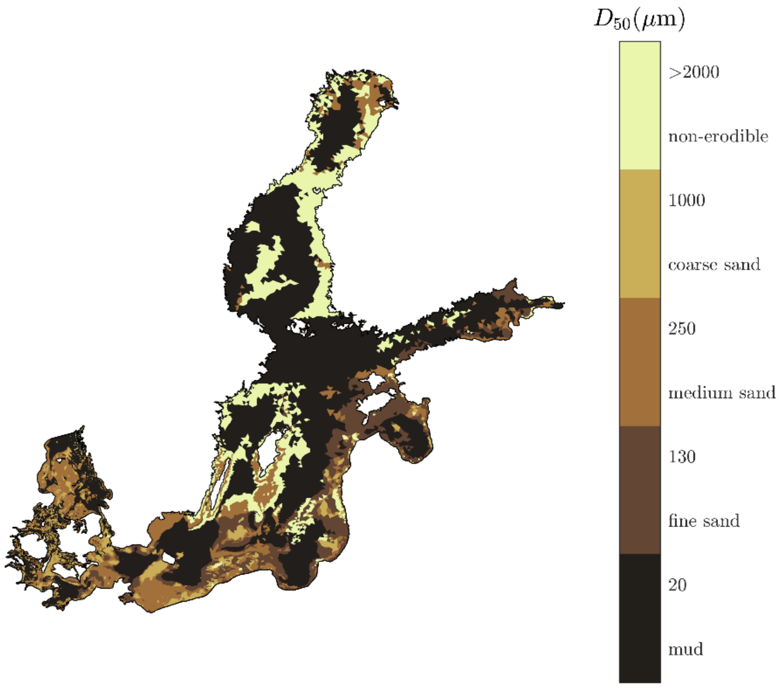

Figure 2. Median surface grain size map of Baltic Sea surface sediments according to Bobertz et al. (2009).

2. Physical Processes Controlling Mud Depocenter Development on Continental Shelves – Geological, Oceanographic, and Modeling Concepts

This chapter contains a paper, which was published in Marine Geology as:

Porz, L., Zhang, W., Hanebuth, T.J., Schrum, C., 2021. Physical processes controlling mud depocenter development on continental shelves – Geological, oceanographic, and modeling concepts. Marine Geology 432.

The contribution of Lucas Porz and co-other authors to this paper is as follows:

TH conceived the review. LP collected the literature and wrote the manuscript in consultation with WZ, TH and CS. TH processed the core radiography. All authors revised the manuscript.

Marine Geology 432 (2021) 106402

Contents lists available at ScienceDirect

Marine Geology

journal homepage: www.elsevier.com/locate/margo

Physical processes controlling mud depocenter development on continental shelves – Geological, oceanographic, and modeling concepts

Lucas Porz [a,*], Wenyan Zhang [a], Till J.J. Hanebuth [b], Corinna Schrum [a,c]

[a] Institute of Coastal Research, Helmholtz-Zentrum Geesthacht, Max-Planck-Strasse 1, Geesthacht 21502, Germany
[b] Department of Coastal and Marine Systems Science, Coastal Carolina University, 301 Allied Drive, Conway, SC 29528, USA
[c] Institute of Oceanography, Center for Earth System Research and Sustainability, University of Hamburg, Bundesstrasse 53, Hamburg 20146, Germany

ARTICLE INFO

Keywords:
Mud
Depocenters
Shelf processes
Sediment transport
Numerical models

ABSTRACT

Mud depocenters (MDCs) represent major proximal-marine sinks for fine-grained terrigenous material, carbon, and contaminants on modern continental shelves. Throughout the past decades, several studies have shed light on the physical processes controlling MDC development at various timescales, ranging from controlled flume experiments and in-situ oceanographic monitoring, to stratigraphic analyses of recent and ancient deposits based on seismo-acoustic and sediment-core data. Thereby, key mechanisms related to the formation and maintenance dynamics of MDCs have been discovered: a) cross-shore bottom transport of suspended mud through *gravity flows*, b) interaction of mud with density gradients associated with *oceanic fronts*, c) resuspension and dispersal control of mud by *internal waves*, d) *bedload deposition of mud* forming laminated bedding under energetic flow conditions, and e) mud resuspension resulting from *chronic bottom trawling*.

Among the physical processes identified or proposed, three conceptual paradigms for MDC development can be distinguished: 1. *continuous supply*, associated with a steady sediment supply and hemipelagic settling in relatively calm conditions; 2. *continual resuspension-deposition cycles*, wherein parts of an MDC area are subject to multiple cycles of resuspension, redeposition and reworking before ultimate burial; and 3. *episodic sedimentation and erosion*, in which extreme events such as riverine floods and atmospheric storms dominate the total, long-term sediment flux. Although the predominance of each of these paradigms within a single MDC depends to a large degree on the timescales considered, case studies tend to emphasize processes associated with only one of these three paradigms. As a result, the relative, long-term contribution of individual processes remains largely uncertain for many MDCs.

The ability of numerical models to accurately predict medium to long-term mud accumulation is restricted not only by computational costs, but also by insufficient parametrizations of the muddy sedimentation process. These remain challenging to constrain due to the multiplicity and complexity of factors affecting the cohesive properties of mud, including its state of consolidation, and the amount and type of organic matter present. Bridging the gap between individual events and long-term accumulation is the key to a more complete understanding of sedimentation processes in MDCs.

1. Introduction

Mud depocenters (MDCs) represent major shallow-marine, thus most proximal to the continent, sinks for fine-grained terrigenous material on modern shelves (Hanebuth et al., 2015). Various types of MDC have been categorized, according to their position on the shelf, topographic situation, hydrodynamic conditions, and sediment supply (McCave, 1972; McKee et al., 2004; Walsh and Nittrouer, 2009; Gao and Collins, 2014; Hanebuth et al., 2015). Comprising primarily silt (grain size <63 μm) and often some amount of organic matter (referred to collectively as “fines” hereafter), these sediment depocenters contain geological records important to the study of past climatic, oceanographic, and continental conditions (Potter et al., 2005). Moreover, MDCs serve as habitats and cradle for benthic life (Snelgrove, 1999; Thrush and Dayton, 2002) and as significant sinks, and maybe sources, for anthropogenic contaminants (Mahiquesde et al., 2015; Hanebuth et al., 2018), making them crucial components in ecosystem functioning. As major carbon storage areas (Blair and Aller, 2011; Bauer et al., 2013), MDCs

* Corresponding author.
E-mail address: lucas.porz@hzg.de (L. Porz).

https://doi.org/10.1016/j.margeo.2020.106402
Received 11 June 2020; Received in revised form 13 December 2020; Accepted 16 December 2020
Available online 29 December 2020
0025-3227/

may be considered an important element in the regional biotic and abiotic carbon cycles (Oberle et al., 2014; Hanebuth et al., subm.), and – on geological timescales – a potential source rock for hydrocarbons (Arthur and Sageman, 1994).

Prompted by their significance regarding ecology and environment, considerable effort has gone into the study of MDCs in the past decades, and various physical mechanisms involved in the formation and reworking of MDC deposits have been identified or proposed (e.g. Swift et al., 1972; Palinkas and Nittrouer, 2007; Wu et al., 2016b). Geological analyses of modern MDCs and their underlying late-Pleistocene to early-Holocene strata have provided insight into long-term formation mechanisms and the conditions under which MDCs initiate and continue developing, including shelf topography, relative sea level variations, and mean oceanic bottom-currents (e.g. Mountain et al., 2007; Syvitski et al., 2007; Hanebuth et al., 2015). Such approaches fundamentally lack, however, the temporal resolution needed to determine various short-term processes that are relevant for the overall shaping and growth of an MDC. To this end, oceanographic studies have progressed in determining the fluid mechanical processes bounding the appearance of MDCs, such as near-bottom gravity flows, internal waves, and oceanic density fronts (e.g. Traykovski et al., 2000; Cheriton et al., 2014; Liu et al., 2018; Williams et al., 2019; Zhang et al., 2019). These advances have encouraged a search for signatures of depositional processes in the microstratigraphy of ancient mudstone analogues (e.g. Leithold, 1989; Macquaker et al., 2010; Lazar et al., 2015; Wilson and Schieber, 2017; Boulesteix et al., 2019). In-situ monitoring and experimental flume studies have shed light on the hemipelagic and near-bed transport and sedimentation mechanisms of fines, including material flocculation dynamics, hindered settling of high-concentration suspensions, and consolidation and erosion processes (e.g. Le Hir et al., 2008; Schieber and Yawar, 2009; Mathew and Winterwerp, 2017; Xiong et al., 2017; Thompson et al., 2019). These results have, in turn, informed process-based numerical methods by constraining parametrizations related to the cohesive nature of mud (e.g. Mehta, 1991; Papanicolaou et al., 2008; Neumeier et al., 2008; Amoudry and Souza, 2011; Sherwood et al., 2018; Winterwerp et al., 2018). Meanwhile, increasing attention to ecosystem functioning has raised new questions regarding the role of benthic and hemipelagic biogeochemistry as well as anthropogenic impacts on the physical properties of mud (e.g. Le Hir et al., 2007; Andersen and Pejrup, 2011; Oberle et al., 2016a). It seems, thus, evident that a combined effort of various stratigraphic analyses, in-situ hydrodynamic monitoring, numerical coastal ocean modeling, and ecosystem research is required in order to advance our understanding of MDC development and functioning.

The goals of this review are to synthesize and structure the existing knowledge on physical mechanisms relating to the formation and shaping of MDCs, including the evaluation of hydrodynamic processes and of the geological record. Referring to existing literature, we discuss unresolved mechanistic problems and underline the necessity of an interdisciplinary approach in order to properly address and fully understand the relevant processes. A focus lies on the representation of physical mechanisms crucial for reproducing the local morphodynamics of MDCs in coastal sediment-transport models. While several of the individual concepts described herein are applicable to sediment dispersal systems in general, this study places emphasis on those mechanisms that are related to the dynamics of MDCs on continental shelves in particular.

The review is structured as follows: Beginning with a chronological assessment of existing literature relevant to the topic, we discuss MDCs from a sedimentological perspective, and present various points of view regarding their formation and maintenance dynamics. The next section describes mud sources and known physical processes involved in locally confined shelf mud accumulation. This compilation includes a discussion on the current state of coastal sediment-transport models required to resolve MDC dynamics. Finally, we summarize recent advances and remaining challenges in this field.

2. Existing concepts

2.1. Past reviews on mud depocenter dynamics

A handful of review articles exists on the topic of shelf mud sedimentation, each with a different focus, and some authors have proposed a classification of muddy shelf sedimentary systems.

McCave (1972) in his seminal work recognized that sites of mud accumulation on continental shelves are controlled by near-bed concentration of fines, particle sinking velocity, and the ratio of bed shear stress and critical shear stress for deposition. Further conceptualizing shelf mud deposition as a balance between near-bed suspended particle concentration and bottom hydrodynamic energy, he suggested five types of depositional mud patterns according to their distances from the coast, from proximal to distal: a) *Coastal* and b) *nearshore* mud deposits form during hydrodynamically calm periods, allowing for the development of sufficient cohesive strength at the seabed to withstand storm conditions. For c) *mid-shelf* deposits, waves and tidal currents limit shoreward accumulation, whereas an acceleration of tidal currents near the shelf edge limits its seaward extent. d) *Outer-shelf* deposits are attributed to settling from river-fed, high-concentration mud flows where storm waves cannot counteract supply. Lastly, e) *mud blankets* draping the entire shelf develop primarily off deltas with high riverine sediment discharge. The study identified advective hydrodynamic processes to be dominant over (non-directed) diffusion. By example of the East Coast of North America, Stanley et al. (1983) presented the concept of a “mudline” to denote the shoreward limitation of mud accumulation. More specifically, the mudline is defined as the boundary beyond which silt and clay content of the sediment increases substantially. The mudline serves as a natural energy level marker that defines the boundary between mobilization and settling of fines, and it may be located anywhere from the inner continental shelf to the middle continental slope depending on the long-term hydrodynamic conditions. Principle factors governing the regional mudline depth are shelf width (often in combination with shelf gradient), volume of sediment supply, and magnitude of bottom current energy. High sediment supply and low bottom-current energy were described as prerequisites for mud to accumulate on a shelf. This relationship was suggested to intensify with narrowing shelf width, that is, a narrower shelf would require higher sediment supply and/or lower bottom-current energy in order to sustain an MDC compared to a broader shelf.

In the ongoing effort to explain the range of the site-specific appearance and geometry of MDCs, a shift of focus over time from the water column to the near-bed environment took place. Most particulate transport occurs, according to Nittrouer and Wright (1994), near the seabed. They identified the mid-shelf as a primary location of MDC development globally and determined wind-driven flows, internal waves, surface waves during storms, infra-gravity waves, buoyant plumes, and surf-zone processes as important mechanisms for cross-shelf transport of sediment. By example of the Northern California shelf, Sommerfield et al. (2007) stressed the importance of an interaction between shelf bathymetry and near-bottom currents, which influences the lateral pattern and rate of mud accumulation on a wide range of temporal and spatial scales. They found that most of the mud transport to the Northern California shelf occurs during river flooding stages, where mud is sequestered through both static and dynamic trapping mechanisms within the bottom boundary layer (BBL: the part of the water column above the stationary seabed that is affected by the drag of ocean currents on the seafloor, typically with a thickness on the order of 10^0-10^1 m, Trowbridge and Lentz, 2018). Static trapping refers to deposition inside local topographic depressions in the receiving submarine basin, while dynamic trapping is characterized by particle flocculation, convergent circulation, and water column stratification leading to rapid sedimentation and sequestration of event deposits. During the past decades, increasing attention has been directed towards local hydrodynamics and biological activity. Gorsline (1984), for example, acknowledged bottom currents causing continual reworking of fines at the seabed, and biological activity leading to pelletization and bioturbation, which may alter the stratigraphic record significantly.

Some authors have focused on processes of mud dispersion related to riverine suspension plumes. McKee et al. (2004) differentiated four basic categories of riverine dispersal-dominated depocenters with respect to their relative position on the shelf and the main hydrodynamic forcing mechanism: a) *deltaic,* b) *subaqueous detached,* c) *shelf escape,* and d) *combined*. This classification is somewhat analogous to that of McCave (1972), though it is specific to river-dominated ocean margins and takes into account shore-parallel and vertical variability in depositional patterns. McKee et al. (2004) emphasized that the region 1-2 m above the sediment/water interface and the mobile upper region of the seabed is an important zone for the transport of fines and for the remineralization of organic matter and nutrients, but they concluded that knowledge of these processes was insufficient at that stage to discern their role in controlling fluxes of fines. Geyer et al. (2004) elucidated dispersal mechanisms of sediment associated with buoyant river plumes, including frontal trapping, particle flocculation and settling, and near-bottom fluxes of suspended fines. Their study emphasized the role of oceanic frontal dynamics in both trapping sediment on the shelf as well as generating high-concentration near-bottom layers that promote cross-shelf transport and deposition.

Walsh and Nittrouer (2009) distinguished five types of riverine-to-marine dispersal systems based on their geographic positions relative to the source, namely a) *estuarine-accumulation-dominated* (EA), b) *proximal-accumulation-dominated* (PAD), c) *marine-dispersal-dominated* (MDD), d) *subaqueous-delta-clinoform* (SDC), and e) *canyon-captured* (CC). Compared to previous classifications by McCave (1972) and McKee et al. (2004), the first two systems (EA and PAD) may be sorted into a nearshore/deltaic type, MDD is analogous to a mid-shelf deposit, SDC may extend from inner to mid-shelf regions, and CC refers to special cases where a submarine canyon is directly connected to the river mouth. A hierarchical decision tree based on fluvial discharge, shelf width, mean significant wave height, and tidal range allowed a prediction of the respective type of system for most of the world's largest riverine dispersal systems. Flocculation of solids dominates in nearshore depositional systems (EA and PD), while suspended sediment gravity flow and current-driven dispersion are the significant mechanisms acting in the dispersal systems where sediment accumulates further offshore (MDD, SDC, and CC). It was found that the distance of an MDC to its sediment source increases with significant wave height and with tidal range. These strong relationships led to the suggestion that in general, dispersal systems may not be sorted into discrete types but rather exist on a continuum as a consequence of the multi-parameter control on their geographic location, shape, size, internal architecture, sediment accumulation rates, and material composition.

Other reviews have focused on the problem of linking short-term transport and sedimentation processes to the overall, long-term geometry and stratigraphy of MDCs. Wright and Nittrouer (1995) differentiated river-supplied sediment dispersal processes on the shelf into four successive stages: 1. *offshore plume dispersal*, 2. *rapid initial deposition*, 3. *resuspension and transport*, and 4. *long-term net accumulation*. The initial Stages 1 and 2 were suggested to be dominant in some shelf systems (e.g. Huanghe and Mississippi), while the subsequent Stages 3 and 4 control other systems (e.g. Amazon and Yangtze). The authors stressed that the timescale of interest is important when considering the dispersal processes; in-situ measurements may not reflect long-term accumulation patterns, because Stage 3 and 4 processes may alter the record lastingly by repeated mobilization or erosion, transport, and redeposition of particles. Gao and Collins (2014) distinguished between wide and narrow shelf topographies under either abundant sediment supply or material starved conditions. MDCs were proposed to develop primarily under a regime of abundant sediment supply. This study inferred that most shelves have incomplete Holocene sedimentary records, and stressed that the duplicity between event-based and average sedimentation can lead to a misinterpretation of the sedimentary record. It was suggested that numerical models may aid in this effort by simulating the formation, post-depositional alteration, and preservation potential of these deposits.

Hanebuth et al. (2015) have recently undertaken an attempt to classify MDCs on continental shelves from a geological perspective, defining eight types with regard to their three-dimensional architecture and long-term depositional pattern. Shelf morphology, sea level, local hydrodynamic regime, and sediment supply were identified as primary factors controlling the depositional geometries. High sediment supply favors the formation of a) extensive *prodeltas* and b) *subaqueous deltas,* attached or in proximity to the river mouth; c) scattered *mud patches* and d) widespread *mud blankets* might occur across the whole shelf and reflect the amount of sediment available. Hydrodynamic forcing produces e) elongated mid-shelf *mudbelts* and f) shallow-water *contourite drifts,* both detached from the fluvial point source. Finally, topography controls the formation of g) local *mud entrapments* and h) *mud wedges,* which deposit inside seabed depressions and behind morphological jumps.

2.2. Paradigms of mud depocenter development

A simple, yet valuable conceptualization of MDC development is based on local mass conservation as described by the Exner equation (Exner, 1925; Paola and Voller, 2005), which can be expressed as

$$\frac{d\eta}{dt} = -A\nabla\cdot\boldsymbol{U} \tag{1}$$

where $\eta(x,y)$ is bed elevation, t is time, $A > 0$ is a coefficient related to bulk density of the deposited grains, and $\boldsymbol{U} = \vec{U}(x,y)$ is a vector field of horizontal sediment flux. In general, sedimentation occurs wherever there is a negative gradient in lateral flux ($\nabla\cdot\boldsymbol{U} < 0$), that is, wherever deposition outweighs erosion. Variations of Eq. (1) are implemented in long-term morphodynamic models (e.g. Zhang et al., 2012) as well as short-term, process-based models (e.g Amoudry and Souza, 2011) alike. Accordingly, the validity and interpretation of Eq. (1) depends upon the temporal and spatial scales considered.

The fact that apparent sedimentation rates scale inversely with the averaged timespan has motivated the concept of *stratigraphic completeness*, i.e. the amount of time and space preserved in a sediment column (Sadler, 1981). As for most modern shelves, MDCs typically exhibit high sedimentation rates (on the order of 1 mm/yr), exceeding those in most other open-ocean environments by an order of magnitude or more. However, stratigraphic completeness may vary widely from one MDC to another. On a 1000 yr scale, completeness may vary from 20–50% on strongly tidal deltaic shelves to 50–90% on calm-water accretionary shelves (Sommerfield, 2006). In systems with high sediment supply, depositional events are often sporadic and followed by phases of reduced input or even erosion. Thus, stratigraphic completeness is usually highest and accumulation rates are most steady in locations where both sediment supply and hydrodynamic energy are low. This (somewhat counterintuitive) insight reflects the episodic nature of sedimentation and erosion. Although completeness tends to be higher in deeper topographic settings, water depth is not a robust predictor of completeness due to the variety of mechanisms influencing sediment accretion on continental margins such as wave and tidal currents, wind-driven flows, sediment supply, and bottom trawling.

In view of the variability of horizontal sediment fluxes and stratigraphic completeness on different timescales, the identified mechanisms related to the formation of MDCs frequently correspond to one of three paradigms: *continuous supply*, *continual resuspension-deposition cycles*, and *episodic erosion and sedimentation events* (Fig. 1).

2.2.1. Continuous supply

The first paradigm pertains to the concept of advective and diffusive

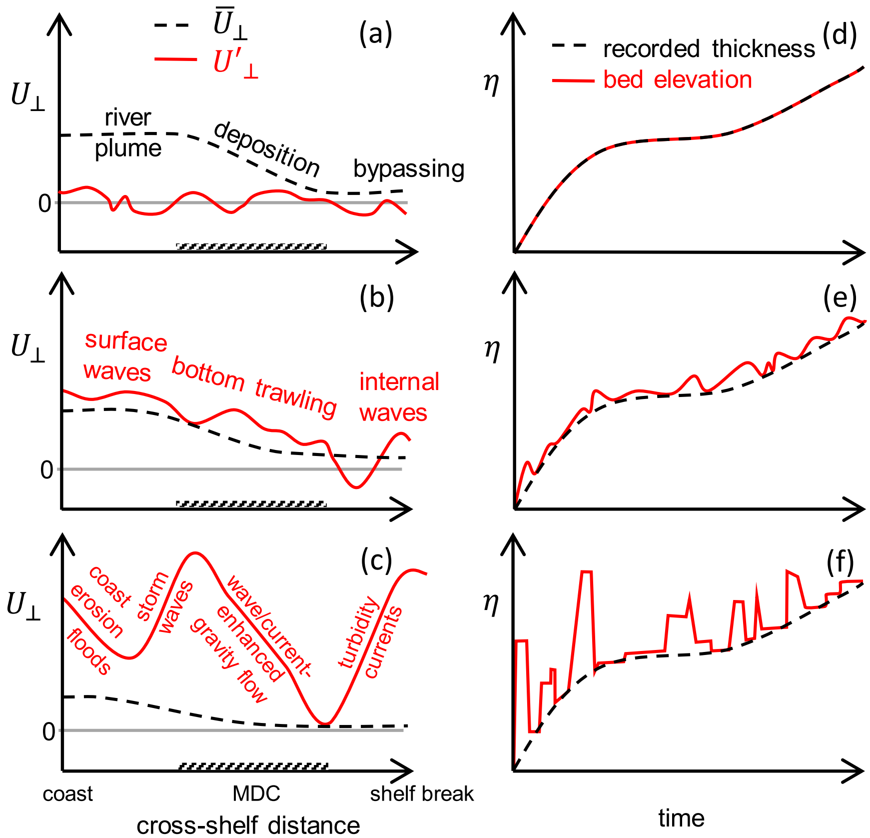

Fig. 1. Conceptual illustration of MDC development and likely processes based on (a-c) the cross-shelf component of mud fluxes $U_\perp$ and (d-f) possible time-series of MDC thickness η for (a, d) low-energy settings, (b, e) resuspension-dominated settings and (c, f) event-dominated settings. Here, all scenarios result in the same recorded thickness (d-f, dashed) and MDC position. Deposition occurs where the flux gradient is negative, and negative fluxes are directed onshore. In the cases of (b) and (c), the background flux $\overline{U}_\perp$ (dashed) must not correspond to the position of the MDC on the shelf. In (a, d) low-energy settings, the recorded MDC thickness (dashed) is close to the instantaneous bed elevation (solid), while the recorded thickness deviates from the instantaneous thickness in the cases of (b, e) and (c, f), induced by short-term (hourly to seasonal) deviations $U'_\perp$ (a-c, solid) during high-flux events.

offshore sediment transport and hemipelagic settling out of nepheloid layers as first described by McCave (1972). The reasoning behind this paradigm is that fines tend to deposit from suspension under calm hydrodynamic conditions. Accordingly, conditions which allow long-term accumulation of fines into an MDC should be exceptionally quiescent. Within the MDC, the presence of such conditions may be expressed in the form of mm-scale mud lamination, as described for many recent and ancient MDCs (e.g. Stanley, 1983; Kuehl et al., 1988; O'Brien, 1996; Potter et al., 2005; Schimmelmann et al., 2016), although this internal layering often becomes lost secondarily due to endobenthic bioturbation. These fine deposits typically display a distinct internal, sub-parallel sediment-acoustic reflection pattern as well (Damuth and Hayes, 1977). This architectural MDC stratification of highest temporal resolution and with an aggradational, sometimes progradational growth history evokes a rather (semi-) continuous picture of sedimentation wherein the MDC is more or less consistently supplied with fresh material. Such a system would be expected to have exceptionally high stratigraphic completeness.

An argument in line with this paradigm was recently made by Williams et al. (2019), who suggested that tidal-current circulation patterns are responsible for retaining fines within patchy MDCs around the British Isles. Regions of cyclonic tidal currents exhibit thinner BBLs than their Coriolis-supported, anti-cyclonic counterparts, because the BBL cannot fully develop within a tidal period in the former situation. A limited BBL thickness promotes enhanced accumulation by a settling of fines from the low-turbulence zone above the BBL and by a limitation of the upward-directed flux of resuspended mud to within the BBL. This study posited that such persisting "background" mechanisms dominate other broad, low-energy shelves as well.

The *continuous supply* paradigm pertains to a state of morphodynamic equilibrium, such that $\nabla \cdot U < 0$ across the MDC. This situation corresponds to steady-state sedimentation, as has been described by regime theory (Swift and Thorne, 1992). When U becomes constant over the entire depositional area, no further net deposition takes place. In such a system, the accommodation space available is completely filled and new deposits are no longer preserved but subject to cross-shelf material export. This type of equilibrium seems to have established in most modern dispersal systems after sea level has stabilized over the later Holocene (Sommerfield et al., 2007; Hanebuth et al., 2015 and references therein).

2.2.2. *Continual resuspension-deposition cycles*

The second paradigm contends that mud deposition is not a straightforward source-to-sink process, but rather dynamic, and includes multiple cycles of suspension, advection, and vertical mixing before final settling and consolidation. This view is supported by oceanographic monitoring, which shows that short-term peak energy conditions cause frequent resuspension events (Cacchione et al., 1987; Ogston et al., 2000; Cheriton et al., 2014; e.g. Zhang et al., 2019). On timescales from seconds to months, hydrodynamic conditions are highly variable, leading to recurrent phases of resuspension or erosion in geographic areas of net deposition. Such phases are often largely unrelated to variations in river discharge or secondary mud sources in the upper water column (Walsh and Nittrouer, 1999). Intermittent mobilization by internal waves, tidal waves, marine storms, eddies, and secondary bottom-circulation have been found to strongly determine MDC morphology (Zhang et al., 2016; Zhang et al., 2019). As a result, the sedimentary succession (material grain size) in most of the MDCs is either vertically homogenized or graded due to slight material sorting trends, with little visual or stratigraphic evidence of small-scale layering. The result is an acoustically transparent seismo-acoustic signature in-between major, sub-parallel internal reflections (Hanebuth et al., 2015).

Flume experiments have shown that fines can accrete as laminated mud layers even under energetic conditions of sustained bottom flow at a current speed of up to 25 cm/s, (Schieber et al., 2007; Schieber and

Yawar, 2009). In these experiments, clay suspensions formed aggregates that transferred to bedload, developing migrating, low-angle ripples, and finally accreted into cm-thick mud beds. Subsequent compaction results in randomly interspersed clay and coarse silt laminae. Increased shear in the boundary layer led to destruction of clay flocs and allowed only silt grains to settle to the bottom and form a silt layer. These laminae are conspicuously similar to those found in many recent muddy depositional environments and ancient geologic mudstone successions, in which a careful examination often reveals signs of energetic deposition or reworking (e.g. Nittrouer and Sternberg, 1981; Macquaker et al., 2010; Ghadeer and Macquaker, 2012; Plint, 2014). Thus, other than solely hemipelagic settling, the mechanism of bedload-transported flocculated mud offered an alternative explanation for the ubiquity of lamination found in MDCs (Yawar and Schieber, 2017).

Within the paradigm of *continual resuspension-deposition cycles*, perturbations of the steady-state become meaningful, and U is to be understood as an instantaneous value. Thus, the horizontal flux may be split into a long-term mean and a fluctuating part which represent deviations from the mean (Sommerfield, 2006): $U = \overline{U} + U'$. In the context of MDCs, $\overline{U}$ may be interpreted as the multi-decadal average background flux related to hemipelagic dispersal and sedimentation and U' are deviations from the average flux occurring on hourly to seasonal time scales due to intermittent disruption, e.g. by storm waves or bottom trawling activities. According to this paradigm, stratigraphic completeness of MDCs should generally be limited compared to a scenario of *continuous supply*, but the resulting stratigraphic gaps might be minimal to negligible, though frequent, depending on event duration and intensity.

2.2.3. Episodic erosion and sedimentation

Contrasting the idea of *continuous supply*, the third paradigm refers to *episodic erosion and sedimentation* processes. In this context, the term "event" is commonly used to describe such environmental fluctuations where $|U'| \geq \left|\overline{U}\right|$ with periods from minutes to a few weeks, often triggered by river flood stages or atmospheric storm events. The main justification for this paradigm is rooted in the observation that events of high material flux can sometimes be distinguished from in the geological record, and that they are occasionally observed in the field, leading several studies to term them the main driving mechanisms of mud sedimentation. For example, Ulses et al. (2008) and Dufois et al. (2014) have found that storms and floods play a crucial role on mud dispersal and off-shelf material export in the Gulf of Lions. Marion et al. (2010) described for the Rhone prodelta multi-cm rises in local seabed elevation shortly after a river flood event, and seabed lowering during storms. Similarly, Collins et al. (2017) have described the shelf off northwest Borneo as an alternating storm vs. flood dominated setting, resulting in depositional event beds. Frequent flood events and subsequent near-bottom gravity flows have also been designated as the responsible mechanisms for MDC development on the Eel shelf off California (USA) and in the Adriatic Sea (Traykovski et al., 2000, 2007).

Though isolated, sandy event beds seem to be conspicuously absent in the record of modern storm-dominated MDCs, the imprints of stormy conditions have been presumed in the record of ancient muddy shelves in the form of tempestite beds (e.g. Pedersen, 1985). Myrow and Southard (1996) identified three endmembers of tempestites according to sedimentary stratification and the presence of sole marks associated with different storm-related processes: wave action (isotropic hummocky cross-stratification), geostrophic current-induced bottom flow (low-angle current ripples), and gravity-driven density flow (shallow-water turbidites).

However, not all events are preserved as a depositional horizon and many of them become disturbed or eliminated after initial deposition. A useful concept in this context is that of the *preservation potential*, i.e. the likelihood that a particular sediment layer will escape total long-term disruption (Wheatcroft, 1990). A muddy bed is more likely to be preserved when its resistance to erosion increases quickly following deposition, or when it is buried by a subsequent sediment layer before it can be destroyed by an event of high bed shear stress (Wheatcroft et al., 2007). Examples of the high preservation potential of flood deposits include the Eel River margin (Sommerfield and Nittrouer, 1999) and the Waipaoa River, New Zealand (Carter et al., 2010). Systems with a low preservation potential are found in the Taiwan Strait (Milliman et al., 2007) and on the Washington shelf off the Elwha River (Eidam et al., 2019).

Fig. 2 shows a radiographic image from an MDC in a high-energy environment which contains different features corresponding to all of the three paradigms; laminated background sedimentation (*continuous supply*), flood layers (*episodic sedimentation*), and disturbed layers (*continual resuspension-deposition cycles*).

3. Controlling factors on mud depocenter formation

Two prerequisites of MDC development are a sufficient supply of fines to the coastal ocean, and a hydrodynamic situation which allows their accumulation on the shelf. This section aims to summarize current knowledge on the sources which deliver mud the coast, the mechanisms which disperse them on the shelf, and the conditions under which mud deposits on the seabed. These mechanisms are linked, wherever possible, to the paradigms introduced in Section 2.2.

3.1. Mud sources

While rivers are considered the dominant supplier of fines to the coastal ocean, aeolian and coast-erosional sources do contribute significantly in some settings. These sources often overlap in proximity to the coast and their roles may only become apparent through detailed provenance analyses. As McCave and Hall (2006) put it, "clearly there are some sources that do not produce gravel or coarse sand, but few that supply something fail to provide mud […]"

It is noteworthy that precipitates in the form of biogenic carbonate, silicate, and organic matter do contribute as secondary sources to MDC development (e.g. Nittrouer et al., 1988). Though the amount of carbonate-producing algae is generally limited in siliciclastic systems, some amount of production does occur alongside the terrigenous input (Mount, 1984; Milliman and Droxler, 1996), as may in-situ synthesis of clay minerals in the sediment (Michalopoulos and Aller, 1995; Holland, 2005). The description of these (minor) autochthonous and authigenic sources is, however, beyond the scope of this article.

3.1.1. Fluvial

Most studies of MDCs have focused on river-dominated margins, and this inclination is reflected in the classifications presented by McKee et al. (2004), Walsh and Nittrouer (2009), and Hanebuth et al. (2015). Indeed, most MDCs can be easily traced back to one or more riverine sources, often extending directly from the rivers' mouths. Though turbid river plumes seem impressive as seen from aerial images, their total load is small compared to near-bottom modes of suspended particle transport and their lateral extent often does not match the geographical location of depocenters (Geyer et al., 2004; Walsh and Nittrouer, 2009; Hanebuth et al., 2015). In a global survey of mudline depths at various river-dominated ocean margins, George and Hill (2008) found no strong correlation between the position of the mudline and the load of nearby rivers. Cross-shelf sediment transport of large river systems seems to be largely uncorrelated with the extent of the freshwater plume, as sediment is quickly lost from the plume and initially deposits near the river's mouth (e.g. Geyer et al., 2004; Nowacki et al., 2012; Pawlowicz et al., 2017).

According to Meade (1996), less than 5 % of the river sediment delivered to the global coastal ocean reach the deep sea; the vast majority becomes trapped in estuaries, floodplains and on the continental shelf. The exact apportionment of the proximally trapped sediment is

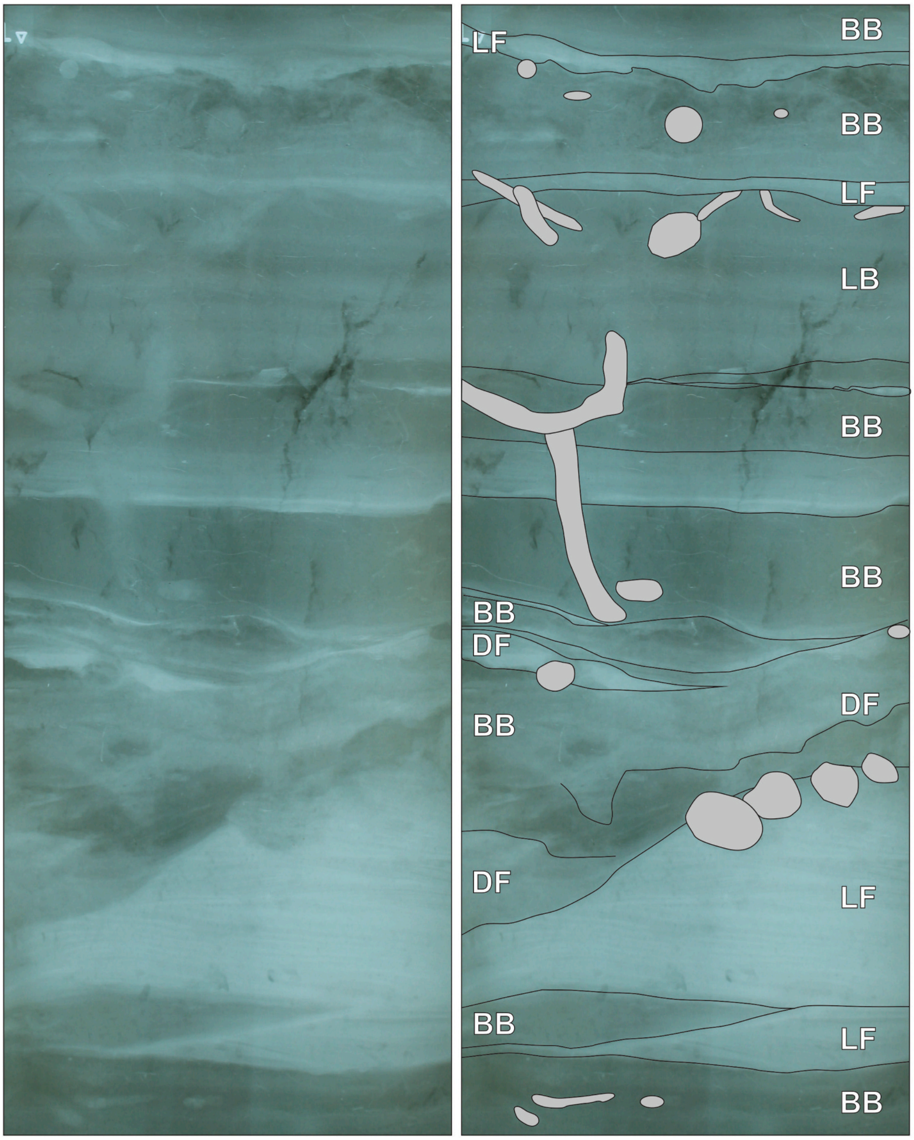

Fig. 2. Radiography of a proximal prodeltaic MDC (Guadalquivir River, Gulf of Cadiz, southern Spain). This section illustrates hemipelagic sedimentation (darker) interrupted by recurrent flood event layers (lighter). BB - bioturbated background sedimentation; LB - laminated background sedimentation; LF - laminated flood layer; DF - disturbed flood layer; gray ellipsoids - large burrows; dark, vertical (root-like) features: cracks in slab sample. Core GeoB 19520-2, 20 km off the river mouth, 20 m water depth, 320-345 cm sample depth, 11x25 cm image size, 0.7 cm slab thickness.

not known, as most sampling surveys and monitoring stations of rivers are located considerably far upstream of the rivers' mouths. However, some estimates for the amount of solids that escape the coastal zone have been compiled, and it is thought that this portion is dominated by fines (McCave, 2003). Beusen et al. (2005) estimated that 11,000-27,000 Mt/yr of total suspended solids are exported to coastal seas. These estimates are in fair agreement with those of Ludwig and Probst (1998) of 16,000 Mt/yr. Asia is by far the largest contributor (>50 %) with an estimated river export of 12,000 Mt/yr. Dürr et al. (2011) estimated that almost 9000 Mt/yr of the overall global solid discharge are particulate silica (lithic rock and mineral grains), amounting to roughly half of the total suspended solid fraction. Although nearly half of the sediments are delivered by the worlds 25 larges rivers (Milliman and Meade, 1983), Milliman and Syvitski (1992) first established the importance of small mountainous rivers for the delivery of large amounts of sediment to the global ocean. Usually found along active margins with steep topographic gradients, regions dominated by small mountainous rivers, such as the western side of North and South America, southern Europe, and southeastern Asia, exhibit high sediment yields compared to their small drainage basins, and are especially susceptible to events such as floods and mudslides.

Anthropogenic activity impacts riverine sediment discharge in two opposing ways. Increasing erosion due to overuse of land and river bank diking both promote sediment export, while reservoir damming suppresses it significantly by retaining a large amount of material. The amount of fluvial material that is retained by such reservoirs and thus withheld from the coastal ocean has been estimated to 50 % on average (Ouillon, 2018), though values of up to 95 % have been reported regionally (Vörösmarty et al., 2003; Yang et al., 2011). Though the global effects of sediment starving on delta shorelines seems to be limited thus far, the overall trend points toward the ultimate demise of many deltas by the combination of reduced fluvial supply and wave action (Anthony, 2015; Besset et al., 2019). This disequilibrium is perhaps most apparent in subaqueous delta systems, as found off the Yangtze (Yang et al., 2011), Mekong (Unverricht et al., 2013), Danube (Giosan, 2007), and Mississippi Rivers (Maloney et al., 2018). An impressive example was documented at the Minjiang River of southern China, where the subaqueous delta deposits recorded an acceleration followed by a collapse in sedimentation rates in response to increasing soil erosion and progressing dam construction, respectively (Ai-jun et al., 2020).

3.1.2. Aeolian

Airborne particles, including those generated due to wind-driven soil erosion and volcanic eruptions, are known to travel over remarkably large distances before settling (Grousset et al., 2003; Stuut et al., 2009; Van der Does et al., 2018). Yet, the potential role of dust input to the shelf sediment budget is not yet fully explored. Atmospheric dust plumes' contributions to MDC budgets are associated with great uncertainties regarding total mass due to their strong spatial diffusivity. For example, estimates for Saharan dust production vary widely, ranging from 130 to 460 Mt/yr (Swap et al., 1996), to up to 1400 Mt/yr (Ginoux et al., 2004).

Sand and coarse silt fractions tend to be carried through the atmosphere for relatively short durations (Stuut et al., 2009), though instances of their travel over several thousands of kms have been reported (van der Does et al., 2018). In contrast, fine silt and finer particles may be considered aerosols which, in extreme cases, traverse the entire globe before being washed out by precipitation (Grousset et al., 2003). Some success has been reported in distinguishing fluvial from aeolian inputs in deep sea settings using end-member analyses of grain sizes, where the aeolian fraction occupies the coarser end-member (e.g. Weltje and Prins, 2003; Holz et al., 2007). However, the ambiguities of such methods increase with closer proximity to the coast as the grain size signal becomes more heavily muddled. Aeolian fluxes to the shelf have been studied mainly in the context of paleoclimate to reconstruct past wind directions, distinguish material sources, or identify arid periods. Data from Nizou et al. (2011) suggest, for instance, that the quantity of material carried as dust plumes from the Sahelian and Saharan regions matches that of the fluvial runoff supplied to the MDCs off the coast of Senegal during arid periods. The authors used a combination of grain size and elemental distribution data to find suitable proxies for fluvial and aeolian material. Here, the fluvial fraction was both finer and contained a larger amounts of aluminum and iron. This contrasted previous studies which had used iron as a proxy for short-lasting dust outbreaks in the Mauritanian mud wedge (Hanebuth and Lantzsch, 2008; Hanebuth and Henrich, 2009). Such ambiguities highlight the difficulty in separating aeolian and fluvial material in an MDC.

Saharan dust was also recognized to contribute to MDCs in the Mediterranean (Martin et al., 1989; Stuut et al., 2009; Wu et al., 2016a) and on the Moroccan shelf (Summerhayes et al., 1976). In fact, Martin et al. (1989) estimated the volume of aeolian input to the same order of magnitude as that of all rivers discharging into the western Mediterranean. Aeolian input also contributes as a secondary source to the MDCs on the inner shelf of the East China Sea compared to the material discharge provided by the Yangtze River (Liu et al., 2014).

3.1.3. *Coast-erosional*

Another source mechanism that may supply fines to the coast is the physical erosion of consolidated coastal material. According to Young and Carilli (2019), cliffs comprise about 50 % of the world's coasts and they occur, in contrast to rivers, more commonly in mid- and high latitudes than in low-latitudes in both hemispheres. Strong storms and freeze-thaw-cycles are known to have strong impacts on mid- and high-latitude coasts, respectively (Davies and Clayton, 1980). As cliff erosion takes place primarily during storms, this mode of supply is often episodic and subject to strong temporal variability. The frequencies and intensities of storms are modulated by the regional climate, but erosion rates are also expected to increase with sea level rise (Dickson et al., 2007). For example, cliff retreat rates on parts of the Polish coast have almost tripled, from 0.55 to 1.49 m/yr on average, over the past decades compared to the previous century (Uścinowicz et al., 2004). At the same time, coastal protection measures combating cliffy shoreline retreat act to reduce erosion, but also hinder the supply of cliff-derived material towards offshore depocenters, by as much as 75 % in the case of the Norfolk Cliffs in the UK, for instance (Clayton, 1989).

Prémaillon et al. (2018) compiled a database of coastal cliff erosion rates from 1530 cliffs worldwide. Their statistical analysis concluded that lithology, specifically rock resistance, is the dominant predictor of erosion rate. Marine forcing such as wave height, leading to cliff undercutting and material out-washing, and climatic variables show a much smaller correlation with the rate of erosion. Somewhat surprisingly, the number of frost days is the only climatic variable that shows a significant positive correlation with erosion rates, while marine climate (such as wave forcing) exhibits a weaker influence.

Syvitski et al. (2003) estimated that about 400 Mt/yr of material erode from coastal cliffs globally, though this number is deemed particularly uncertain compared to their fluvial and aeolian counterparts. Although many studies have focused on the role of eroding cliffs in delivering sand to beaches and its alongshore transport, little is known about the transport and fate of the fine fractions supplied in this way. There has long been consensus that fines tend to be moved beyond the shoreface by subsequent winnowing of waves, such that horizontal gradients of hydrodynamic bottom energy are reflected the grain size gradients on the seabed (e.g. McCave, 1978; Swift and Thorne, 1992; Anthony and Aagaard, 2020). It seems, thus, indubitable that this material may become available for further transport and potential deposition in MDCs. Yet, potential connections of cliff erosion to MDC development have remained tentative.

For the southern Baltic Sea, about 90 % of the material stored in MDCs of the central basins was estimated to derive from erosion of soft cliffs in Germany and Poland (Gingele and Leipe, 2001). The overall regional riverine sediment discharge plays, in contrast, only a minor role. Similarly, sediment supply to the East Anglian coast is dominated by erosion of the chalk cliffs of Norfolk, Suffolk and Holderness in the UK (McCave, 1987), some of which may deposit in the mud patches in the North Sea (McCave, 1973; Dronkers et al., 1990).

Along the California coast, the situation is reversed, with rivers accounting for the bulk (90 %) of fines, while cliff erosion makes up about 10 % (Farnsworth and Warrick, 2007). Cliff erosion, nonetheless, might become locally significant: The contribution of cliff-supplied material is expected to close the budget of the mudbelt on the shelf off Santa Cruz and Davenport (Xu et al., 2002). A large amount of the silty offshore deposits comprises cliff-sourced material near Santa Monica (Limber et al., 2008). Because this material does not remain on the beach for long after initial erosion, it is reasonable to assume that it is transported cross-shore and contributes to the MDCs on the shelf. An extensive survey of the grain size composition of coastal cliffs of Southern California was carried out by Young et al. (2010), where fines comprise 23% of the cliff material on average. However, even the sand fraction does not necessarily remain on beaches entirely, as part of the fine sand bypasses the coastal zone and deposits offshore. In this context, a useful concept is that of the littoral cutoff diameter (Limber et al., 2008; Carlin et al., 2019), i.e. the minimum grain size that is retained on the beach, while grains smaller than this diameter travel farther offshore. This cutoff may be significantly larger than 63 μm (~125 μm at the Californian coast; Limber et al., 2008), which has important implications for the potential of cliff erosion to contribute to MDCs, as neglecting the grain size window between 63 μm and the littoral cutoff diameter underestimates the amount of sediment supplied to the offshore (by up to 124% in the case of Californian cliffs; Limber et al., 2008). In a sediment core from the Monterey Bay, Carlin et al. (2019) attributed higher amounts of sand in this grain size window to periods of enhanced cliff erosion by storms while sections lacking sand in this grain size window suggested periods of fewer storms. Notably, these trends were found to be independent of the total sand fraction within the muddy deposit. Thus, the amount of littoral sand found within an MDC seems to be a useful proxy for cliff material.

3.2. *Mud dispersal on continental shelves*

Following the delivery to the shallow coastal ocean, various hydrodynamic processes are responsible for the transport of fines across a continental shelf, and three particular types of processes have received much attention recently: gravity-driven flows, internal waves, and dynamics of hydrographic fronts. During the last century, material transport within the BBL in the form of dilute bottom nepheloid layers and their advection by bottom currents was identified as a highly effective dispersal mechanism of fines on continental shelves (Hill and McCave, 2001). Here, a *dilute* suspension is one of relatively low concentration (<1 g/l) in a bottom flow in which turbulence is fully developed. In natural conditions, turbulent mixing dominates at these concentration levels, and interactions of the suspension with flow dynamics (through self-stratification) and with itself (through particle-interactions) are usually not observed. Several occurrences of bottom nepheloid layers on the shelf associated with resuspension by atmospheric storms were reported during this time (e.g. Sternberg, 1986; Cacchione et al., 1990; Sherwood et al., 1994), showing the pervasiveness of recurring resuspension and transport events in shelf settings. On the mid-shelf mudbelt off of the Russian River in Northern California, storm-induced bottom currents are responsible for up to half of the total sediment flux (Drake and Cacchione, 1985). Sahl et al. (1987) attributed mud deposition on the Texas shelf to river-derived bottom nepheloid layers, which are maintained by riverine input, waves and currents in the nearshore, and by the action of internal waves on the outer shelf. Vitorino et al. (2002) observed bottom nepheloid layers several meters in thickness during storm conditions on the Portuguese shelf.

Although the concept of dilute near-bottom suspension is appealing as an analogy to the Rouse-like equilibrium suspension profiles common in open-channel flows, such as they occur in most rivers and estuaries, the focus of research has shifted towards modes of high-concentration near-bottom flows. Based on data from different coastal settings, Friedrichs et al. (2000) found that resuspension within the BBL may lead to a negative feedback loop, by which the density stratification induced by the suspension dampens turbulence, thus hindering additional resuspension. The resulting concentration remains nearly constant within the boundary layer, deviating markedly from the Rouse-like profiles expected under open-channel flow conditions.

3.2.1. Gravity-driven flow

Gravity-driven flows of sediment suspension are short lasting, thus episodic, events of high lateral flux. They form when the density of the near-bottom suspension is high enough with respect to the surrounding fluid that it moves down-gradient in the form of a fluid layer separated from the overlying water column as a result of gravitational acceleration. This phenomenon is well known from the continental slope and from submarine canyons, where steep bathymetric gradients (>0.7°) lead to auto-suspending flows and, ultimately, to the formation of turbidites (Bouma et al., 1985). These turbidity currents represent the primary conduit for the escaping of sediment from the shelf to the deep ocean, and considerable effort has been carried out recently to analyze the flow structures of such events and their corresponding deposits (e.g. Payo-Payo et al., 2017; Maier et al., 2019; Simmons et al., 2020). Although the continental shelf is generally not steep enough to allow for this form of auto-suspension, gravity-driven bottom flows have been shown to form on the shelf under the influence of wave- or current-enhanced near-bottom energy (Wright and Friedrichs, 2006), or in vicinity of a river mouth and along the submarine part of river deltas with high sediment loading, leading to hyperpycnal (negatively buoyant) conditions.

Three preconditions for gravity-driven flows to develop seem to be a high sediment concentration at the bottom, weak (ambient) onshore-directed currents, and a sufficiently steep slope (≲0.03°, Wright and Friedrichs, 2006). However, the precise combination of parameters required to trigger gravity-driven flows are not yet understood, because their episodic nature makes them difficult to observe directly, and the environments in which they have been observed often differ strongly from one another. The general trend of both in-situ and geological studies seems to point toward gravity-driven flows as a very common, if not ubiquitous phenomenon on continental shelves globally (e.g. Macquaker et al., 2010; Plint, 2014; Zhang et al., 2016; Denommee et al., 2016; Peng et al., 2020).

The occurrence of gravity-driven flows derived from river discharge was, for a long time, considered rare because the net buoyancy of the initially outflowing freshwater plume with respect to the receiving ocean waters is usually positive. Thus, extremely high sediments concentrations are required for hyperpycnal plumes to evolve at river mouth areas (>36 g/l, according to Mulder et al., 2003). Recent studies from the Elwha River dam-removal experiment in Washington State suggest that gravity flows are unlikely to form in tidally energetic systems and that the major mechanisms for transport are tidal current-induced bedload transport and river-plume advection (Eidam et al., 2016; Eidam et al., 2019). Those results highlight the limitations for forming hyperpycnal river plumes within tidally energetic systems, even in case of an extremely turbid river. In these systems, the traces of major sediment delivery events may, instead, be erased from the sedimentary record within weeks after material settling. Increasing evidence shows, however, that in environments with steep bathymetric gradients, gravity-driven flows do occur at considerably lower concentrations than previously thought (e.g. Parsons et al., 2001). In the Squamish Delta, Canada, Hage et al. (2019) observed a gravity flow at only 0.07 g/l which was triggered during a period of high water discharge which forced the turbidity maximum towards the steeper part of the delta. Similar conditions shortly after did not result in comparable gravity flow, the likely reason being that no more erodible mud was available to maintain the self-sustaining flow.

In shelf settings that are less steep, instead of forming directly from river efflux, gravity-driven flows may occur at a later stage, when settled material is being resuspended or kept in suspension temporarily by currents or waves. Conceptually predicted by Moore (1969) and confirmed by observations on the Amazon (Sternberg et al., 1996), Eel (Traykovski et al., 2000), and the Waipaoa (Walsh et al., 2014; Hale and Ogston, 2015) and Waiapu continental shelves in New Zealand (Ma et al., 2008), among others, wave- and current-enhanced sediment gravity flows have solved a contradiction that challenged traditional views of plume settling; Measurements on the Eel shelf indicated that rapid deposition of flood sediment occurs beneath the river plume in near-coastal waters, but long-term accumulation is centered on the mid-outer shelf (Sommerfield and Nittrouer, 1999; Wheatcroft and Borgeld, 2000). Here, wave-induced mobilization of the initial, muddy flood deposits and subsequent seaward density flow has been identified as the key mechanisms leading to cross-shelf transport. The majority of cross-shelf sediment flux is associated with a few major flood and storm events which occur over short time windows of just one to two weeks every few years. A comparable process has since been observed for the low-energy Adriatic shelf (Traykovski et al., 2007) and in several other geographic areas, as summarized by Wright and Friedrichs (2006).

To what extent gravity-driven flows play a role with regard to the net material budget of a late Holocene MDC is still unclear. For example, while Friedrichs and Scully (2007) have attributed the majority of the large flood deposit from the Po River to wave-enhanced gravity flows, Traykovski et al. (2007) have posited along-shore advection by mean currents to be the main transport mechanism.

In the rock record, "wave-modified turbidites" associated with wave-supported sediment gravity flows have been identified (Myrow et al., 2002; Lamb et al., 2008). Here, normal grading associated with decelerating flows are overprinted by hummocky cross-stratification due to waves. Reverse-to-normal grading occurs in some distal parts and point towards deposition under waxing-to-waning conditions which are common in sediment gravity flows. Lamb and Mohrig (2009) have shown in a model study that bedforms and sediment grading patterns in gravity flow deposits can record multiple episodes of flow waxing-waning pulses even during a simple single-peaked flooding event. Mulder et al. (2003) defined the "hyperpycnite" sequence as a "compound of a basal coarsening-up unit, deposited during the waxing period of discharge, and a top fining-up unit deposited during the waning period of discharge". Muddy hyperpycnites typically show distinct lamination with sharp, erosional contacts and little bioturbation, reflecting near-instantaneous sedimentation, in contrast to the gradual, hemipelagic settling of mud from suspension (Bhattacharya and MacEachern, 2009).

3.2.2. Internal waves and intermediate nepheloid layers

Internal waves play a crucial role within the paradigm of continual resuspension-deposition cycles. They are ubiquitous in stratified waters and they occur in a wide range of amplitudes and wavelengths (5-50 m and 0.5-15 km, respectively; Shanmugam, 2013). Interaction of internal waves with the seafloor can lead to resuspension of seabed sediment which may feed one or more intermediate nepheloid layers (INLs, e.g. McPhee-Shaw and Kunze, 2002). These layers of elevated sediment concentration are detached from the seafloor and spread seaward along isopycnals. Much attention has been directed toward resuspension by internal waves at the shelf break (as reviewed by McPhee-Shaw, 2006), where INLs often occur due to reflection and breaking of incoming open-ocean internal waves, which transport shelf sediment offshelf. Sediment resuspension by internal waves that form due to the hydraulic jump where a shelf current runs over the shelf edge has also been observed (Bogucki et al., 1997; Klymak and Moum, 2003; Bogucki et al., 2005; Quaresma et al., 2007). The mechanisms of resuspension and transport by internal waves were recently summarized by Boegman and Stastna (2019), but the full range of effects on MDC development is not yet fully understood.

The potential role of internal waves in MDC development is twofold: Firstly, winnowing of fines by incoming and shoaling internal waves provides a mechanism which constrains the seaward limit of an MDC, as found on the narrow, high-energy Iberian shelf (Zhang et al., 2019). Secondly, transport within INLs that are generated by an interaction of internal waves with the seabed may disperse mud laterally (McPhee-Shaw et al., 2004). When internal waves break due to a shallowing seabed topography, a short pulse of shoreward sediment transport (run-up) is followed by a prolonged phase of seaward transport (back-wash). While the net shoreward transport is mostly restricted to coarse-grained bedload material, fines are usually injected into the water column and transported offshelf within the INL (Sahl et al., 1987; Bourgault et al., 2014). Cheriton et al. (2014) have shown, however, that INLs caused by internal wave resuspension may also transport fines shoreward and, thus, add to MDC material accumulation.

Pomar et al. (2012) have suggested that internal waves are responsible for hummocky cross-stratification on the mid- and outer shelf below the maximum storm base. A conceptual facies model has been developed on the basis of an ancient carbonate ramp in order to distinguish the characteristics of such “internalites” from those of turbidites at the continental slope and tempestites in shallower areas (Bádenas et al., 2012). Though all three deposit types show a basal erosion surface and a subsequent depositional phase, internalites do not show the coarsening and thickening upward trend induced by differential settling in storm deposits. Furthermore, internalites thin out gradually to disappear in both up- and downdip directions.

3.2.3. Hydrographic front dynamics

The dynamics of oceanic fronts may encompass all of the aforementioned mechanisms, and both episodic and long-term stable fronts have been associated with MDC development. In a general sense, the term “front” describes a sharp lateral density contrasts between water masses, often marking a boundary to lateral fluxes. A front needs not be stationary, but can vary spatially with winds, tides, seasons, or over geological time intervals (e.g. Geyer et al., 2004; Bender et al., 2013).

Stable fronts, linked to the paradigm of continuous supply, have been characterized as traps for suspended matter on shelves (Geyer et al., 2004). The water column is often well-mixed on the shallow inner shelf due to highly turbulent conditions associated with river outflow, waves, and tides. This well-mixed zone transitions to a stratified marine environment in the frontal zone. As a mechanism analogous to estuarine sediment trapping, the phenomenon of frontal trapping due to flow convergence in the near-bottom layer leads to a high concentration of suspended mud in the frontal zone, which may deposit rapidly due to particle aggregation and water column self-stratification. For example, Castaing et al. (1999) have shown that the locations of thermohaline fronts coincide with the sites of patchy MDCs on the Gironde shelf during winter. The study documented a sharp decrease in bottom water turbidity beyond this front and postulated that the front acts as a permanent barrier to the seaward escape of fines. Interpreting the decrease of turbidity across the front as a decrease in U according to Eq. (1) explains the presence of these MDCs. Another example for a modern MDC under frontal control is the 1000 km long mudbelt extending from the mouth of the Yangtze River southward along the Chinese coast and into the Taiwan Strait. Liu et al. (2018) have identified a laterally dynamic, stratification-induced vertical oceanographic barrier as a key mechanism, which prevents suspended mud to escape seaward during winter . The hydrodynamics of the front result from an interplay of river plume and coastal currents, leading to isopycnals that prevent cross-shelf flow, confining the mud within the mud belt. Wang et al. (2019) have described a similar mechanism in the Yellow Sea: A seasonally shifting, vertical thermal front determines the lateral boundary of the MDC east of the Chinese Shandong Peninsula. Bi et al. (2010) explained the dispersion patterns of fines from the Yellow River by tidal shear forces that prevent transport of suspended fines beyond the shear front, mitigating transport to the submarine delta.

On the high-energy northwest Iberian shelf, a different type of frontal mechanism occurs, which is more episodic in nature. Here, storm-driven, downwelling-promoted thermohaline fronts limit the shoreward accumulation of the MDC (Zhang et al., 2016; Villacieros-Robineau et al., 2019). This phenomenon has been explained conceptually by Kämpf (2019), who showed that during episodes of coastal downwelling due to sustained strong winds, extreme bed shear stress at the shoreward side of an oceanic density front may erode the seabed as far as 20 km offshore. In a 2D numerical model experiment, downwelling-favorable winds induced a cross-shore circulation that mixed the nearshore waters, in turn shutting down the cross-shore circulation. This shutdown was accompanied by a strong along-shelf jet at the frontal zone between mixed and stratified waters, which extended downward to the seabed. The jet moved offshore with the front, essentially “plowing” the seabed. At the Dutch coast, Horner-Devine et al. (2017) described the mechanism of “frontal pumping” which transports fines resuspended by waves in the nearshore to the inner shelf. In this case, fronts occur in the form of fresh water lenses that emanate from the Rhine River and then propagate onshore and alongshore. During the passage of these fronts, a two-layer, counter-rotating velocity field associated with tidal straining develops, where the velocity is directed offshore in the bottom layer.

3.3. Settling and post-depositional alteration

Aside from the hydrodynamic mechanisms described above, the properties of mud itself and its modification by biological and human activity, both in suspension and at the seabed, have proven crucial when explaining MDC appearance. In contrast to sandy and coarser sediment, the cohesive nature of fines complicates the description of both vertical mud flux and post-settling processes (e.g. van Rijn, 1993; Winterwerp, 2011). These processes are of particular importance during the *rapid initial deposition* and *resuspension and transport* phases (stages 2 and 3 of the sedimentation process described by Wright and Nittrouer, 1995). It is this timeframe which, to a large extent, determines the long-term preservation potential of newly formed mud layers. An excellent summary of mud settling and resuspension mechanisms was given by Winterwerp (2011), and the effects of biota on sediment transport processes were reviewed by Andersen and Pejrup (2011).

3.3.1. Cohesive properties

A distinction has been made between silt particles smaller and larger than 10 μm (McCave et al., 1995; Chang et al., 2006). Around this size, a transition is thought to occur between cohesive and non-cohesive behavior. The finer sized particles (<10 μm) settle and erode as aggregates, while the coarser silt size (10-63 μm) has been termed "sortable silt", allowing its applicability as a paleo-current proxy in deep-sea deposits (McCave et al., 1995). This approach has not been established for MDCs, where primary productivity and, thus, the effect of aggregation is potentially larger than in the deep sea. For example, erosion experiments by Law et al. (2008) using sediment samples from the Gulf of Lions pointed to a size cutoff for non-cohesive behavior, i.e. "sortability", at 16 μm. Most of our knowledge of the cohesive and rheological properties of natural muds stem from studies in mud flats, estuaries, and embayments, but the cohesive properties of those nearshore sediments may differ strongly from those of mid- and outer shelf MDCs. Fettweis and Lee (2017), for example found a strong increase in aggregate sizes and porosities from the nearshore to the offshore in the North Sea. Overall, little consensus seems to have been achieved regarding the general description of cohesive mud properties.

Fines tend to collide into aggregates which can be many times larger than the individual particles. The maximum diameter of aggregates is thought to be limited to the local microscale of turbulence, which usually does not exceed 1 mm in coastal and shelf seas (e.g. Fettweis et al., 2006; van der Lee et al., 2009). Aggregation occurs both in the form of coagulation (also termed "salt flocculation"; Eisma, 1986; Wolanski and Gibbs, 1995) due to attractive forces inherent to clay mineral grains in a saline environment, and in the form of flocculation, resulting from the binding of sediment components by sticky extracellular polymeric substances (EPS), which are excreted by fungi, bacteria, and plankton (Grabowski et al., 2011; Tourney and Ngwenya, 2014). Both flocculation and coagulation may take place simultaneously and are therefore difficult to discern even in a laboratory setting. However, studies of estuarine sediments have suggested that, whenever a substantial amount of organic matter is present, biogenic flocculation is the dominant process over coagulation (Andersen and Pejrup, 2011), and a robust correlation seems to exist between maximal floc size and the ratio of algae concentration and to sediment concentration (Fettweis and Lee, 2017; Deng et al., 2019).

The main effect of aggregation of particles on sediment transport is accelerated sinking of the aggregates compared to that of individual grains. The difference in effective sinking velocity may span orders of magnitude, for instance, few mm/s for an aggregate versus 0.01 mm/s for a single clay particle under quiescent conditions. It is, thus, not surprising that aggregation is considered a major and indispensable controlling factor in the development of MDCs (Hill et al., 2007). Enhanced deposition due to aggregation has been evoked to explain the appearance of different kinds of river-fed MDCs around the world. Examples include the wide, supply-rich, high-energy Amazon shelf (Cacchione et al., 1995), the narrow, low-supply, event-dominated Eel shelf (Hill et al., 2000), and the epicontinental, sediment-starved, low-energy Po-shelf (Fox et al., 2004; Milligan et al., 2007). Accelerated sinking of aggregates does not, however, necessarily lead to equally enhanced deposition. This discrepancy is due to the secondary breakup of aggregates at increasing shear stress near the seabed (Dyer, 1989; Manning and Dyer, 2002). Thus, while aggregation can encourage mud deposition by rapid deposition directly off a river mouth, it may also enhance the development of a highly concentrated bottom layer, which may convey the material further offshore.

The collision and interaction of particles with each other within a high-density fluid transport medium generally leads to a decrease in particle sinking speed. This phenomenon is referred to as *hindered settling*, and its effect enhances with increasing suspended particle concentration. In the case of cohesive particles, aggregation and hindered settling take place simultaneously. At low particle concentrations, aggregation is the dominant effect over hindered settling, resulting in a net downward acceleration in particle sinking. At concentrations of a few g/l, hindered settling overpowers the aggregation effect, leading to a net deceleration in sinking (Fig. 3; Winterwerp, 2002). A conceptual model of Kämpf and Myrow (2014) revealed that for a given shear stress, mud suspensions of both low and high concentrations remain in suspension more easily than those of intermediate concentrations as a direct result of the hindered settling effect. This represents a possible mechanism for the development of high-concentration suspensions that travel downslope as a gravity-driven flows (section 3.2.1). Conversely, self-stratification of the suspension hinders turbulent mixing, creating a positive feedback that may lead to a collapse of the suspension. In the absence of significant turbulent mixing, the result is a highly concentrated bottom layer that allows for rapid settling. A one-dimensional model by Winterwerp (2001) predicted that above a certain saturation concentration of the suspension, the concentration profile will quickly collapse into a thin fluid mud bottom layer. This behavior is remarkably similar to the dampened turbulence induced by self-stratification observed in coastal zones by Friedrichs et al. (2000; see Section 3.2). In both cases, a stability criterion involving density stratification and vertical turbulence is evoked, the ratio of which (i.e. Richardson number) determines whether a stably stratified near-bed layer may develop.

Along with aggregation, consolidation, i.e. the compaction and strengthening of a deposit with time by expulsion of pore water, is a key characteristic of mud that limit its offshelf transport. In fact, modeling studies by Harris and Wiberg (2002) have suggested that, without these two mechanisms, all mud would eventually be removed from the shelf. The general effect of consolidation is both lowering the height of the seabed and increasing substrate resistance to erosion with time. The latter is especially significant in those high-energy settings in which short-term events dominate the sediment supply. In those settings, the time between deposition and development of sufficient shear strength determines whether a deposit will remain in place or whether it will be remobilized during the next episode of high bottom shear stress. The stabilizing effect of cohesion on the sediment architecture in an energetic setting was demonstrated by experiments of Straub et al. (2015): Compared to the non-cohesive case, the cohesive experiment exhibited significantly higher variability in overall relief. The most apparent natural display of this effect is found in deltas, which develop deep, avulsing channels. The reason for the high lateral variability is that cohesion increases the maximum steepness that can be sustained across a landscape. Wherever bottom currents influence an MDC's surface, one can therefore expect higher lateral variability in thickness compared to a

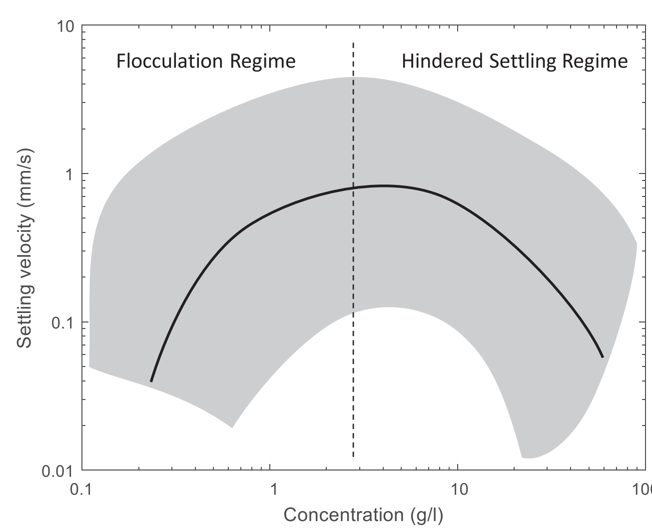

Fig. 3. Conceptual diagram of the relationship between suspended sediment concentration and settling velocity (solid black line). For concentrations below 2-3 g/l, settling velocity increases with higher concentration due to flocculation. Above that concentration, particle interactions with each other decrease the settling velocity. The shaded area encloses data sets of estuarine mud flocs compiled by Winterwerp (2002).

sandy deposit in an equivalent settings.

Aside from strengthening through self-weight consolidation alone, the role of biota in altering the resistance of mud to erosion has received increasing attention over recent decades (e.g. Le Hir et al., 2007; Andersen and Pejrup, 2011). Remarkably low contents of clay and EPS are found to dramatically alter the deposit response to particle mobilization. Field studies by Lichtman et al. (2018) found that an increase in EPS content up to 0.05 % drastically lowers the material transport rate compared to clean sand substrate. Besides microalgae, it has been recognized that secondary production of EPS by heterotrophic bacteria assemblages, which are ubiquitous in muds, contribute to biostabilization (Gerbersdorf and Wieprecht, 2015). Valentine et al. (2014) and Valentine and Mariotti (2020) studied the effect of biofilms on deposit erodibility and found that the presence of a biofilm always reduces erodibility at low shear strengths (~0.1 Pa), while only a "mature" biofilm (>3 weeks old) reduces erodibility at moderate shear strength (~0.4 Pa). Notably, this effect seems to overpower that of material consolidation by pore water expulsion on timescales of a few weeks.

As opposed to the stabilizing effect of microbenthos, macrobenthos generally has a destabilizing effect: Its physical presence enhances seabed roughness, sometimes by an order of magnitude compared to a smooth muddy seabed (Pope et al., 2006), leading to enhanced near-bottom turbulence. Bioturbation through burrowing further increases erodibility, either by reducing shear strength, or through direct bioresuspension (Le Hir et al., 2007). It has also been proposed that enhanced permeability created by burrows and tubes directly promotes sediment dewatering and, thus, can accelerate consolidation (Richardson et al., 2002).

Typical values for the critical shear stress of soft beds lie in the range of 0.1-5 Pa (Winterwerp et al., 2012), depending on its state of consolidation, though much smaller and much larger values are possible for freshly deposited and well-consolidated muds, respectively. Thompson et al. (2019), for example, measured critical shear stresses as low as 0.02 Pa at muddy sites in the Celtic Sea. Based on extensive in-situ erosion measurements, they parametrized critical shear stress with a range of sediment characteristics (organic carbon and bulk density, sorting, kurtosis, porosity, percentage fines and chlorophyll a concentration). Though the resulting model fits the data well (R^2=0.99), the authors concluded that generalized predictions of critical erosion thresholds from sediment properties are not yet possible and that instead, localized parametrizations are still necessary. One reason for this is that the stress history, i.e. the history of resuspension, swelling, and consolidation phases is not captured by these parametrizations. In this light, a period of "high preservation" seems just as important for mud accumulation as a period of high sediment flux, as pointed out by Paola et al. (2018).

3.3.2. Bottom trawling

As a common, often chronic anthropogenic contribution, resuspension by the fishing practice of bottom trawling is a dominant erosion mechanism on many MDCs (Oberle et al., 2018). The deployment of heavy gear pulled over the seafloor disturbs the upper few cm to dm of the seabed, frequently resuspending a large amount of fines.

According to Amoroso et al. (2018), 14 % of the continental shelf and slope regions worldwide are affected by bottom trawling, reaching >50 % in some European seas. Oberle et al. (2016a) estimated a total of 21,870 Mt/yr of sediment is resuspended globally in this way, which is at the same order of magnitude as the global riverine supply. Mengual et al. (2016) linked a 30 % decrease in mud content in the seabed deposits of the Bay of Biscay since 1967 to intense bottom trawling. Similarly, Palanques et al. (2014) found an artificial coarsening-upward trend within the uppermost 20 cm of the muddy Ebro prodelta. Puig et al. (2015) described redeposition of mud from the flanks of a canyon in the NW Mediterranean, forming a new depocenter along the canyon's deeper axis. Some attempts have been made to quantify the net effect of off-shelf export of fines caused by chronic bottom trawling. On the NW Iberian shelf, Oberle et al. (2016a) calculated a six-fold increase in off-shelf sediment transport due to bottom trawling compared to natural (storm-driven) conditions, assuming all recurrently resuspended fines are eventually advected into the deep ocean. Churchill (1989) estimated that bottom trawling is responsible for about 10 % of the resuspended mud in the New England Mud Patch. Applying a simple model that assumes constant off-shelf directed current velocity, he concluded that bottom trawling does not seem to cause significant net erosion. Similarly, Ferré et al. (2008) posed that trawling-induced resuspension contributed a few percent to the total export of fines on the Gulf of Lions shelf.

From these examples, it seems that fate of fines resuspended by bottom trawling depends largely on the strength and direction of bottom currents prevailing during and after resuspension in the trawled area. In any case, bottom trawling imparts a significant signal onto the sub-recent record of MDCs, which may manifest as material contortion, homogenization, winnowing, and re-sorting of the preexisting near-surface stratigraphy, including organism disturbance, substrate ventilation, and nutrient recirculation (Oberle et al., 2016b).

3.4. Numerical modeling of mud sedimentation processes

During the past decades, numerous numerical models have been developed to describe sedimentation processes of mud in estuarine and coastal shelf environments (e.g. Scully et al., 2003; Harris et al., 2005; Neumeier et al., 2008; Hsu et al., 2009; Bourgault et al., 2014; Zhang et al., 2016, 2019). They have proven indispensable tools in comprehending the influences of short-term hydrodynamic processes on MDC development. A survey of such models was conducted by Amoudry and Souza (2011), who summarized that the predictive ability of regional sediment transport models was limited by inadequate parametrizations of several important processes, including erosion, flocculation, consolidation, and biological effects. We find many of the general shortcomings laid out by those authors to still be valid today.

Process-based models of mud transport and dynamics fall into two categories: 1) high-resolution (10^{-2}-10^{0} m scale) one-dimensional or two-dimensional vertical models (1DV or 2DV), and 2) coarse-resolution (10^{1}-10^{3} m scale) three-dimensional (3D) models. Models of the first category directly resolve two- (or multi-) layer flow where an inviscid water layer overlays a mud layer with specific rheological properties (e.g. Longo, 2005; Hsu et al., 2009; Amoudry and Liu, 2010; Espath et al., 2014). The limitation to one- or two-dimensional vertical planes allows resolving a detailed interaction between turbulence and mud by the use of Direct Numerical Simulation (DNS) or Large-Eddy Simulation (LES) approaches (e.g. Hu et al., 2012; Deng et al., 2017). The theoretical soundness and satisfactory performance of these models in capturing small-scale physical interactions between fluid and mud has been demonstrated for various flow conditions in laboratory in settling tank and open channel experiments (e.g. Chauchat et al., 2013). However, the expensive computational cost of such models often impedes their use for studying large-scale coastal MDC dynamics.

Models of the second category are often called "coastal ocean sediment transport models", which are meant to capture the transitional nature of sediment dynamics between coastal shelf environments and deep ocean (Kirby, 2017; Fringer et al., 2019). Coastal ocean models must be able to simulate both highly frictional, ageostrophic motions governing sediment dynamics in estuaries and coastal shelf seas and the dispersal of fine particles across shelf towards the open ocean. These models are normally discretized at a scale (10^{1}-10^{3} m in space and 10^{0}-10^{2} s in time, Warner et al., 2008; Syvitski et al., 2010; Zhang et al., 2018; Fringer et al., 2019) that is much larger than the one on which turbulence, sediment particle-particle interactions and particle-fluid interactions occur (10^{-2}-10^{0} m in space and 10^{-2}-10^{0} s in time). Therefore, the small-scale processes have to be either solved by sub-grid modeling or simplified by empirical formulae (Zhang, 2016). Coastal ocean sediment transport models treat sediment as a continuum rather than individual particles and assume that suspended sediment particles effectively follow the water flow and their concentration is small enough (normally less than 1 g/l) to ignore particle-particle interactions. The presence of sediment in a spatial unit is in this case represented by a concentration value. By integrating a mass balance equation of sediment into the Reynolds-Averaged Navier-Stokes equations of water flow, coastal ocean models have the capability to resolve sediment transport and deposition on continental shelves to the first order of approximation (Amoudry and Souza, 2011).

Most coastal-ocean sediment-transport models divide sediment into two or multiple grain size classes to consider contrasting transport modes regarding a specific particle size distribution (e.g. Warner et al., 2008; Erikson et al., 2013; van Maren and Cronin, 2016; Kirby, 2017). In almost all existing models, the modeling of sand and mud classes is still separated assuming that these different classes do not influence or interact with each other in the water column (Warner et al., 2008; van Maren and Cronin, 2016; Kirby, 2017; Sherwood et al., 2018; Delft3D-Flow, 2020). Their interactions are considered only for a thin layer (normally within a few cm) near the seabed in the case of high sediment concentration (>10 g/l) that may significantly affect settling (e.g. through hindered settling) and resuspension (Styles and Glenn, 2000; Zhang et al., 2016).

Parameterization of the settling velocity of mud is particularly important in coastal shelf seas where mud is transported mainly in the form of aggregates (Winterwerp, 2011; Soulsby et al., 2013). Aggregation and break-up of mud poses a great challenge in modeling using the multiple grain size division approach because the variation of floc size changes with environmental factors such as turbulence shear and stratification (Zhang et al., 2020). By now, no coastal ocean model explicitly couples a biological model with a sediment transport model to account for mud flocculation and de-flocculation. Instead, a common method is to ignore flocculation parameterizations and assume static floc sizes with behavior that is essentially tuned to match observations (Soulsby et al., 2013; Fringer et al., 2019). The difficulty of achieving a flocculation model which matches observations is illustrated by the model of Soulsby et al. (2013): Their formulas for sinking velocities of macro- and microflocs include a total of eleven tunable parameters, the calibration of which requires an extensive experimental dataset. Spearman and Roberts (2002) concluded from an inter-comparison of different flocculation models with field data that adding complexity to flocculation models does not necessarily improve their performance, and that a simple power law model, or even a fixed (mean) settling velocity, often produce the most accurate results.

Diaz et al. (2020) recently demonstrated the high sensitivity of simulated mud fluxes on settling and erosion parameterizations. Using a numerical model of the Gironde estuary an adjacent shelf which was extensively calibrated against near-surface sediment concentrations in the estuary, they showed that vastly different sediment parametrizations could reproduce the measured near-surface sediment concentrations with similar skill. Meanwhile, uncertainties of residual mud fluxes among the model runs using different parameter sets reached up to 93 %. This shows the importance of near-bottom measurements of suspended sediment for validating numerical models in order to mitigate uncertainties associated with equifinal parameter sets.

The realistic modeling of the consolidation process of soft mud is critical for a quantitative modeling of MDC development. While some approaches deal exclusively with reduction of porosity and the associated subsiding of the bed (e.g. Toorman, 1999; Merckelbach and Kranenburg, 2004), others focus on the increase of critical shear stress for erosion with time and with depth below the seabed surface (e.g. Sanford, 2008). An approach where both effects are treated simultaneously was implemented by Le Hir et al. (2011), who related shear strength to relative mud mass concentration through a simple power law. It may be argued that within MDC modeling, the evolution of critical shear stress is of far greater concern than the evolution of bed height, as even a pluricentimetric subsidence of a bed due to consolidation will not substantially alter the hydrodynamics in water depths of several meters or more. In fact, both a coastal ocean model's vertical grid spacing and uncertainties in the model bathymetry are usually far greater than the consolidation effect on the timescales covered by such models.

Some of the most important processes for mud transport and deposition occur near the seabed, as described above. However, the bottom-closest layer in coastal ocean models is normally too thick to resolve these processes, in particular wave-supported sediment gravity flow, which is confined to the wave boundary layer that is limited to not more than 20 cm above seafloor (Zhang et al., 2016). To bridge the gap in a model between the seafloor and the bottom-most grid point (which is normally higher than a few tens of centimeter above the seafloor), parameterizations of the BBL are used in coastal ocean models. The classic theory describing the BBL under the combined effects of currents and surface gravity waves by Grant and Madsen (1979) was later extended to include the effect of sediment-induced stratification in the near-bottom water column (e.g. Glenn and Grant, 1987; Styles and Glenn, 2000). Application of BBL parameterization taking into account the effect of sediment-induced stratification of the wave boundary layer proved helpful in modeling the development of coastal shelf mud deposits (e.g. Wang, 2002; Zhang et al., 2016). To account for the transport of gravity-driven sediment flows (e.g. fluid muds or wave-supported sediment gravity flows) on the seafloor in coastal ocean models, either two-layer approaches resolving the Reynolds-averaged fluid mud transport in the BBL (e.g. Hsu et al., 2009) or simplified formulations by the use of gradient Richardson number and buoyancy anomaly across the lutocline to approximate the transport velocity of gravity-driven sediment flows (Scully et al., 2003; Harris et al., 2005; Wright and Friedrichs, 2006; Zhang et al., 2016; Zang et al., 2020) have been applied. Though these models are not able to represent the internal structure of the flow, they were able to predict the positions of gravity-flow deposits with good accuracy.

Most coastal ocean sediment transport models are based on the hydrostatic primitive equations under the Boussinesq approximation – a valid approximation for mesoscale and submesoscale (≥1 km) water motions which have a horizontal scale much larger than its vertical scale (Marshall et al., 1997). However, non-hydrostatic pressure becomes important when water motions that are much smaller than the local water depth have significant impact on sediment transport (Quaresma et al., 2007; Masunaga et al., 2017; Shi et al., 2017; Zhang et al., 2019). These motions include internal solitary waves, oceanic fronts, tidal bores, convective overturning, and water flow over short-wavelength bedforms such as dunes and ripples. Resolving such processes in coastal shelf seas is computationally expensive because it requires very high resolution in both time (second-scale) and space (meter-scale), which often impedes the use of 3D coastal ocean sediment transport models for studying mud dispersal associated with these fine-scale processes (Fringer et al., 2019). Nevertheless, 2D versions of non-hydrostatic coastal ocean models using a cross-shelf vertical plane and neglecting along-shelf variations proved useful in understanding mud dispersal by single processes such as internal solitary waves (Masunaga et al., 2017).

Although process-based coastal ocean models are robust in capturing sediment transport and deposition/erosion patterns on short time scales such as days and months, direct application of these models to longer-term (decadal-to-millennial scale) is severely restricted and they can hardly perform better than behavior-oriented models built on assumptions of morphological equilibrium or quasi-equilibrium in response to certain driving forces (Zhang et al., 2012; French et al., 2016). Exclusion of the impacts of stochastic extreme climatic events (storms and floods), system self-organization and biophysical factors in process-based models often leads to results that systematically deviate from observations (e.g. Zhang et al., 2010). Hybrid models, which combine the advantages of process-based modeling (for mechanisms that can be both mathematically and physically well described) and behavior-oriented formulations (for less-known intrinsic self-organization, morphological equilibrium and biological impacts), seem to be the best choice for modeling long-term development of complex coastal sedimentary systems including MDCs (Roelvink, 2006; Brown and Davies, 2009; Zhang et al., 2014; French et al., 2016). Nevertheless, the development of such models is in a very early stage and there is still lack of consensus on tackling the difficulty in upscaling, coupling, localization, thresholds, scale invariance and interwoven biology and geochemistry (Syvitski et al., 2010).

4. Discussion and conclusions

Many of the tasks facing MDC research relate to the ubiquitous scale problem in sedimentary geology: Modern subaqueous deposits lack signatures induced by low-order effects such as climatic variations and tectonics, which usually dominate ancient strata, while in-situ and laboratory studies tend to be biased towards individual, high-flux events. Therefore, any comparison of ancient geological records, modern soft-sediment deposits, and in-situ/laboratory monitoring and experiments faces a fundamental difficulty. This disparity has been summarized by Woodroffe and Murray-Wallace (2012): "*Coastal scientists presently have a relatively good understanding of coastal behavior at millennial timescales, and process operation at contemporary timescale. However, there is less certainty about how coasts [and continental shelves] change on decadal to century timescales*". Particularly the relationship of individual events occurring in periods of minutes to weeks with multidecadal patterns remains an open challenge. This issue was raised some time ago by Dott (1983, 1996) and expanded on recently by Miall (2015) and Paola et al. (2018), who surmised that the rare events that lead to long-term preservation of a deposit are not catastrophic transport events but short-lived intervals of rapid deposition that trap the background sedimentation.

The three paradigms of MDC development – *continuous supply, continual resuspension-deposition cycles*, and *episodic erosion and sedimentation events* (Section 2.2) – offer alternative explanations for the development dynamics of MDCs, and specifically for the occurrence and thickness of individual strata within MDCs. The disparity of timescales of oceanographic versus geological approaches makes it challenging to reach a conclusion about the validity of each of the paradigms regarding a specific MDC. In general, high-flux processes that influence an MDC's morphology, such as gravity flows, occur locally, while stable hydrographic fronts influence regional scales. On timescales longer than those on which episodic events and bedform-scale perturbations take place, depositional processes are implicitly time-averaged, and U in Eq. (1) represents the steady-state, or residual flux. In contrast, an equilibrium is seldom observed on time-scales on which the lateral flux of fines is dominated by individual events, where $|\boldsymbol{U}'| \gtrsim |\overline{\boldsymbol{U}}|$ (Zhou et al., 2017). Thus, the extent to which perturbations effect the morphology depends upon frequency and amplitude of U', which are correlated with the environmental statistics (e.g. frequency and intensity of storms and floods, or biological activity). In relatively calm settings with low supply of fines, $|\boldsymbol{U}'| \ll |\overline{\boldsymbol{U}}|$ and the overall extent and geometry of an MDC may be reasonably represented by the conceptualization of dynamic equilibrium driven by hemipelagic settling and mean current patterns. In high-supply and high-energy settings, events and perturbations become important for explaining the overall geometry and extent of a MDC. In both cases, fluctuations of U' influence small-scale shape variations as well and individual laminae within the record. This treatment is in line with that of Nittrouer and Sternberg (1981), who tackled the problem of strata development by considering the ratio of vertical mixing rate to accumulation rate. As this ratio increases, structures become less distinct and strata become more homogeneous. The variability of strata preserved through time is controlled by the relationship between the residence time of particles within the surface mixed layer and the natural cyclic period of sedimentation, i.e. the time after which extreme flood or storm depositional products are averaged out (in the range of 10^0-10^2 yrs, Curray et al., 1964). An important consequence of the former two paradigms (*continuous supply* and *continual resuspension-deposition cycles)* is that an MDC will tend to deteriorate when sediment supply decreases (Hanebuth et al., 2015). The reason is that, assuming other environmental factors remain unchanged, a decrease in $\overline{\boldsymbol{U}}$ from the landward side of an MDC will lead to a decrease in $\nabla \cdot \boldsymbol{U}$ on the seaward side. This connection is not necessarily true for the third paradigm (*episodic erosion and sedimentation*); for example, flood deposits may accrete even when the mean sediment supply decreases.

Three general conclusions may be drawn regarding MDC development:

1. Episodic, high-flux events are highly likely to influence MDC development in a range of oceanographic settings.
2. The three paradigms of MDC development – continuous supply, continual resuspension-deposition cycles, and episodic erosion and sedimentation - may be partially reconciled by consideration of various spatial and temporal scales on which the sedimentary processes take place.
3. The relative contributions of episodic events to long-term MDC development is not known for many systems.

Since the introduction of the *mudline* as the shoreward limit of muddy deposition on the continental margin, considerable progress has elucidated those processes responsible for moving fines from the sediment source along- and cross-shore. For fines, the shear stress threshold for initiation of motion is close to that of resuspension. For this reason, fines have commonly been treated as either suspended or settled, and bedload transport by rolling/saltation such as observed in sand is typically not associated with fines. However, researchers have become increasingly aware that in many settings, energetic modes of near-bottom transport are the dominant dispersal mechanism for fines. Among the recent developments in explaining the appearance of MDCs, five discoveries stand out:

The mechanism of *wave- or current-enhanced sediment gravity flow* explained why some MDCs are located considerably further offshore than would result from plume advection alone. Similarly, episodic, *storm-generated density fronts* associated with strong bottom shear stress have been shown to keep the inner shelf free of mud. By contrast, the seaward limit of mud deposition has remained more elusive. To this end, resuspension by *internal waves* and shielding of deposits by lateral density gradients associated with *stable density fronts* have been identified as processes which increase and decrease, respectively, the seaward extension of MDCs. The observation that mud can accrete through *bedload-deposition of fines* showed that MDCs may develop in environments which are more energetic than commonly assumed and offered some explanation of mm-scale laminae found within many recent and ancient deposits. Finally, the impact of *chronic bottom trawling* on many MDCs has been shown to significantly enhance off-shelf transport and rework the top few dm of the seabed. Relevant processes discussed in this review are summarized in Fig. 4.

Though numerical modeling was proven to be an indispensable tool for the study of MDC dynamics, the implementations of morphodynamic processes into 3D coastal circulation models continue to lag behind their hydrodynamic counterparts (Fringer et al., 2019). Discrepancies between predictions and measurements of one order of magnitude remain common for near-bed sediment concentration and suspended-load transport, making further improvement on parametrizations of muddy transport processes necessary. In addition, many of the parametrizations developed for the processes of erosion, settling, and consolidation were realized using mud samples taken from to estuaries, bays, or mudflats. The applicability of those coastal parametrizations to those offshore settings, where most MDCs are found, is yet to be demonstrated. This effort would likely contribute to the solution of the aforementioned timescale problem; for example, a more sophisticated parametrization of

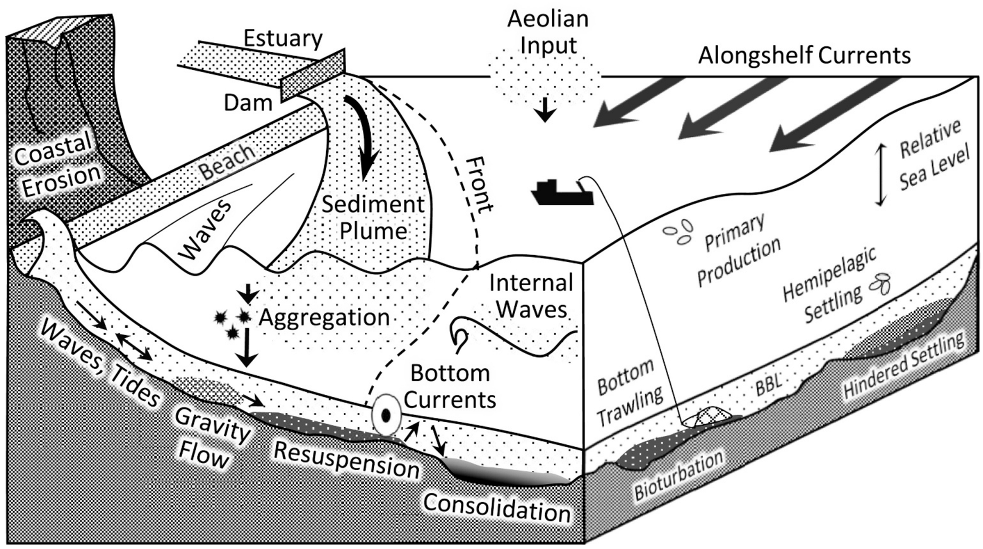

Fig. 4. Conceptual diagram illustrating the major source-to-sink processes influencing MDC development. Modified after Nittrouer and Wright (1994).

material consolidation at the seabed should be able to predict whether a deposited sediment layer will lastingly remain in place or be destroyed during one of the following erosive events. Applying high-resolution, process-based models to long-term morphological changes also represents a challenge due to limits in computational resources. A compromise between model accuracy and computational cost may be achieved by reducing processes to their main driving terms on the scale of interest while omitting or averaging small-scale processes. The obvious drawback of this approach is that it requires a priori knowledge of the significant mechanisms, determining the contribution of which is usually the objective of a modeling study. Another common method is the use of a morphological acceleration factor to speed up the adjustment of landscapes to hydrodynamic forcing. For large acceleration factors or strong forcing, this approach may lead to issues with stability and accuracy of predicted bed levels, when nonlinearities in the hydrodynamic response occur (Jones et al., 2007).

Bridging the gap between short-term processes and long-term accumulation patterns through the identification of morphological equilibrium–disequilibrium cycles is the key towards a more complete understanding of sedimentation at and around MDCs.

Data statement

No data was used in the preparation of this article.

Declaration of Competing Interest

The authors declare that they have no known competing financial interests or personal relationships that could have appeared to influence the work reported in this paper.

Acknowledgements

This study is a contribution by the Helmholtz Association through the PACES II program. W. Zhang acknowledges the support from the I^{2}B project "Unravelling the linkages between benthic biological functioning, biogeochemistry and coastal morphodynamics – from big data to mechanistic modeling" funded by Helmholtz-Zentrum Geesthacht. We thank two anonymous reviewers for their detailed comments which helped to improve this manuscript.

References

Ai-jun, W., Xiang, Y., Zhen-kun, L., Liang, W., Jing, L., 2020. Response of sedimentation processes in the Minjiang River subaqueous delta to anthropogenic activities in the river basin. Estuar. Coast. Shelf Sci. 232, 106484. https://doi.org/10.1016/j.ecss.2019.106484.

Amoroso, R.O., Pitcher, C.R., Rijnsdorp, A.D., McConnaughey, R.A., Parma, A.M., Suuronen, P., Eigaard, O.R., Bastardie, F., Hintzen, N.T., Althaus, F., Baird, S.J., Black, J., Buhl-Mortensen, L., Campbell, A.B., Catarino, R., Collie, J., Cowan, J.H., Durholtz, D., Engstrom, N., Fairweather, T.P., Fock, H.O., Ford, R., Gálvez, P.A., Gerritsen, H., Góngora, M.E., González, J.A., Hiddink, J.G., Hughes, K.M., Intelmann, S.S., Jenkins, C., Jonsson, P., Kainge, P., Kangas, M., Kathena, J.N., Kavadas, S., Leslie, R.W., Lewis, S.G., Lundy, M., Makin, D., Martin, J., Mazor, T., Gonzalez-Mirelis, G., Newman, S.J., Papadopoulou, N., Posen, P.E., Rochester, W., Russo, T., Sala, A., Semmens, J.M., Silva, C., Tsolos, A., Vanelslander, B., Wakefield, C.B., Wood, B.A., Hilborn, R., Kaiser, M.J., Jennings, S., 2018. Bottom trawl fishing footprints on the world's continental shelves. Proc. Natl. Acad. Sci. U. S. A. 115, E10275 https://doi.org/10.1073/pnas.1802379115.

Amoudry, L.O., Liu, P.L.-F., 2010. Parameterization of near-bed processes under collinear wave and current flows from a two-phase sheet flow model. Cont. Shelf Res. 30, 1403–1416.

Amoudry, L.O., Souza, A.J., 2011. Deterministic coastal morphological and sediment transport modeling: A review and discussion. Rev. Geophys. 49.

Andersen, T.J., Pejrup, M., 2011. Biological Influences on Sediment Behavior and Transport. In: Wolanski, E., McClusky, D. (Eds.), Treatise on Estuarine and Coastal Science. Academic Press, Waltham, pp. 289–309.

Anthony, E.J., 2015. Wave influence in the construction, shaping and destruction of river deltas: A review. Mar. Geol. 361, 53–78. https://doi.org/10.1016/j.margeo.2014.12.004.

Anthony, E.J., Aagaard, T., 2020. The lower shoreface: Morphodynamics and sediment connectivity with the upper shoreface and beach. Earth Sci. Rev. 210, 103334. https://doi.org/10.1016/j.earscirev.2020.103334.

Arthur, M.A., Sageman, B.B., 1994. Marine Black Shales: Depositional Mechanisms and Environments of Ancient Deposits. Annu. Rev. Earth Planet. Sci. 22, 499–551. https://doi.org/10.1146/annurev.ea.22.050194.002435.

Bádenas, B., Pomar, L., Aurell, M., Morsilli, M., 2012. A facies model for internalites (internal wave deposits) on a gently sloping carbonate ramp (Upper Jurassic, Ricla, NE Spain). Sediment. Geol. 271–272, 44–57. https://doi.org/10.1016/j.sedgeo.2012.05.020.

Bauer, J.E., Cai, W.-J., Raymond, P.A., Bianchi, T.S., Hopkinson, C.S., Regnier, P.A.G., 2013. The changing carbon cycle of the coastal ocean. Nature 504, 61–70. https://doi.org/10.1038/nature12857.

Bender, V.B., Hanebuth, T.J., Chiessi, C.M., 2013. Holocene shifts of the Subtropical Shelf Front off southeastern South America controlled by high and low latitude atmospheric forcings. Paleoceanography 28, 481–490. https://doi.org/10.1002/palo.20044.

Besset, M., Anthony, E.J., Bouchette, F., 2019. Multi-decadal variations in delta shorelines and their relationship to river sediment supply: An assessment and review. Earth Sci. Rev. 193, 199–219. https://doi.org/10.1016/j.earscirev.2019.04.018.

Beusen, A.H.W., Dekkers, A.L.M., Bouwman, A.F., Ludwig, W., Harrison, J., 2005. Estimation of global river transport of sediments and associated particulate C, N, and P. Global Biogeochemical Cycles 19. https://doi.org/10.1029/2005GB002453.

Bhattacharya, J.P., MacEachern, J.A., 2009. Hyperpycnal Rivers and Prodeltaic Shelves in the Cretaceous Seaway of North America. J. Sediment. Res. 79, 184–209. https://doi.org/10.2110/jsr.2009.026.

Bi, N., Yang, Z., Wang, H., Hu, B., Ji, Y., 2010. Sediment dispersion pattern off the present Huanghe (Yellow River) subdelta and its dynamic mechanism during normal river discharge period. Estuar. Coast. Shelf Sci. 86, 352–362. https://doi.org/10.1016/j.ecss.2009.06.005.

Blair, N.E., Aller, R.C., 2011. The Fate of Terrestrial Organic Carbon in the Marine Environment. Annu. Rev. Mar. Sci. 4, 401–423. https://doi.org/10.1146/annurev-marine-120709-142717.

Boegman, L., Stastna, M., 2019. Sediment Resuspension and Transport by Internal Solitary Waves. Annu. Rev. Fluid Mech. 51, 129–154. https://doi.org/10.1146/annurev-fluid-122316-045049.

Bogucki, D.J., Dickey, T., Redekopp, L.G., 1997. Sediment Resuspension and Mixing by Resonantly Generated Internal Solitary Waves. J. Phys. Oceanogr. 27, 1181–1196.

Bogucki, D.J., Redekopp, L.G., Barth, J., 2005. Internal solitary waves in the Coastal Mixing and Optics 1996 experiment: Multimodal structure and resuspension. J. Geophys. Res. Oceans 110. https://doi.org/10.1029/2003JC002253.

Boulesteix, K., Poyatos-Moré, M., Flint, S.S., Taylor, K.G., Hodgson, D.M., Hasiotis, S.T., 2019. Transport and deposition of mud in deep-water environments: Processes and stratigraphic implications. Sedimentology 66, 2894–2925. https://doi.org/10.1111/sed.12614.

Bouma, A.H., Normark, W.R., Barnes, N.E. (Eds.), 1985. Submarine Fans and Related Turbidite Systems. Springer, New York, NY.

Bourgault, D., Morsilli, M., Richards, C., Neumeier, U., Kelley, D.E., 2014. Sediment resuspension and nepheloid layers induced by long internal solitary waves shoaling orthogonally on uniform slopes. Cont. Shelf Res. 72, 21–33. https://doi.org/10.1016/j.csr.2013.10.019.

Brown, J.M., Davies, A.G., 2009. Methods for medium-term prediction of the net sediment transport by waves and currents in complex coastal regions. Cont. Shelf Res. 29, 1502–1514. https://doi.org/10.1016/j.csr.2009.03.018.

Cacchione, D.A., Drake, D.E., Kayen, R.W., Sternberg, R.W., Kineke, G.C., Tate, G.B., 1995. Measurements in the bottom boundary layer on the Amazon subaqueous delta. Mar. Geol. 125, 235–257. https://doi.org/10.1016/0025-3227(95)00014-P.

Cacchione, D.A., Drake, D.E., Losada, M.A., Medina, R., 1990. Bottom-boundary-layer measurements on the continental shelf off the Ebro River, Spain. Mar. Geol. 95, 179–192.

Cacchione, D.A., Grant, W.D., Drake, D.E., Glenn, S.M., 1987. Storm-dominated bottom boundary layer dynamics on the Northern California Continental Shelf: Measurements and predictions. J. Geophys. Res. Oceans 92, 1817–1827. https://doi.org/10.1029/JC092iC02p01817.

Carlin, J., Addison, J., Wagner, A., Schwartz, V., Hayward, J., Severin, V., 2019. Variability in Shelf Sedimentation in Response to Fluvial Sediment Supply and Coastal Erosion Over the Past 1,000 Years in Monterey Bay, CA, United States. Front. Earth Sci. 7, 113. https://doi.org/10.3389/feart.2019.00113.

Carter, L., Orpin, A.R., Kuehl, S.A., 2010. From mountain source to ocean sink–the passage of sediment across an active margin, Waipaoa Sedimentary System, New Zealand. Mar. Geol. 270, 1–10.

Castaing, P., Froidefond, J., Lazure, P., Weber, O., Prud'homme, R., Jouanneau, J.M., 1999. Relationship between hydrology and seasonal distribution of suspended sediments on the continental shelf of the Bay of Biscay. Deep-Sea Res. II Top. Stud. Oceanogr. 46, 1979–2001. https://doi.org/10.1016/S0967-0645(99)00052-1.

Chang, T.S., Bartholomä, A., Flemming, B.W., 2006. Seasonal Dynamics of Fine-Grained Sediments in a Back-Barrier Tidal Basin of the German Wadden Sea (Southern North Sea). J. Coast. Res. 2006, 328–338. https://doi.org/10.2112/03-0085.1.

Chauchat, J., Guillou, S., van Pham Bang, D., Dan Nguyen, K., 2013. Modelling sedimentation–consolidation in the framework of a one-dimensional two-phase flow model. J. Hydraul. Res. 51, 293–305. https://doi.org/10.1080/00221686.2013.768798.

Cheriton, O.M., McPhee-Shaw, E.E., Shaw, W.J., Stanton, T.P., Bellingham, J.G., Storlazzi, C.D., 2014. Suspended particulate layers and internal waves over the southern Monterey Bay continental shelf: An important control on shelf mud belts? J. Geophys. Res. Oceans 119, 428–444. https://doi.org/10.1002/2013JC009360.

Churchill, J.H., 1989. The effect of commercial trawling on sediment resuspension and transport over the Middle Atlantic Bight continental shelf. Cont. Shelf Res. 9, 841–865. https://doi.org/10.1016/0278-4343(89)90016-2.

Clayton, K.M., 1989. Sediment Input from the Norfolk Cliffs, Eastern England A Century of Coast Protection and Its Effect. J. Coast. Res. 5, 433–442.

Collins, D.S., Johnson, H.D., Allison, P.A., Guilpain, P., Damit, A.R., 2017. Coupled 'storm-flood' depositional model: Application to the Miocene-Modern Baram Delta Province, north-west Borneo. Sedimentology 64, 1203–1235.

Curray, J.R., Moore, D.G., van Andel, T.H., Shor, G.G., JR., 1964. Pleistocene Deltaic Progradation of Continental Terrace, Costa de Nayarit, Mexico, In: van Andel, T.H., Shor, G.G., Marine Geology of the Gulf of California: a symposium, vol. 3. American Association of Petroleum Geologists.

Damuth, J.E., Hayes, D.E., 1977. Echo character of the East Brazilian continental margin and its relationship to sedimentary processes. Mar. Geol. 24, 73–95. https://doi.org/10.1016/0025-3227(77)90002-0.

Davies, J.L., Clayton, K.M., 1980. Geographical variation in coastal development. Longman, London.

Deltares, 2020. Delft3D-Flow: Simulation of Multi-Dimensional Hydrodynamic Flows and Transport Phenomena, Including Sediments. User Manual. Version 3.15, Delft. https://content.oss.deltares.nl/delft3d/manuals/Delft3D-FLOW_User_Manual.pdf. Accessed 21 September 2020.

Deng, Z., He, Q., Safar, Z., Chassagne, C., 2019. The role of algae in fine sediment flocculation: In-situ and laboratory measurements. Mar. Geol. 413, 71–84. https://doi.org/10.1016/j.margeo.2019.02.003.

Deng, B.-Q., Hu, Y., Guo, X., Dalrymple, R.A., Shen, L., 2017. Numerical study on the dissipation of water waves over a viscous fluid-mud layer. Comput. Fluids 158, 107–119. https://doi.org/10.1016/j.compfluid.2017.04.015.

Denommee, K.C., Bentley, S.J., Harazim, D., Macquaker, J.H., 2016. Hydrodynamic controls on muddy sedimentary-fabric development on the Southwest Louisiana subaqueous delta. Mar. Geol. 382, 162–175. https://doi.org/10.1016/j.margeo.2016.09.013.

Diaz, M., Grasso, F., Le Hir, P., Sottolichio, A., Caillaud, M., Thouvenin, B., 2020. Modeling Mud and Sand Transfers Between a Macrotidal Estuary and the Continental Shelf: Influence of the Sediment Transport Parameterization. J. Geophys. Res. Oceans 125. https://doi.org/10.1029/2019JC015643 e2019JC015643.

Dickson, M.E., Walkden, M.J.A., Hall, J.W., 2007. Systemic impacts of climate change on an eroding coastal region over the twenty-first century. Clim. Chang. 84, 141–166. https://doi.org/10.1007/s10584-006-9200-9.

Dott, R.H., 1983. Episodic sedimentation - how normal is average? How rare is rare? Does it matter?. In: 1982 SEPM presidential address. Journal of Sedimentary Petrology, 53, pp. 5–23.

Dott, R.H., 1996. Episodic event deposits versus stratigraphic sequences—shall the twain never meet? Sediment. Geol. 104, 243–247. https://doi.org/10.1016/0037-0738(95)00131-X.

Drake, D.E., Cacchione, D.A., 1985. Seasonal variation in sediment transport on the Russian River shelf, California. Cont. Shelf Res. 4, 495–514.

Dronkers, J., van Alphen, J.S.L.J., Borst, J.C., 1990. Suspended Sediment Transport Processes in the Southern North Sea. In: Cheng, R.T. (Ed.), Coastal and Estuarine Studies - Residual Currents and Long-term Transport. Springer, New York, NY, pp. 302–320.

Dufois, F., Verney, R., Le Hir, P., Dumas, F., Charmasson, S., 2014. Impact of winter storms on sediment erosion in the Rhone River prodelta and fate of sediment in the Gulf of Lions (North Western Mediterranean Sea). Cont. Shelf Res. 72, 57–72. https://doi.org/10.1016/j.csr.2013.11.004.

Dürr, H.H., Meybeck, M., Hartmann, J., Laruelle, G.G., Roubeix, V., 2011. Global spatial distribution of natural riverine silica inputs to the coastal zone. Biogeosciences 8, 597–620. https://doi.org/10.5194/bg-8-597-2011.

Dyer, K.R., 1989. Sediment processes in estuaries: Future research requirements. J. Geophys. Res. Oceans 94, 14327–14339. https://doi.org/10.1029/JC094iC10p14327.

Eidam, E.F., Ogston, A.S., Nittrouer, C.A., 2019. Formation and Removal of a Coastal Flood Deposit. J. Geophys. Res. Oceans 124, 1045–1062. https://doi.org/10.1029/2018JC014360.

Eidam, E.F., Ogston, A.S., Nittrouer, C.A., Warrick, J.A., 2016. Tidally dominated sediment dispersal offshore of a small mountainous river: Elwha River, Washington State. Cont. Shelf Res. 116, 136–148. https://doi.org/10.1016/j.csr.2016.01.009.

Eisma, D., 1986. Flocculation and de-flocculation of suspended matter in estuaries. Neth. J. Sea Res. 20, 183–199. https://doi.org/10.1016/0077-7579(86)90041-4.

Erikson, L.H., Wright, S.A., Elias, E., Hanes, D.M., Schoellhamer, D.H., Largier, J., 2013. The use of modeling and suspended sediment concentration measurements for quantifying net suspended sediment transport through a large tidally dominated inlet. Mar. Geol. 345, 96–112. https://doi.org/10.1016/j.margeo.2013.06.001.

Espath, L., Pinto, L.C., Laizet, S., Silvestrini, J.H., 2014. Two- and three-dimensional Direct Numerical Simulation of particle-laden gravity currents. Comput. Geosci. 63, 9–16. https://doi.org/10.1016/j.cageo.2013.10.006.

Exner, F.M., 1925. Über die Wechselwirkung zwischen Wasser und Geschiebe in Flüssen. Akad. Wiss. Wien Math. Naturwiss. Klasse 134, 165–204.

Farnsworth, K.L., Warrick, J.A., 2007. Sources, dispersal, and fate of fine sediment supplied to coastal California. In: Scientific Investigations Report 2007-5254. U.S. Geological Survey, Reston, VA, p. 86.

Ferré, B., Durrieu de Madron, X., Estournel, C., Ulses, C., Le Corre, G., 2008. Impact of natural (waves and currents) and anthropogenic (trawl) resuspension on the export of particulate matter to the open ocean: Application to the Gulf of Lion (NW Mediterranean). Cont. Shelf Res. 28, 2071–2091. https://doi.org/10.1016/j.csr.2008.02.002.

Fettweis, M., Francken, F., Pison, V., van den Eynde, D., 2006. Suspended particulate matter dynamics and aggregate sizes in a high turbidity area. Mar. Geol. 235, 63–74. https://doi.org/10.1016/j.margeo.2006.10.005.

Fettweis, M., Lee, B.J., 2017. Spatial and seasonal variation of biomineral suspended particulate matter properties in high-turbid nearshore and low-turbid offshore zones. Water 9, 694.

Fox, J.M., Hill, P.S., Milligan, T.G., Boldrin, A., 2004. Flocculation and sedimentation on the Po River Delta. Mar. Geol. 203, 95–107. https://doi.org/10.1016/S0025-3227(03)00332-3.

French, J., Payo, A., Murray, B., Orford, J., Eliot, M., Cowell, P., 2016. Appropriate complexity for the prediction of coastal and estuarine geomorphic behaviour at decadal to centennial scales. Geomorphology 256, 3–16. https://doi.org/10.1016/j.geomorph.2015.10.005.

Friedrichs, C.T., Scully, M.E., 2007. Modeling deposition by wave-supported gravity flows on the Po River prodelta: From seasonal floods to prograding clinoforms. Cont. Shelf Res. 27, 322–337. https://doi.org/10.1016/j.csr.2006.11.002.

Friedrichs, C.T., Wright, L.D., Hepworth, D.A., Kim, S.C., 2000. Bottom-boundary-layer processes associated with fine sediment accumulation in coastal seas and bays. Cont. Shelf Res. 20, 807–841. https://doi.org/10.1016/S0278-4343(00)00003-0.

Fringer, O.B., Dawson, C.N., He, R., Ralston, D.K., Zhang, Y.J., 2019. The future of coastal and estuarine modeling: Findings from a workshop. Ocean Model. 143, 101458. https://doi.org/10.1016/j.ocemod.2019.101458.

Gao, S., Collins, M.B., 2014. Holocene sedimentary systems on continental shelves. Mar. Geol. 352, 268–294. https://doi.org/10.1016/j.margeo.2014.03.021.

George, D.A., Hill, P.S., 2008. Wave climate, sediment supply and the depth of the sand–mud transition: A global survey. Mar. Geol. 254, 121–128. https://doi.org/10.1016/j.margeo.2008.05.005.
Gerbersdorf, S.U., Wieprecht, S., 2015. Biostabilization of cohesive sediments: revisiting the role of abiotic conditions, physiology and diversity of microbes, polymeric secretion, and biofilm architecture. Geobiology 13, 68–97. https://doi.org/10.1111/gbi.12115.
Geyer, W.R., Hill, P.S., Kineke, G.C., 2004. The transport, transformation and dispersal of sediment by buoyant coastal flows. Cont. Shelf Res. 24, 927–949. https://doi.org/10.1016/j.csr.2004.02.006.
Ghadeer, S.G., Macquaker, J.H., 2012. The role of event beds in the preservation of organic carbon in fine-grained sediments: Analyses of the sedimentological processes operating during deposition of the Whitby Mudstone Formation (Toarcian, Lower Jurassic) preserved in northeast England. Mar. Pet. Geol. 35, 309–320. https://doi.org/10.1016/j.marpetgeo.2012.01.001.
Gingele, F.X., Leipe, T., 2001. Southwestern Baltic Sea—A sink for suspended matter from the North Sea? Geology 29, 215. https://doi.org/10.1130/0091-7613(2001)029<0215:SBSASF>2.0.CO;2.
Ginoux, P., Prospero, J.M., Torres, O., Chin, M., 2004. Long-term simulation of global dust distribution with the GOCART model: correlation with North Atlantic Oscillation. Environ. Model Softw. 19, 113–128.
Giosan, L., 2007. Morphodynamic feedbacks on deltaic coasts: lessons from the wave-dominated Danube delta. In: Kraus, N.C., Rosati, J.D. (Eds.), Coastal Sediments '07, pp. 828–841.
Glenn, S.M., Grant, W.D., 1987. A suspended sediment stratification correction for combined wave and current flows. J. Geophys. Res. Oceans 92, 8244–8264.
Gorsline, D.S., 1984. A review of fine-grained sediment origins, characteristics, transport and deposition. Geol. Soc. Lond., Spec. Publ. 15, 17–34. https://doi.org/10.1144/GSL.SP.1984.015.01.02.
Grabowski, R.C., Droppo, I.G., Wharton, G., 2011. Erodibility of cohesive sediment: The importance of sediment properties. Earth Sci. Rev. 105, 101–120. https://doi.org/10.1016/j.earscirev.2011.01.008.
Grant, W.D., Madsen, O.S., 1979. Combined wave and current interaction with a rough bottom. J. Geophys. Res. Oceans 84, 1797–1808. https://doi.org/10.1029/JC084iC04p01797.
Grousset, F.E., Ginoux, P., Bory, A., Biscaye, P.E., 2003. Case study of a Chinese dust plume reaching the French Alps. Geophys. Res. Lett. 30.
Hage, S., Cartigny, M.J.B., Sumner, E.J., Clare, M.A., Hughes Clarke, J.E., Talling, P.J., Lintern, D.G., Simmons, S.M., Silva Jacinto, R., Vellinga, A.J., Allin, J.R., Azpiroz-Zabala, M., Gales, J.A., Hizzett, J.L., Hunt, J.E., Mozzato, A., Parsons, D.R., Pope, E. L., Stacey, C.D., Symons, W.O., Vardy, M.E., Watts, C., 2019. Direct Monitoring Reveals Initiation of Turbidity Currents From Extremely Dilute River Plumes. Geophys. Res. Lett. 46, 11310–11320. https://doi.org/10.1029/2019GL084526.
Hale, R.P., Ogston, A.S., 2015. In situ observations of wave-supported fluid-mud generation and deposition on an active continental margin. J. Geophys. Res. Earth Surf. 120, 2357–2373. https://doi.org/10.1002/2015JF003630.
Hanebuth, T.J., Henrich, R., 2009. Recurrent decadal-scale dust events over Holocene western Africa and their control on canyon turbidite activity (Mauritania). Quat. Sci. Rev. 28, 261–270. https://doi.org/10.1016/j.quascirev.2008.09.024.
Hanebuth, T.J., King, M.L., Mendes, I., Lebreiro, S., Lobo, F.J., Oberle, F.K., Antón, L., Ferreira, P.A., Reguera, M.I., 2018. Hazard potential of widespread but hidden historic offshore heavy metal (Pb, Zn) contamination (Gulf of Cadiz, Spain). Sci. Total Environ. 637-638, 561–576. https://doi.org/10.1016/j.scitotenv.2018.04.352.
Hanebuth, T.J., Lantzsch, H., 2008. A Late Quaternary sedimentary shelf system under hyperarid conditions: Unravelling climatic, oceanographic and sea-level controls (Golfe d'Arguin, Mauritania, NW Africa). Mar. Geol. 256, 77–89. https://doi.org/10.1016/j.margeo.2008.10.001.
Hanebuth, T.J., Lantzsch, H., Nizou, J., 2015. Mud depocenters on continental shelves—appearance, initiation times, and growth dynamics. Geo-Mar. Lett. 35, 487–503. https://doi.org/10.1007/s00367-015-0422-6.
Harris, C.K., Traykovski, P.A., Geyer, W.R., 2005. Flood dispersal and deposition by near-bed gravitational sediment flows and oceanographic transport: A numerical modeling study of the Eel River shelf, northern California. J. Geophys. Res. Oceans 110. https://doi.org/10.1029/2004JC002727.
Harris, C.K., Wiberg, P.L., 2002. Across-shelf sediment transport: Interactions between suspended sediment and bed sediment. J. Geophys. Res. Oceans 107. https://doi.org/10.1029/2000JC000634, 8-1-8-12.
Hill, P.S., Fox, J.M., Crockett, J.S., Curran, K.J., Friedrichs, C.T., Geyer, W.R., Milligan, T. G., Ogston, A.S., Puig, P., Scully, M.E., Traykovski, P.A., Wheatcroft, R.A., 2007. Sediment Delivery to the Seabed on Continental Margins. In: Nittrouer, C.A., Austin, J.A., Field, M.E., Kravitz, J.H., Syvitski, J.P., Wiberg, P.L. (Eds.), Continental margin sedimentation. From sediment transport to sequence stratigraphy. Blackwell Pub, Malden, MA.
Hill, P.S., McCave, I.N., 2001. Suspended particle transport in benthic boundary layers. In: Boudreau, B.P., Jorgensen, B.B. (Eds.), The benthic boundary layer: Transport processes and biogeochemistry. Oxford University Press, pp. 78–103.
Hill, P.S., Milligan, T.G., Geyer, W.R., 2000. Controls on effective settling velocity of suspended sediment in the Eel River flood plume. Cont. Shelf Res. 20, 2095–2111. https://doi.org/10.1016/S0278-4343(00)00064-9.
Holland, H.D., 2005. Sea level, sediments and the composition of seawater. Am. J. Sci. 305, 220–239.
Holz, C., Stuut, J.-B.W., Henrich, R., Meggers, H., 2007. Variability in terrigenous sedimentation processes off northwest Africa and its relation to climate changes: Inferences from grain-size distributions of a Holocene marine sediment record. Sediment. Geol. 202, 499–508. https://doi.org/10.1016/j.sedgeo.2007.03.015.
Horner-Devine, A.R., Pietrzak, J.D., Souza, A.J., McKeon, M.A., Meirelles, S., Henriquez, M., Flores, R.P., Rijnsburger, S., 2017. Cross-shore transport of nearshore sediment by river plume frontal pumping. Geophys. Res. Lett. 44, 6343–6351. https://doi.org/10.1002/2017GL073378.
Hsu, T.-J., Ozdemir, C.E., Traykovski, P.A., 2009. High-resolution numerical modeling of wave-supported gravity-driven mudflows. J. Geophys. Res. 114, F04016. https://doi.org/10.1029/2008JC005006.
Hu, Y., Guo, X., Lu, X., Liu, Y., Dalrymple, R.A., Shen, L., 2012. Idealized numerical simulation of breaking water wave propagating over a viscous mud layer. Phys. Fluids 24, 112104. https://doi.org/10.1063/1.4768199.
Jones, O.P., Petersen, O.S., Kofoed-Hansen, H., 2007. Modelling of complex coastal environments: Some considerations for best practise. Coast. Eng. 54, 717–733. https://doi.org/10.1016/j.coastaleng.2007.02.004.
Kämpf, J., 2019. Extreme bed shear stress during coastal downwelling. Ocean Dyn. 69, 581–597. https://doi.org/10.1007/s10236-019-01256-4.
Kämpf, J., Myrow, P., 2014. High-Density Mud Suspensions and Cross-Shelf Transport: On the Mechanism of Gelling Ignition. J. Sediment. Res. 84, 215–223. https://doi.org/10.2110/jsr.2014.20.
Kirby, J.T., 2017. Recent advances in nearshore wave, circulation, and sediment transport modeling. J. Mar. Res. 75, 263–300. https://doi.org/10.1357/002224017821836824.
Klymak, J.M., Moum, J.N., 2003. Internal solitary waves of elevation advancing on a shoaling shelf. Geophys. Res. Lett. 30 https://doi.org/10.1029/2003GL017706.
Kuehl, S.A., Nittrouer, C.A., DeMaster, D.J., 1988. Microfabric study of fine-grained sediments; observations from the Amazon subaqueous delta. J. Sediment. Res. 58, 12–23. https://doi.org/10.1306/212F8CFB-2B24-11D7-8648000102C1865D.
Lamb, M.P., Mohrig, D., 2009. Do hyperpycnal-flow deposits record river-flood dynamics? Geology 37, 1067–1070.
Lamb, M.P., Myrow, P.M., Lukens, C., Houck, K., Strauss, J., 2008. Deposits from Wave-Influenced Turbidity Currents: Pennsylvanian Minturn Formation, Colorado, U.S.A. J. Sediment. Res. 78, 480–498. https://doi.org/10.2110/jsr.2008.052.
Law, B.A., Hill, P.S., Milligan, T.G., Curran, K.J., Wiberg, P.L., Wheatcroft, R.A., 2008. Size sorting of fine-grained sediments during erosion: Results from the western Gulf of Lions. Cont. Shelf Res. 28, 1935–1946. https://doi.org/10.1016/j.csr.2007.11.006.
Lazar, O.R., Bohacs, K.M., Macquaker, J.H., Schieber, J., Demko, T.M., 2015. Capturing Key Attributes of Fine-Grained Sedimentary Rocks In Outcrops, Cores, and Thin Sections: Nomenclature and Description Guidelines. J. Sediment. Res. 85, 230–246. https://doi.org/10.2110/jsr.2015.11.
Le Hir, P., Cann, P., Waeles, B., Jestin, H., Bassoullet, P., 2008. Erodibility of natural sediments: experiments on sand/mud mixtures from laboratory and field erosion tests. In: Kusuda, T., Yamanishi, H., Spearman, J., Gailani, J.Z. (Eds.), Proceedings in Marine Science : Sediment and Ecohydraulics, vol. 9. Elsevier, pp. 137–153.
Le Hir, P., Cayocca, F., Waeles, B., 2011. Dynamics of sand and mud mixtures: A multiprocess-based modelling strategy. Continental Shelf Research 31, S135–S149. https://doi.org/10.1016/j.csr.2010.12.009.
Le Hir, P., Monbet, Y., Orvain, F., 2007. Sediment erodability in sediment transport modelling: Can we account for biota effects? Continental Shelf Research 27, 1116–1142. https://doi.org/10.1016/j.csr.2005.11.016.
Leithold, E.L., 1989. Depositional processes on an ancient and modern muddy shelf, northern California. Sedimentology 36, 179–202. https://doi.org/10.1111/j.1365-3091.1989.tb00602.x.
Lichtman, I.D., Baas, J.H., Amoudry, L.O., Thorne, P.D., Malarkey, J., Hope, J.A., Peakall, J., Paterson, D.M., Bass, S.J., Cooke, R.D., Manning, A.J., Davies, A.G., Parsons, D.R., Ye, L., 2018. Bedform migration in a mixed sand and cohesive clay intertidal environment and implications for bed material transport predictions. Geomorphology 315, 17–32. https://doi.org/10.1016/j.geomorph.2018.04.016.
Limber, P.W., Patsch, K.B., Griggs, G.B., 2008. Coastal sediment budgets and the littoral cutoff diameter: a grain size threshold for quantifying active sediment inputs. J. Coast. Res. 24, 122–133.
Liu, J.T., Hsu, R.T., Yang, R.J., Wang, Y.P., Wu, H., Du, X., Li, A., Chien, S.C., Lee, J., Yang, S., Zhu, J., Su, C.-C., Chang, Y., Huh, C.-A., 2018. A comprehensive sediment dynamics study of a major mud belt system on the inner shelf along an energetic coast. Sci. Rep. 8, 4229. https://doi.org/10.1038/s41598-018-22696-w.
Liu, S., Shi, X., Fang, X., Dou, Y., Liu, Y., Wang, X., 2014. Spatial and temporal distributions of clay minerals in mud deposits on the inner shelf of the East China Sea: Implications for paleoenvironmental changes in the Holocene. Quat. Int. 349, 270–279. https://doi.org/10.1016/j.quaint.2014.07.016.
Longo, S., 2005. Two-Phase Flow Modeling of Sediment Motion in Sheet-Flows above Plane Beds. J. Hydraul. Eng. 131, 366–379. https://doi.org/10.1061/(ASCE)0733-9429(2005)131:5(366).
Ludwig, W., Probst, J.-L., 1998. River sediment discharge to the oceans; present-day controls and global budgets. Am. J. Sci. 298, 265–295.
Ma, Y., Wright, L.D., Friedrichs, C.T., 2008. Observations of sediment transport on the continental shelf off the mouth of the Waiapu River, New Zealand: evidence for current-supported gravity flows. Cont. Shelf Res. 28, 516–532.
Macquaker, J.H., Bentley, S.J., Bohacs, K.M., 2010. Wave-enhanced sediment-gravity flows and mud dispersal across continental shelves: Reappraising sediment transport processes operating in ancient mudstone successions. Geology 38, 947–950. https://doi.org/10.1130/G31093.1.
Mahiquesde, M.M., Hanebuth, T.J., Martins, C.C., Montoya-Montes, I., Alcántara-Carrió, J., Figueira, R.C.L., Bícego, M.C., 2015. Mud depocentres on the continental shelf: a neglected sink for anthropogenic contaminants from the coastal zone. Environ. Earth Sci. 75, 44. https://doi.org/10.1007/s12665-015-4782-z.
Maier, K.L., Gales, J.A., Paull, C.K., Rosenberger, K., Talling, P.J., Simmons, S.M., Gwiazda, R., McGann, M., Cartigny, M.J.B., Lundsten, E., Anderson, K., Clare, M.A.,

Xu, J., Parsons, D., Barry, J.P., Wolfson-Schwehr, M., Nieminski, N.M., Sumner, E.J., 2019. Linking Direct Measurements of Turbidity Currents to Submarine Canyon-Floor Deposits. Front. Earth Sci. 7, 144. https://doi.org/10.3389/feart.2019.00144.
Maloney, J.M., Bentley, S.J., Xu, K., Obelcz, J., Georgiou, I.Y., Miner, M.D., 2018. Mississippi River subaqueous delta is entering a stage of retrogradation. Mar. Geol. 400, 12–23. https://doi.org/10.1016/j.margeo.2018.03.001.
Manning, A.J., Dyer, K.R., 2002. The use of optics for the in situ determination of flocculated mud characteristics. J. Opt. A Pure Appl. Opt. 4, S71–S81. https://doi.org/10.1088/1464-4258/4/4/366.
Marion, C., Dufois, F., Arnaud, M., Vella, C., 2010. In situ record of sedimentary processes near the Rhône River mouth during winter events (Gulf of Lions, Mediterranean Sea). Cont. Shelf Res. 30, 1095–1107. https://doi.org/10.1016/j.csr.2010.02.015.
Marshall, J., Hill, C., Perelman, L., Adcroft, A., 1997. Hydrostatic, quasi-hydrostatic, and nonhydrostatic ocean modeling. J. Geophys. Res. Oceans 102, 5733–5752. https://doi.org/10.1029/96JC02776.
Martin, J.M., Elbaz-Poulichet, F., Guieu, C., Loÿe-Pilot, M.D., Han, G., 1989. River versus atmospheric input of material to the Mediterranean Sea: an overview. Mar. Chem. 28, 159–182. https://doi.org/10.1016/0304-4203(89)90193-X.
Masunaga, E., Arthur, R.S., Fringer, O.B., Yamazaki, H., 2017. Sediment resuspension and the generation of intermediate nepheloid layers by shoaling internal bores. J. Mar. Syst. 170, 31–41. https://doi.org/10.1016/j.jmarsys.2017.01.017.
Mathew, R., Winterwerp, J.C., 2017. Surficial sediment erodibility from time-series measurements of suspended sediment concentrations: Development and validation. Ocean Dyn. 67, 691–712. https://doi.org/10.1007/s10236-017-1055-2.
McCave, I., 1972. Transport and escape of fine-grained sediment from shelf areas. In: Swift, D.J.P., Duane, D., Pilkey, O. (Eds.), Shelf sediment transport: process and pattern. Dowden, Hutchinson and Ross, Stroudsburg, pp. 225–244.
McCave, I.N., 1973. Mud in the North Sea. In: Goldberg, E.D. (Ed.), North Sea Science. MIT Press, Cambridge, Mass., pp. 75–100
McCave, I.N., 1978. Grain-size trends and transport along beaches: Example from eastern England. Mar. Geol. 28, M43–M51. https://doi.org/10.1016/0025-3227(78)90092-0.
McCave, I.N., 1987. Fine sediment sources and sinks around the East Anglian Coast (UK). J. Geol. Soc. 144, 149–152. https://doi.org/10.1144/gsjgs.144.1.0149.
McCave, I.N., 2003. Sedimentary settings on continental margins—an overview. In: Wefer, G., Billet, D., Hebbeln, D., Jorgensen, B.B., Schlüter, M., van Weering, T.C.E. (Eds.), Ocean margin systems. Springer, pp. 1–14.
McCave, I.N., Hall, I.R., 2006. Size sorting in marine muds: Processes, pitfalls, and prospects for paleoflow-speed proxies. Geochem. Geophys. Geosyst. 7 https://doi.org/10.1029/2006GC001284.
McCave, I.N., Manighetti, B., Robinson, S.G., 1995. Sortable silt and fine sediment size/composition slicing: Parameters for palaeocurrent speed and palaeoceanography. Paleoceanography 10, 593–610. https://doi.org/10.1029/94PA03039.
McKee, B.A., Aller, R.C., Allison, M.A., Bianchi, T.S., Kineke, G.C., 2004. Transport and transformation of dissolved and particulate materials on continental margins influenced by major rivers: Benthic boundary layer and seabed processes. Cont. Shelf Res. 24, 899–926. https://doi.org/10.1016/j.csr.2004.02.009.
McPhee-Shaw, E., 2006. Boundary–interior exchange: Reviewing the idea that internal-wave mixing enhances lateral dispersal near continental margins. Ocean Mixing 53, 42–59. https://doi.org/10.1016/j.dsr2.2005.10.018.
McPhee-Shaw, E.E., Kunze, E., 2002. Boundary layer intrusions from a sloping bottom: A mechanism for generating intermediate nepheloid layers. J. Geophys. Res. Oceans 107. https://doi.org/10.1029/2001JC000801.
McPhee-Shaw, E.E., Sternberg, R.W., Mullenbach, B.L., Ogston, A.S., 2004. Observations of intermediate nepheloid layers on the northern California continental margin. Cont. Shelf Res. 24, 693–720. https://doi.org/10.1016/j.csr.2004.01.004.
Meade, R.H., 1996. River-sediment inputs to major deltas. In: Milliman, J.D., Haq, B.U. (Eds.), Sea-level rise and coastal subsidence. Springer, pp. 63–85.
Mehta, A.J., 1991. Understanding fluid mud in a dynamic environment. Geo-Mar. Lett. 11, 113–118. https://doi.org/10.1007/BF02430995.
Mengual, B., Cayocca, F., Le Hir, P., Draye, R., Laffargue, P., Vincent, B., Garlan, T., 2016. Influence of bottom trawling on sediment resuspension in the 'Grande-Vasière' area (Bay of Biscay, France). Ocean Dyn 66, 1181–1207. https://doi.org/10.1007/s10236-016-0974-7.
Merckelbach, L.M., Kranenburg, C., 2004. Equations for effective stress and permeability of soft mud–sand mixtures. Géotechnique 54, 235–243. https://doi.org/10.1680/geot.2004.54.4.235.
Miall, A.D., 2015. Updating uniformitarianism: Stratigraphy as just a set of 'frozen accidents'. Geol. Soc. Lond., Spec. Publ. 404, 11–36. https://doi.org/10.1144/SP404.4.
Michalopoulos, P., Aller, R.C., 1995. Rapid Clay Mineral Formation in Amazon Delta Sediments: Reverse Weathering and Oceanic Elemental Cycles. Science 270, 614. https://doi.org/10.1126/science.270.5236.614.
Milligan, T.G., Hill, P.S., Law, B.A., 2007. Flocculation and the loss of sediment from the Po River plume. Cont. Shelf Res. 27, 309–321. https://doi.org/10.1016/j.csr.2006.11.008.
Milliman, J.D., Droxler, A.W., 1996. Neritic and pelagic carbonate sedimentation in the marine environment: ignorance is not bliss. Geol. Rundsch. 85, 496–504. https://doi.org/10.1007/BF02369004.
Milliman, J.D., Lin, S.W., Kao, S.J., Liu, J.P., Liu, C.S., Chiu, J.K., Lin, Y.C., 2007. Short-term changes in seafloor character due to flood-derived hyperpycnal discharge: Typhoon Mindulle, Taiwan, July 2004. Geology 35, 779–782.
Milliman, J.D., Meade, R.H., 1983. World-Wide Delivery of River Sediment to the Oceans. J. Geol. 91, 1–21.
Milliman, J.D., Syvitski, J.P.M., 1992. Geomorphic/Tectonic Control of Sediment Discharge to the Ocean: The Importance of Small Mountainous Rivers. J. Geol. 100, 525–544. https://doi.org/10.1086/629606.
Moore, D.G., 1969. Reflection profiling studies of the California continental borderland: structure and Quaternary turbidite basins. Geol. Soc. Am. Spec. Pap. 107.
Mount, J.F., 1984. Mixing of siliciclastic and carbonate sediments in shallow shelf environments. Geology 12, 432–435.
Mountain, G.S., Burger, R.L., Delius, H., Fulthorpe, C.S., Austin, J.A., Goldberg, D.S., Steckler, M.S., McHugh, C.M., Miller, K.G., Monteverde, D.H., 2007. The long-term stratigraphic record on continental margins. In: Nittrouer, C.A., Austin, J.A., Field, M.E., Kravitz, J.H., Syvitski, J.P., Wiberg, P.L. (Eds.), Continental margin sedimentation.From sediment transport to sequence stratigraphy. Blackwell Pub, Malden, MA, pp. 381–458.
Mulder, T., Syvitski, J.P.M., Migeon, S., Faugères, J.-C., Savoye, B., 2003. Marine hyperpycnal flows: initiation, behavior and related deposits. A review. Mar. Pet. Geol. 20, 861–882. https://doi.org/10.1016/j.marpetgeo.2003.01.003.
Myrow, P.M., Fischer, W., Goodge, J.W., 2002. Wave-modified turbidites: combined-flow shoreline and shelf deposits, Cambrian, Antarctica. J. Sediment. Res. 72, 641–656.
Myrow, P.M., Southard, J.B., 1996. Tempestite deposition. J. Sediment. Res. 66, 875–887.
Neumeier, U., Ferrarin, C., Amos, C.L., Umgiesser, G., Li, M.Z., 2008. Sedtrans05: An improved sediment-transport model for continental shelves and coastal waters with a new algorithm for cohesive sediments. Comput. Geosci. 34, 1223–1242. https://doi.org/10.1016/j.cageo.2008.02.007.
Nittrouer, C.A., Bergenback, B.E., DeMaster, D.J., Kuehl, S.A., 1988. Chapter 9 Accumulation of Mixed Carbonate and Siliciclastic Muds on the Continental Shelf of Eastern Spain. In: Doyle, L.J., Roberts, H.H. (Eds.), Developments in Sedimentology : Carbonate – Clastic Transitions, vol. 42. Elsevier, pp. 251–269.
Nittrouer, C.A., Sternberg, R.W., 1981. The formation of sedimentary strata in an allochthonous shelf environment: The Washington continental shelf. Mar. Geol. 42, 201–232. https://doi.org/10.1016/0025-3227(81)90164-X.
Nittrouer, C.A., Wright, L.D., 1994. Transport of particles across continental shelves. Rev. Geophys. 32, 85–113. https://doi.org/10.1029/93RG02603.
Nizou, J., Hanebuth, T.J., Vogt, C., 2011. Deciphering signals of late Holocene fluvial and aeolian supply from a shelf sediment depocentre off Senegal (north-west Africa). J. Quat. Sci. 26, 411–421. https://doi.org/10.1002/jqs.1467.
Nowacki, D.J., Horner-Devine, A.R., Nash, J.D., Jay, D.A., 2012. Rapid sediment removal from the Columbia River plume near field. Cont. Shelf Res. 35, 16–28. https://doi.org/10.1016/j.csr.2011.11.013.
O'Brien, N.R., 1996. Shale lamination and sedimentary processes. Geol. Soc. Lond., Spec. Publ. 116, 23. https://doi.org/10.1144/GSL.SP.1996.116.01.04.
Oberle, F.K.J., Hanebuth, T.J., Baasch, B., Schwenk, T., 2014. Volumetric budget calculation of sediment and carbon storage and export for a late Holocene mid-shelf mudbelt system (NW Iberia). Cont. Shelf Res. 76, 12–24. https://doi.org/10.1016/j.csr.2013.12.012.
Oberle, F.K.J., Puig, P., Martín, J., 2018. Fishing Activities. In: Micallef, A., Krastel, S., Savini, A. (Eds.), Submarine Geomorphology. Springer International Publishing, Cham, pp. 503–534.
Oberle, F.K.J., Storlazzi, C.D., Hanebuth, T.J., 2016a. What a drag: Quantifying the global impact of chronic bottom trawling on continental shelf sediment. J. Mar. Syst. 159, 109–119. https://doi.org/10.1016/j.jmarsys.2015.12.007.
Oberle, F.K.J., Swarzenski, P.W., Reddy, C.M., Nelson, R.K., Baasch, B., Hanebuth, T.J., 2016b. Deciphering the lithological consequences of bottom trawling to sedimentary habitats on the shelf. J. Mar. Syst. 159, 120–131. https://doi.org/10.1016/j.jmarsys.2015.12.008.
Ogston, A.S., Cacchione, D.A., Sternberg, R.W., Kineke, G.C., 2000. Observations of storm and river flood-driven sediment transport on the northern California continental shelf. Cont. Shelf Res. 20, 2141–2162. https://doi.org/10.1016/S0278-4343(00)00065-0.
Ouillon, S., 2018. Why and How Do We Study Sediment Transport? Focus on Coastal Zones and Ongoing Methods. Water 10. https://doi.org/10.3390/w10040390.
Palanques, A., Puig, P., Guillén, J., Demestre, M., Martín, J., 2014. Effects of bottom trawling on the Ebro continental shelf sedimentary system (NW Mediterranean). Cont. Shelf Res. 72, 83–98. https://doi.org/10.1016/j.csr.2013.10.008.
Palinkas, C.M., Nittrouer, C.A., 2007. Modern sediment accumulation on the Po shelf, Adriatic Sea. Cont. Shelf Res. 27, 489–505. https://doi.org/10.1016/j.csr.2006.11.006.
Paola, C., Ganti, V., Mohrig, D., Runkel, A.C., Straub, K.M., 2018. Time Not Our Time: Physical Controls on the Preservation and Measurement of Geologic Time. Annu. Rev. Earth Planet. Sci. 46, 409–438. https://doi.org/10.1146/annurev-earth-082517-010129.
Paola, C., Voller, V.R., 2005. A generalized Exner equation for sediment mass balance. J. Geophys. Res. Earth Surf. 110. https://doi.org/10.1029/2004JF000274.
Papanicolaou, A.N., Elhakeem, M., Krallis, G., Prakash, S., Edinger, J., 2008. Sediment Transport Modeling Review—Current and Future Developments. J. Hydraul. Eng. 134, 1–14. https://doi.org/10.1061/(ASCE)0733-9429(2008)134:1(1).
Parsons, J.D., Bush, J.W.M., Syvitski, J.P.M., 2001. Hyperpycnal plume formation from riverine outflows with small sediment concentrations. Sedimentology 48, 465–478. https://doi.org/10.1046/j.1365-3091.2001.00384.x.
Pawlowicz, R., Di Costanzo, R., Halverson, M., Devred, E., Johannessen, S., 2017. Advection, surface area, and sediment load of the Fraser River plume under variable wind and river forcing. Atmosphere-Ocean 55, 293–313.
Payo-Payo, M., Jacinto, R.S., Lastras, G., Rabineau, M., Puig, P., Martin, J., Canals, M., Sultan, N., 2017. Numerical modeling of bottom trawling-induced sediment transport and accumulation in La Fonera submarine canyon, northwestern

Mediterranean Sea. Mar. Geol. 386, 107–125. https://doi.org/10.1016/j.margeo.2017.02.015.
Pedersen, G.K., 1985. Thin, fine-grained storm layers in a muddy shelf sequence: an example from the Lower Jurassic in the Stenlille 1 well, Denmark. J. Geol. Soc. 142, 357. https://doi.org/10.1144/gsjgs.142.2.0357.
Peng, Y., Olariu, C., Steel, R.J., 2020. Recognizing tide- and wave-dominated compound deltaic clinothems in the rock record. Geology. https://doi.org/10.1130/G47767.1.
Plint, G.A., 2014. Mud dispersal across a Cretaceous prodelta: Storm-generated, wave-enhanced sediment gravity flows inferred from mudstone microtexture and microfacies. Sedimentology 61, 609–647. https://doi.org/10.1111/sed.12068.
Pomar, L., Morsilli, M., Hallock, P., Bádenas, B., 2012. Internal waves, an under-explored source of turbulence events in the sedimentary record. Earth Sci. Rev. 111, 56–81. https://doi.org/10.1016/j.earscirev.2011.12.005.
Pope, N.D., Widdows, J., Brinsley, M.D., 2006. Estimation of bed shear stress using the turbulent kinetic energy approach—A comparison of annular flume and field data. Cont. Shelf Res. 26, 959–970. https://doi.org/10.1016/j.csr.2006.02.010.
Potter, P.E., Maynard, J.B., Depetris, P.J. (Eds.), 2005. Mud and Mudstones: Introduction and Overview. Springer Berlin Heidelberg, Berlin, Heidelberg.
Prémaillon, M., Regard, V., Dewez, T.J.B., Auda, Y., 2018. GlobR2C2 (Global Recession Rates of Coastal Cliffs): a global relational database to investigate coastal rocky cliff erosion rate variations. Earth Surface Dynamics 6, 651.
Puig, P., Martin, J., Masqué, P., Palanques, A., 2015. Increasing sediment accumulation rates in La Fonera (Palamós) submarine canyon axis and their relationship with bottom trawling activities. Geophys. Res. Lett. 42, 8106–8113. https://doi.org/10.1002/2015GL065052.
Quaresma, L.S., Vitorino, J., Oliveira, A., da Silva, J., 2007. Evidence of sediment resuspension by nonlinear internal waves on the western. Portuguese mid-shelf. Mar. Geol. 246, 123–143. https://doi.org/10.1016/j.margeo.2007.04.019.
Richardson, M.D., Briggs, K.B., Bentley, S.J., Walter, D.J., Orsi, T.H., 2002. The effects of biological and hydrodynamic processes on physical and acoustic properties of sediments off the Eel River, California. Mar. Geol. 182, 121–139. https://doi.org/10.1016/S0025-3227(01)00231-6.
Roelvink, J.A., 2006. Coastal morphodynamic evolution techniques. Coast. Eng. 53, 277–287. https://doi.org/10.1016/j.coastaleng.2005.10.015.
Sadler, P.M., 1981. Sediment accumulation rates and the completeness of stratigraphic sections. J. Geol. 89, 569–584.
Sahl, L.E., Merrell, W.J., McGrail, D.W., Webb, J.A., 1987. Transport of mud on continental shelves: Evidence from the Texas Shelf. Mar. Geol. 76, 33–43. https://doi.org/10.1016/0025-3227(87)90015-6.
Sanford, L.P., 2008. Modeling a dynamically varying mixed sediment bed with erosion, deposition, bioturbation, consolidation, and armoring. Comput. Geosci. 34, 1263–1283. https://doi.org/10.1016/j.cageo.2008.02.011.
Schieber, J., Southard, J.B., Thaisen, K., 2007. Accretion of Mudstone Beds from Migrating Floccule Ripples. Science 318, 1760. https://doi.org/10.1126/science.1147001.
Schieber, J., Yawar, Z., 2009. A new twist on mud deposition: mud ripples in experiment and rock record. The Sedimentary Record 7, 4–8.
Schimmelmann, A., Lange, C.B., Schieber, J., Francus, P., Ojala, A.E., Zolitschka, B., 2016. Varves in marine sediments: A review. Earth Sci. Rev. 159, 215–246. https://doi.org/10.1016/j.earscirev.2016.04.009.
Scully, M.E., Friedrichs, C.T., Wright, L.D., 2003. Numerical modeling of gravity-driven sediment transport and deposition on an energetic continental shelf: Eel River, northern California. J. Geophys. Res. Oceans 108. https://doi.org/10.1029/2002JC001467.
Shanmugam, G., 2013. Modern internal waves and internal tides along oceanic pycnoclines: Challenges and implications for ancient deep-marine baroclinic sands. AAPG Bull. 97, 799–843. https://doi.org/10.1306/10171212101.
Sherwood, C.R., Aretxabaleta, A.L., Harris, C.K., Rinehimer, J.P., Verney, R., Ferré, B., 2018. Cohesive and mixed sediment in the Regional Ocean Modeling System (ROMS v3.6) implemented in the Coupled Ocean–Atmosphere–Wave–Sediment Transport Modeling System (COAWST r1234). Geosci. Model Dev. 11, 1849–1871. https://doi.org/10.5194/gmd-11-1849-2018.
Sherwood, C.R., Butman, B., Cacchione, D.A., Drake, D.E., Gross, T.F., Sternberg, R.W., Wiberg, P.L., Williams, A.J., 1994. Sediment-transport events on the northern California continental shelf during the 1990–1991 STRESS experiment. Cont. Shelf Res. 14, 1063–1099. https://doi.org/10.1016/0278-4343(94)90029-9.
Shi, F., Chickadel, C.C., Hsu, T.-J., Kirby, J.T., Farquharson, G., Ma, G., 2017. High-Resolution Non-Hydrostatic Modeling of Frontal Features in the Mouth of the Columbia River. Estuar. Coasts 40, 296–309. https://doi.org/10.1007/s12237-016-0132-y.
Simmons, S.M., Azpiroz-Zabala, M., Cartigny, M.J., Clare, M.A., Cooper, C., Parsons, D. R., Pope, E.L., Sumner, E.J., Talling, P.J., 2020. Novel Acoustic Method Provides First Detailed Measurements of Sediment Concentration Structure Within Submarine Turbidity Currents. J. Geophys. Res. Oceans 125. https://doi.org/10.1029/2019JC015904 e2019JC015904.
Snelgrove, P.V.R., 1999. Getting to the Bottom of Marine Biodiversity: Sedimentary Habitats: Ocean bottoms are the most widespread habitat on Earth and support high biodiversity and key ecosystem services. BioScience 49, 129–138. https://doi.org/10.2307/1313538.
Sommerfield, C.K., 2006. On sediment accumulation rates and stratigraphic completeness: Lessons from Holocene ocean margins. Cont. Shelf Res. 26, 2225–2240.
Sommerfield, C.K., Nittrouer, C.A., 1999. Modern accumulation rates and a sediment budget for the Eel shelf: a flood-dominated depositional environment. Mar. Geol. 154, 227–241.
Sommerfield, C.K., Ogston, A.S., Mullenbach, B.L., Drake, D.E., Alexander, C.R., Nittrouer, C.A., Borgeld, J.C., Wheatcroft, R.A., Leithold, E.L., 2007. Oceanic Dispersal and Accumulation of River Sediment. In: Nittrouer, C.A., Austin, J.A., Field, M.E., Kravitz, J.H., Syvitski, J.P., Wiberg, P.L. (Eds.), Continental margin sedimentation. From sediment transport to sequence stratigraphy. Blackwell Pub, Malden, MA.
Soulsby, R.L., Manning, A.J., Spearman, J., Whitehouse, R.J., 2013. Settling velocity and mass settling flux of flocculated estuarine sediments. Mar. Geol. 339, 1–12.
Spearman, J., Roberts, W., 2002. Comparison of flocculation models for applied sediment transport modelling. In: Winterwerp, J.C., Kranenburg, C. (Eds.), Proceedings in Marine Science : Fine Sediment Dynamics in the Marine Environment, vol. 5. Elsevier, pp. 277–293.
Stanley, D.J., 1983. Parallel laminated deep-sea muds and coupled gravity flow-hemipelagic settling in the Mediterranean. Smithsonian Institution Press, Washington, D.C.
Stanley, D.J., Addy, S.K., Behrens, E.W., 1983. The Mudline: Variability of its Position Relative to Shelfbreak. In: Stanley, D.J., Moore, G.T. (Eds.), The Shelfbreak: Critical Interface on Continental Margins, vol. 33. SEPM Society for Sedimentary Geology.
Sternberg, R.W., 1986. Transport and accumulation of river-derived sediment on the Washington continental shelf, USA. J. Geol. Soc. 143, 945. https://doi.org/10.1144/gsjgs.143.6.0945.
Sternberg, R.W., Cacchione, D.A., Paulso, B., Kineke, G.C., Drake, D.E., 1996. Observations of sediment transport on the Amazon subaqueous delta. Cont. Shelf Res. 16, 697–715. https://doi.org/10.1016/0278-4343(95)00045-3.
Straub, K.M., Li, Q., Benson, W.M., 2015. Influence of sediment cohesion on deltaic shoreline dynamics and bulk sediment retention: A laboratory study. Geophys. Res. Lett. 42, 9808–9815. https://doi.org/10.1002/2015GL066131.
Stuut, J.-B., Smalley, I., O'Hara-Dhand, K., 2009. Aeolian dust in Europe: African sources and European deposits. Quat. Int. 198, 234–245. https://doi.org/10.1016/j.quaint.2008.10.007.
Styles, R., Glenn, S.M., 2000. Modeling stratified wave and current bottom boundary layers on the continental shelf. J. Geophys. Res. Oceans 105, 24119–24139. https://doi.org/10.1029/2000JC900115.
Summerhayes, C.P., Milliman, J.D., Briggs, S.R., Bee, A.G., Hogan, C., 1976. Northwest African shelf sediments: influence of climate and sedimentary processes. J. Geol. 84, 277–300.
Swap, R., Ulanski, S., Cobbett, M., Garstang, M., 1996. Temporal and spatial characteristics of Saharan dust outbreaks. J. Geophys. Res. Atmos. 101, 4205–4220.
Swift, D.J.P., Duane, D., Pilkey, O. (Eds.), 1972. Shelf sediment transport: process and pattern. Dowden, Hutchinson and Ross, Stroudsburg.
Swift, D.J.P., Thorne, J.A., 1992. Sedimentation on Continental Margins, I: A General Model for Shelf Sedimentation. In: Swift, D.J.P., Oertel, G., Tillman, R., Thorne, J. (Eds.), Shelf sand and sandstone bodies: geometry, facies and sequence stratigraphy. John Wiley & Sons, Hoboken, New Jersey.
Syvitski, J.P.M., Peckham, S.D., Hilberman, R., Mulder, T., 2003. Predicting the terrestrial flux of sediment to the global ocean: a planetary perspective. Sediment. Geol. 162, 5–24.
Syvitski, J.P.M., Pratson, L.F., Wiberg, P.L., Steckler, M.S., García, M.H., Geyer, W.R., Harris, C.K., Hutton, E.W.H., Imran, J., Lee, H.J., 2007. Prediction of margin stratigraphy. In: Nittrouer, C.A., Austin, J.A., Field, M.E., Kravitz, J.H., Syvitski, J.P., Wiberg, P.L. (Eds.), Continental margin sedimentation. From sediment transport to sequence stratigraphy. Blackwell Pub, Malden, MA, pp. 459–529.
Syvitski, J.P.M., Slingerland, R.L., Burgess, P., Meiburg, E., Murray, A.B., Wiberg, P., Tucker, G., Voinov, A.A., 2010. Morphodynamic models: an overview. In: Vionnet, C., García, M., Latrubesse, E., Perillo, G. (Eds.), River, Coastal and Estuarine Morphodynamics - RCEM 2009. Taylor & Francis Group: CRC Press.
Thompson, C., Williams, M.E., Amoudry, L.O., Hull, T., Reynolds, S., Panton, A., Fones, G.R., 2019. Benthic controls of resuspension in UK shelf seas: Implications for resuspension frequency. Cont. Shelf Res. 185, 3–15. https://doi.org/10.1016/j.csr.2017.12.005.
Thrush, S.F., Dayton, P.K., 2002. Disturbance to Marine Benthic Habitats by Trawling and Dredging: Implications for Marine Biodiversity. Annu. Rev. Ecol. Syst. 33, 449–473. https://doi.org/10.1146/annurev.ecolsys.33.010802.150515.
Toorman, E.A., 1999. Sedimentation and self-weight consolidation: constitutive equations and numerical modelling. Géotechnique 49, 709–726. https://doi.org/10.1680/geot.1999.49.6.709.
Tourney, J., Ngwenya, B.T., 2014. The role of bacterial extracellular polymeric substances in geomicrobiology. Chem. Geol. 386, 115–132. https://doi.org/10.1016/j.chemgeo.2014.08.011.
Traykovski, P.A., Geyer, W.R., Irish, J., Lynch, J., 2000. The role of wave-induced density-driven fluid mud flows for cross-shelf transport on the Eel River continental shelf. Cont. Shelf Res. 20, 2113–2140. https://doi.org/10.1016/S0278-4343(00)00071-6.
Traykovski, P.A., Wiberg, P.L., Geyer, W.R., 2007. Observations and modeling of wave-supported sediment gravity flows on the Po prodelta and comparison to prior observations from the Eel shelf. Cont. Shelf Res. 27, 375–399. https://doi.org/10.1016/j.csr.2005.07.008.
Trowbridge, J.H., Lentz, S.J., 2018. The Bottom Boundary Layer. Annu. Rev. Mar. Sci. 10, 397–420. https://doi.org/10.1146/annurev-marine-121916-063351.
Ulses, C., Estournel, C., Durrieu de Madron, X., Palanques, A., 2008. Suspended sediment transport in the Gulf of Lions (NW Mediterranean): Impact of extreme storms and floods. Cont. Shelf Res. 28, 2048–2070. https://doi.org/10.1016/j.csr.2008.01.015.
Unverricht, D., Szczuciński, W., Stattegger, K., Jagodziński, R., Le, X.T., Kwong, L.L.W., 2013. Modern sedimentation and morphology of the subaqueous Mekong Delta, Southern Vietnam. Global and planetary change 110 (Part B), 223–235. https://doi.org/10.1016/j.gloplacha.2012.12.009.

Uścinowicz, S., Zachowicz, J., Graniczny, M., Dobracki, R., 2004. Geological structure of the southern Baltic coast and related hazards. Pol. Geol. Inst. Sp. Papers 15, 61–68.
Valentine, K., Mariotti, G., 2020. Does eutrophication affect the ability of biofilms to stabilize muddy sediments? Estuar. Coast. Shelf Sci. 232, 106490. https://doi.org/10.1016/j.ecss.2019.106490.
Valentine, K., Mariotti, G., Fagherazzi, S., 2014. Repeated erosion of cohesive sediments with biofilms. Adv. Geosci. 39, 9–14. https://doi.org/10.5194/adgeo-39-9-2014.
Van der Does, M., Knippertz, P., Zschenderlein, P., Giles Harrison, R., Stuut, J.-B.W., 2018. The mysterious long-range transport of giant mineral dust particles. Sci Adv 4, eaau2768. https://doi.org/10.1126/sciadv.aau2768.
Van der Lee, E.M., Bowers, D.G., Kyte, E., 2009. Remote sensing of temporal and spatial patterns of suspended particle size in the Irish Sea in relation to the Kolmogorov microscale. Cont. Shelf Res. 29, 1213–1225. https://doi.org/10.1016/j.csr.2009.01.016.
Van Maren, D.S., Cronin, K., 2016. Uncertainty in complex three-dimensional sediment transport models: equifinality in a model application of the Ems Estuary, the Netherlands. Ocean Dynamics 66, 1665–1679. https://doi.org/10.1007/s10236-016-1000-9.
Van Rijn, L.C., 1993. Principles of sediment transport in rivers, estuaries and coastal seas. Aqua publications, Amsterdam.
Villacieros-Robineau, N., Zúñiga, D., Barreiro-González, B., Alonso-Pérez, F., Granda, F., Froján, M., Collins, C.A., Barton, E.D., Castro, C.G., 2019. Bottom Boundary Layer and Particle Dynamics in an Upwelling Affected Continental Margin (NW Iberia). J. Geophys. Res. Oceans. https://doi.org/10.1029/2019JC015619.
Vitorino, J., Oliveira, A., Jouanneau, J.M., Drago, T., 2002. Winter dynamics on the northern Portuguese shelf. Part 2: bottom boundary layers and sediment dispersal. Prog. Oceanogr. 52, 155–170. https://doi.org/10.1016/S0079-6611(02)00004-6.
Vörösmarty, C.J., Meybeck, M., Fekete, B., Sharma, K., Green, P., Syvitski, J.P.M., 2003. Anthropogenic sediment retention: major global impact from registered river impoundments. Glob. Planet. Chang. 39, 169–190.
Walsh, J.P., Corbett, D.R., Kiker, J.M., Orpin, A.R., Hale, R.P., Ogston, A.S., 2014. Spatial and temporal variability in sediment deposition and seabed character on the Waipaoa River margin, New Zealand. Cont. Shelf Res. 86, 85–102. https://doi.org/10.1016/j.csr.2014.07.001.
Walsh, J.P., Nittrouer, C.A., 1999. Observations of sediment flux to the Eel continental slope, northern California. Mar. Geol. 154, 55–68. https://doi.org/10.1016/S0025-3227(98)00103-0.
Walsh, J.P., Nittrouer, C.A., 2009. Understanding fine-grained river-sediment dispersal on continental margins. Mar. Geol. 263, 34–45. https://doi.org/10.1016/j.margeo.2009.03.016.
Wang, X.H., 2002. Tide-Induced Sediment Resuspension and the Bottom Boundary Layer in an Idealized Estuary with a Muddy Bed. J. Phys. Oceanogr 32, 3113–3131.
Wang, A., Ralston, D.K., Bi, N., Cheng, Z., Wu, X., Wang, H., 2019. Seasonal variation in sediment transport and deposition on a muddy clinoform in the Yellow Sea. Cont. Shelf Res. 179, 37–51. https://doi.org/10.1016/j.csr.2019.04.009.
Warner, J.C., Sherwood, C.R., Signell, R.P., Harris, C.K., Arango, H.G., 2008. Development of a three-dimensional, regional, coupled wave, current, and sediment-transport model. Comput. Geosci. 34, 1284–1306. https://doi.org/10.1016/j.cageo.2008.02.012.
Weltje, G.J., Prins, M.A., 2003. Muddled or mixed? Inferring palaeoclimate from size distributions of deep-sea clastics. Climate Impact on Sedimentary Systems 162, 39–62. https://doi.org/10.1016/S0037-0738(03)00235-5.
Wheatcroft, R.A., 1990. Preservation potential of sedimentary event layers. Geology 18, 843–845.
Wheatcroft, R.A., Borgeld, J.C., 2000. Oceanic flood deposits on the northern California shelf: large-scale distribution and small-scale physical properties. Cont. Shelf Res. 20, 2163–2190.
Wheatcroft, R.A., Wiberg, P.L., Alexander, C.R., Bentley, S.J., Drake, D.E., Harris, C.K., Ogston, A.S., 2007. Post-Depositional Alteration and Preservation of Sedimentary Strata. In: Nittrouer, C.A., Austin, J.A., Field, M.E., Kravitz, J.H., Syvitski, J.P., Wiberg, P.L. (Eds.), Continental margin sedimentation. From sediment transport to sequence stratigraphy. Blackwell Pub, Malden, MA, pp. 101–155.
Williams, M.E., Amoudry, L.O., Brown, J.M., Thompson, C., 2019. Fine particle retention and deposition in regions of cyclonic tidal current rotation. Mar. Geol. 410, 122–134. https://doi.org/10.1016/j.margeo.2019.01.006.
Wilson, R.D., Schieber, J., 2017. Sediment transport processes and lateral facies gradients across a muddy shelf: Examples from the Geneseo Formation of central New York, United States. AAPG Bull. 101, 423–431. https://doi.org/10.1306/021417DIG17093.
Winterwerp, J.C., 2001. Stratification effects by cohesive and noncohesive sediment. J. Geophys. Res. Oceans 106, 22559–22574. https://doi.org/10.1029/2000JC000435.
Winterwerp, J.C., 2002. On the flocculation and settling velocity of estuarine mud. Cont. Shelf Res. 22, 1339–1360. https://doi.org/10.1016/S0278-4343(02)00010-9.
Winterwerp, J.C., 2011. The Physical Analyses of Muddy Sedimentation Processes. In: Wolanski, E., McClusky, D. (Eds.), Treatise on Estuarine and Coastal Science. Academic Press, Waltham, pp. 311–360.
Winterwerp, J.C., van Kesteren, W.G.M., van Prooijen, B., Jacobs, W., 2012. A conceptual framework for shear flow–induced erosion of soft cohesive sediment beds. J. Geophys. Res. Oceans 117. https://doi.org/10.1029/2012JC008072.
Winterwerp, J.C., Zhou, Z., Battista, G., van Kessel, T., Jagers, H.R.A., van Maren, D.S., van der Wegen, M., 2018. Efficient Consolidation Model for Morphodynamic Simulations in Low-SPM Environments. J. Hydraul. Eng. 144, 4018055. https://doi.org/10.1061/(ASCE)HY.1943-7900.0001477.
Wolanski, E., Gibbs, R.J., 1995. Flocculation of Suspended Sediment in the Fly River Estuary,Papua New Guinea. J. Coastal Res. 11, 754–762.
Woodroffe, C.D., Murray-Wallace, C.V., 2012. Sea-level rise and coastal change: the past as a guide to the future. Quat. Sci. Rev. 54, 4–11. https://doi.org/10.1016/j.quascirev.2012.05.009.
Wright, L.D., Friedrichs, C.T., 2006. Gravity-driven sediment transport on continental shelves: A status report. Cont. Shelf Res. 26, 2092–2107. https://doi.org/10.1016/j.csr.2006.07.008.
Wright, L.D., Nittrouer, C.A., 1995. Dispersal of river sediments in coastal seas: Six contrasting cases. Estuaries 18, 494–508. https://doi.org/10.2307/1352367.
Wu, J., Ren, J., Liu, H., Qiu, C., Cui, Y., Zhang, Q., 2016b. Trapping and escaping processes of Yangtze River-derived sediments to the East China Sea. Geol. Soc. Lond., Spec. Publ. 429, 153–169.
Xiong, J., Wang, X.H., Wang, Y.P., Chen, J., Shi, B., Gao, J., Yang, Y., Yu, Q., Li, M., Yang, L., Gong, X., 2017. Mechanisms of maintaining high suspended sediment concentration over tide-dominated offshore shoals in the southern Yellow Sea. Estuar. Coast. Shelf Sci. 191, 221–233. https://doi.org/10.1016/j.ecss.2017.04.023.
Xu, J.P., Noble, M.A., Eittreim, S.L., 2002. Suspended sediment transport on the continental shelf near Davenport, California. Mar. Geol. 181, 171–193. https://doi.org/10.1016/S0025-3227(01)00266-3.
Yang, S.L., Milliman, J.D., Li, P., Xu, K., 2011. 50,000 dams later: Erosion of the Yangtze River and its delta. Glob. Planet. Chang. 75, 14–20. https://doi.org/10.1016/j.gloplacha.2010.09.006.
Yawar, Z., Schieber, J., 2017. On the origin of silt laminae in laminated shales. Sedimentary Geology 360, 22–34. https://doi.org/10.1016/j.sedgeo.2017.09.001.
Young, A.P., Carilli, J.E., 2019. Global distribution of coastal cliffs. Earth Surf. Process. Landf. 44, 1309–1316. https://doi.org/10.1002/esp.4574.
Young, A.P., Raymond, J.H., Sorenson, J., Johnstone, E.A., Driscoll, N.W., Flick, R.E., Guza, R.T., 2010. Coarse Sediment Yields from Seacliff Erosion in the Oceanside Littoral Cell. J. Coast. Res. 2010, 580–585. https://doi.org/10.2112/08-1179.1.
Zang, Z., Xue, Z.G., Xu, K., Ozdemir, C.E., Chen, Q., Bentley, S.J., Sahin, C., 2020. A Numerical Investigation of Wave-Supported Gravity Flow During Cold Fronts Over the Atchafalaya Shelf. J. Geophys. Res. Oceans 125 e2019JC015269. 10.1029/2019JC015269.
Zhang, W., 2016. Sediment Transport Models. In: Harff, J., Meschede, M., Petersen, S., Thiede, J. (Eds.), Encyclopedia of Marine Geosciences. Springer Netherlands, Dordrecht, pp. 764–767.
Zhang, J., Chu, D., Wang, D., Cao, A., Lv, X., Fan, D., 2018. Estimation of spatially varying parameters in three-dimensional cohesive sediment transport models by assimilating remote sensing data. J. Mar. Sci. Technol. 23, 319–332. https://doi.org/10.1007/s00773-017-0477-3.
Zhang, W., Cui, Y., Santos, A.I., Hanebuth, T.J., 2016. Storm-driven bottom sediment transport on a high-energy narrow shelf (NW Iberia) and development of mud depocenters. J. Geophys. Res. Oceans 121, 5751–5772. https://doi.org/10.1002/2015JC011526.
Zhang, W., Didenkulova, I., Kurkina, O., Cui, Y., Haberkern, J., Aepfler, R., Santos, A.I., Zhang, H., Hanebuth, T.J., 2019. Internal solitary waves control offshore extension of mud depocenters on the NW Iberian shelf. Mar. Geol. 409, 15–30. https://doi.org/10.1016/j.margeo.2018.12.008.
Zhang, W., Harff, J., Schneider, R., Meyer, M., Zorita, E., Hünicke, B., 2014. Holocene morphogenesis at the southern Baltic Sea: Simulation of multi-scale processes and their interactions for the Darss–Zingst peninsula. J. Mar. Syst. 129, 4–18. https://doi.org/10.1016/j.jmarsys.2013.06.003.
Zhang, W., Harff, J., Schneider, R., Wu, C., 2010. Development of a modelling methodology for simulation of long-term morphological evolution of the southern Baltic coast. Ocean Dyn. 60, 1085–1114. https://doi.org/10.1007/s10236-010-0311-5.
Zhang, Y., Ren, J., Zhang, W., 2020. Flocculation under the control of shear, concentration and stratification during tidal cycles. J. Hydrol. 586, 124908. https://doi.org/10.1016/j.jhydrol.2020.124908.
Zhang, W., Schneider, R., Harff, J., 2012. A multi-scale hybrid long-term morphodynamic model for wave-dominated coasts. Geomorphology 149-150, 49–61. https://doi.org/10.1016/j.geomorph.2012.01.019.
Zhou, Z., Coco, G., Townend, I., Olabarrieta, M., van der Wegen, M., Gong, Z., D'alpaos, A., Gao, S., Jaffe, B.E., Gelfenbaum, G., 2017. Is "morphodynamic equilibrium" an oxymoron? Earth Sci. Rev. 165, 257–267.

3. Density-driven bottom currents control development of muddy basins in the southwestern Baltic Sea

This chapter contains a paper, which was published in Marine Geology as:

Porz, L., Zhang, W., Schrum, C., 2021. Density-driven bottom currents control development of muddy basins in the southwestern Baltic Sea. Marine Geology 438.

The contribution of Lucas Porz and the co-authors to this paper is as follows:

LP and WZ conceived the study. LP carried out the budget calculations, set up the numerical model, processed the model results and the seismo-acoustic data. LP, WZ and CS discussed the results. LP wrote the manuscript in consultation with WZ and CS. All authors revised the manuscript.

Marine Geology 438 (2021) 106523

Contents lists available at ScienceDirect

Marine Geology

journal homepage: www.elsevier.com/locate/margo

Density-driven bottom currents control development of muddy basins in the southwestern Baltic Sea

Lucas Porz [a,*], Wenyan Zhang [a], Corinna Schrum [a,b]

[a] Institute of Coastal Systems, Helmholtz-Zentrum Hereon, Max-Planck-Strasse 1, 21502 Geesthacht, Germany
[b] Institute of Oceanography, Center for Earth System Research and Sustainability, Universität Hamburg, Bundesstrasse 53, 20146 Hamburg, Germany

ARTICLE INFO

Keywords:
Baltic Sea
Mud depocenter
Bottom currents
Density-driven flow
Major Baltic Inflow
Episodic sedimentation

ABSTRACT

The development of two Holocene muddy depocenters in the southwestern Baltic Sea is investigated using sediment budget analysis and numerical modeling. Material derived from the erosion of coastal cliffs surrounding the study area is shown to dominate the supply of fine-grained sediment to the depocenters, while the riverine contribution is an order of magnitude smaller. Comparison with the sink terms, compiled from published geological data, reveals that a substantial additional source of at least 900 kt/yr is required to close the budget, and high-salinity dense inflows from the North Sea carrying suspended sediment are proposed as an additional source mechanism. Seismo-acoustic data show the long-term impact of strong bottom currents, likely linked to dense-water inflows, which produce contouritic deposits in flow-confining channels. We reproduce two distinct inflow events using a coupled hydrodynamic-sediment transport coastal ocean model. The simulations confirm that major inflows are capable of advecting a significant amount of fine-grained sediment into the study area. A scaling relationship based on the simulated fluxes estimates the average amount of sediment imported in this way to the order of 100–900 kt/yr, which is in agreement with the lower limit of the gap in the budget. The amount of sediment advected seems to scale non-linearly with the intensity of the inflow. More field data points are needed in order to improve the accuracy of modeled fluxes and the precision of the scaling relationship. This study shows how the relative contributions of episodic sedimentation events on the longer-term morphology may be quantified.

1. Introduction

In shelf settings, episodically occurring, high flux events such as benthic storms and gravity-driven flows have been shown to have profound impacts on the sedimentary record in both recent and ancient muddy deposits (e.g. Friedrichs and Scully, 2007; Plint, 2014; Schimmelmann et al., 2016; Zhang et al., 2016a). Notably, the depositional and erosional signals induced by such events intermix with those induced by hemipelagic background sedimentation, and one should consider this fact to avoid misinterpretation of the stratigraphic record (Dott, 1996; Miall, 2015). However, the cumulative contributions of event-based sedimentation are difficult to estimate, because their episodic nature makes them difficult to observe in situ, and because hydro- and bioturbation often homogenize the upper few dm of the sediment column following deposition, thereby muddling any individual, laminated event beds (Nittrouer and Sternberg, 1981; Dott, 1983).

The semi-enclosed configuration of the Baltic Sea makes it an ideal laboratory for studying the role of event-driven sedimentation. The muddy sub-basins of the Baltic Sea represent shelf environments where near-stagnant and often hypoxic conditions have allowed mostly undisturbed sedimentation throughout mid- to late-Holocene. However, episodic disturbances do occur here in the form of saline dense-water inflows from the North Sea via the Kattegat Strait, which traverse the Baltic Sea's sub-basins as bottom-hugging, gravity-driven flows. Although the hydrodynamics of dense-water inflows into the Baltic Sea have been studied extensively using hydrodynamic monitoring and modeling (e.g. Matthäus and Franck, 1992; Meier et al., 2006; Hofmeister et al., 2011; Gräwe et al., 2015; Stanev et al., 2018), the interaction of such inflows with the seafloor and suspended particulate matter (SPM) has received little attention.

Few studies have linked muddy contouritic deposits in the Baltic Sea to inflowing dense waters (Sivkov et al., 2002; Stow et al., 2002; Jensen et al., 2017), and Moros et al. (2017) attributed mm-scale, diagenetic manganese-carbonate layers to individual inflow events occurring in the

* Corresponding author.
E-mail address: lucas.porz@hereon.de (L. Porz).

https://doi.org/10.1016/j.margeo.2021.106523
Received 23 December 2020; Received in revised form 17 May 2021; Accepted 23 May 2021
Available online 27 May 2021

last 120 years. Alternative mechanisms that could influence seabed dynamics have been proposed, such as thermal convection (Moros et al., 2020), which has since been shown to be negligible compared to inflow from the North Sea (Giesse et al., 2020). This underlines the role of inflows as dominant events affecting Holocene sedimentation in the Baltic Sea.

The potential physical impact of dense inflows on the morphology of these depocenters is twofold: 1. the inflows themselves may act as an important conveyor of sediments from the North Sea into the Baltic Sea, and 2. the recurring action of density-driven bottom currents associated with the inflows may control the lateral variation in deposit thickness. A mineralogical study by Gingele and Leipe (2001) found that surface sediments show an increase of the chlorite/kaolinite ratio along the inflow pathway, from the Kattegat into the southwestern Baltic Sea. There are no known significant sources of kaolinite in the southwestern Baltic Sea, but kaolinite is found in erodible relict deposits in the North Sea. This observation is the basis for the hypothesis that sediment-laden inflows advect a substantial amount of material into the Baltic Sea from the North Sea. However, no measurements of near-bottom SPM during inflow events have been able to confirm this. In order to test the hypothesis, we perform a sediment budget analysis of two muddy sub-basins of the southwestern Baltic Sea, the Arkona and Bornholm Basins. The impact of inflows on these depocenters is expected to be particularly strong, as the North Sea waters successively traverse these sub-basins first during inflows. The sediment budget allows a tentative approximation of the amount of material advected toward the study area from the North Sea. To aid this analysis, transport of fine-grained sediment during two monitored inflow events, representing moderate and extreme conditions, is simulated using a three-dimensional hydrodynamic-morphodynamic model. Although the small-scale dynamics and magnitude of each event can be different, the general eastward transport direction is the same for all inflow events. At the same time, sedimentation conditions in the study area have remained relatively stable during the mid- to late Holocene, as evidenced by the consistency of both sedimentation rates and patterns in the Baltic Sea during the past few thousand years (Winterhalter et al., 1981; Sivkov et al., 2002). This allows an upscaling of the model results to a longer timescale, thereby bridging the scales between events and long-term accumulation. Based on the outcomes, we aim to derive a more comprehensive understanding of the role of high-energy and high-flux events on the morphology of large-scale depocenters and help disentangle event-driven from hemi-pelagic sedimentation.

2. Study area

The Baltic Sea is a semi-enclosed marginal sea on the northeastern European shelf (Fig. 1). Our study area is in the southwestern part of the Baltic Sea, where two muddy depocenters are located within the Arkona and Bornholm Basins (Fig. 1c). Few narrow and shallow straits connect the Baltic Sea with the North Sea: The Sound between Denmark and Sweden to the northwest and the Belt Sea between Denmark and Germany to the southwest. The Sound is only 2 km wide at its narrowest point and 10 m deep at its shallowest point, Drogden Sill. The connection with the Belt Sea is less restricted. Here, the Darss Sill represents the main hydrographic barrier.

2.1. Geological background

The Littorina transgression from the postglacial, freshwater Ancylus lake to the present-day, semi-enclosed sea occurring between 10,000 and 5300 yr BP resulted in a change of sedimentation from lacustrine, clay-rich material to brackish mud inside of the Baltic Sea sub-basins (Andrén et al., 2000; Rößler et al., 2011; Kostecki and Janczak-Kostecka, 2012). The resulting mud depocenters largely cover the deeper parts of the sub-basins with thicknesses of a few meters. The general grain size distribution within the sub-basins with fining toward the deeper parts reflects the lower near-bottom hydrodynamic energy with increasing depth. As the base of the mud is both well-defined by a strong seismo-acoustic reflection and easily identifiable in sediment cores, it has been established as a key regional stratigraphic marker (Virtasalo et al., 2016). Since the end of the Littorina transgression, the sedimentary environment has remained relatively stable. As the study area is around the isostatic zero-line (Harff et al., 2017), postglacial isostatic adjustments are not expected to have exerted significant control on the morphology of the depocenters.

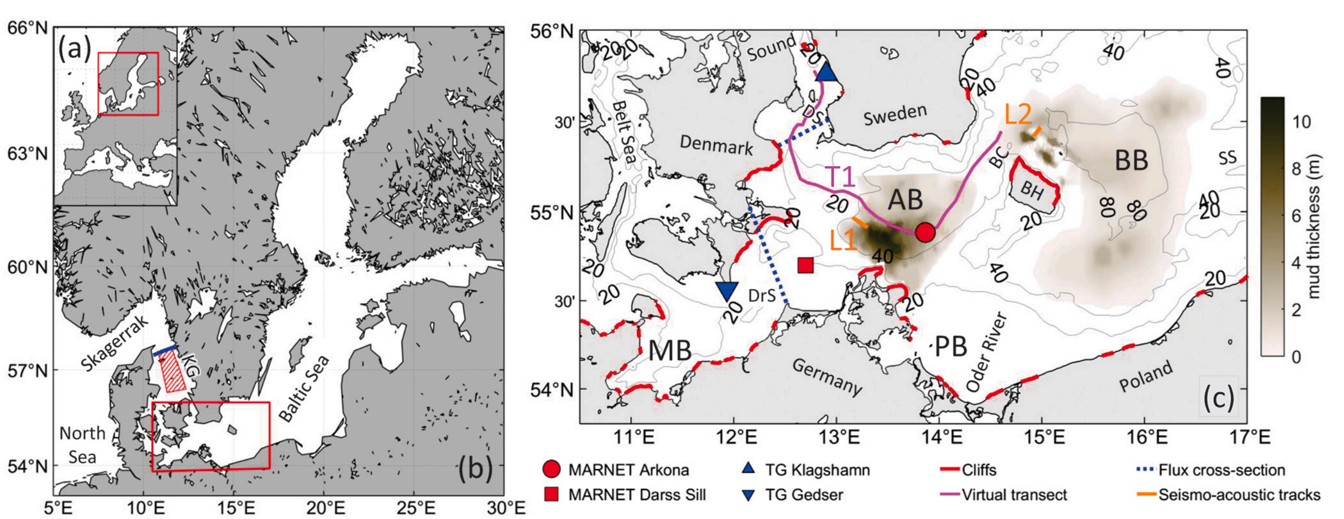

Fig. 1. Location of the Baltic Sea in the (a) European and (b) northern European contexts with the location of the study area (red box), open boundary of the numerical model (solid blue line) and placement of initial surface sediment layer in Kattegat (KG) in the numerical model (red hatched area). (c) Study area with depth contours (BSHC, 2013) at 20, 40 and 80 m. Cliff coasts marked in bold red. Shading indicates the thickness of mud depocenters in the Arkona Basin (AB) and Bornholm Basin (BB) after Lemke (1998) and Bonacker (1996), respectively. MB: Mecklenburg Bight, PB: Pomeranian Bight, BH: Bornholm Island, BC: Bornholm Channel, SS: Stolpe Sill. Blue triangles and red markers denote the positions of the tide gauges and of the monitoring stations, respectively, used to validate the numerical model. Track lines L1 and L2 indicate the positions of the seismo-acoustic profiles shown in Fig. 2. Dotted blue lines represent boundaries in the calculation of salt and sediment fluxes into the study area via the Drogden Sill (DS) and Darss Sill (DrS). Virtual transect T1 is used for the analysis of model results shown in Fig. 8. (For interpretation of the references to colour in this figure legend, the reader is referred to the web version of this article.)

2.2. Morphological configuration

The mud depocenter in the Arkona Basin, located in the western part of the study area, is characterized by a flat, slightly eastwardly dipping modern surface of less than 50 m depth, as shown by a sediment acoustic image of the basin fill (Fig. 2, top). The average thickness of mud in the Arkona Basin is 4.7 m (Lemke, 1998). In contrast to the flat plane of the Arkona Basin fill, the Bornholm Basin's morphology is more variable with depths of more than 90 m. Bornholm Island and its adjacent sills separate the deep waters of these two sub-basins, and their primary hydraulic connection is through the Bornholm Channel north of Bornholm Island, which is a few km in width and branches out into multiple smaller channels as it reaches the Bornholm Basin. A sediment acoustic image across one of these branches shows an asymmetric draping of soft material on one channel levee, indicating the action of bottom currents passing through the channel (Fig. 2, bottom). Mud thickness is less than 1 m in most areas of the Bornholm Basin and 1.1 m on average (Bonacker, 1996). Greater mud thickness is found in local depressions north of Bornholm Island. Outside of the depocenters, there are no known large accumulations of mud in the study area, with most of the seafloor covered by sand, hard (consolidated) clay or hard rock.

2.3. Oceanographic conditions

Because of the limited exchange with the North Sea, the Baltic Sea experiences only a small tidal excursion (<15 cm) and a permanent halocline. The Baltic Sea exhibits an estuarine-like exchange circulation (Fig. 3), with less saline surface water outflowing via the Danish Straits and Kattegat Strait to the North Sea, while denser, more saline water enters in the bottom layer from the North Sea (Burchard et al., 2018). This background exchange is normally not strong enough to ventilate the bottom waters of the Baltic Sea's sub-basins, leading to phases of widespread hypoxia at the bottom of the sub-basins (Carstensen et al., 2014). However, strong pulses of wind-driven inflow, termed Major Baltic Inflows (MBIs), occur episodically and act to replenish the bottom waters of the Baltic Sea (Matthäus and Franck, 1992). During an MBI, a large amount of denser North Sea water travels into the Baltic Sea as a gravity current, and successively spills over the sills into adjacent sub-basins. Statistics of MBI events were recently reviewed by Mohrholz (2018), who found no significant long-term trend of MBI frequency or intensity based on measurements of salinity and water level from 1887 to 2018. The majority of MBIs in the associated dataset is of low intensity with less than 1 Gt of salt import, whereas only few MBIs have been recorded that imported more than 3 Gt of salt. Two specific MBIs, which took place in the winters of 2002/2003 and 2014/2015, are analyzed in this study. In the winter of 2002/2003, an MBI of moderate intensity occurred (Feistel et al., 2003). A very strong MBI took place in the winter of 2014/2015 (Mohrholz et al., 2015; Holtermann et al., 2017). Events of comparable or larger intensity have occurred approximately every 30 years on average in the last century (Mohrholz, 2018).

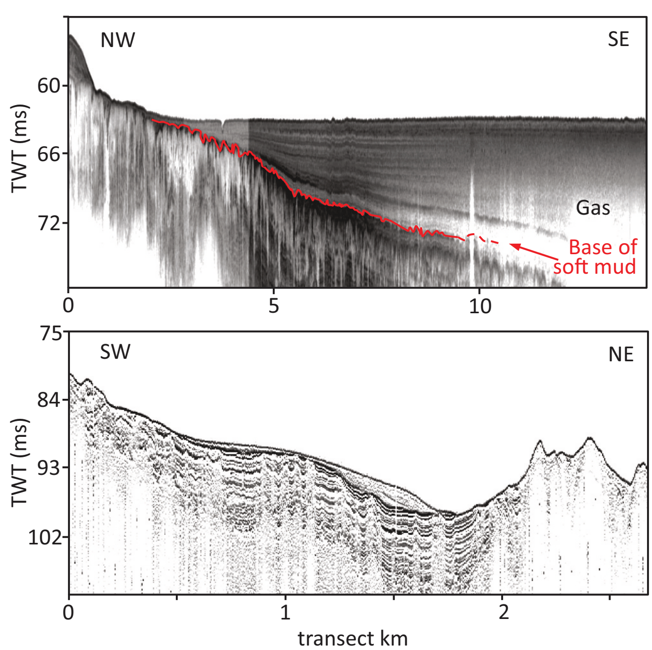

Fig. 2. Sediment acoustic profiles (15 kHz) across parts of the mud depocenters in the study area (see Fig. 1c for locations). Top: Profile L1 across the western margin of the Arkona Basin depocenter. A red line indicates the base of the Holocene soft mud overlying the rough surface of denser Baltic Ice Lake sediments. The occurrence of gas masks the signal toward the center of the basin. Bottom: Profile L2 across the end of the Bornholm Channel leading into the Bornholm Basin. An asymmetric, acoustically transparent layer drapes the southwestern channel levee. (For interpretation of the references to colour in this figure legend, the reader is referred to the web version of this article.)

3. Data and methods

3.1. Budget analysis

Budget analysis of mud fluxes in coastal seas is a useful means to understand sources, sinks, and transport pathways of fine-grained sediment. Examples include the mud budgets compiled for the North Sea by McCave (1973), the western Adriatic Sea by Weltje and Brommer (2011), and for the Bohai, Yellow, and East China Seas by Qiao et al. (2017). We identify and estimate the contribution of three primary source mechanisms to the fine-grained sediment budget of the Arkona and Bornholm Basins: the erosion of soft chalk and moraine cliffs of the surrounding coasts, biogenic production, and fluvial supply of particulate matter. Two primary sink terms are considered: accumulation in the Arkona and Bornholm Basins, and outflow toward the North Sea within the surface waters. We assume that all fine material that enters the study area eventually either ends up in the mud depocenters or leaves the study area toward the west, which is a reasonable assumption considering that the mud depocenters are the only known large accumulations of mud in the study area. In addition, cross-shore transport of fine material from the SW Baltic coast to the center of Arkona Basin has been observed (Emeis et al., 2002), further supporting our assumption of basin-directed transport. Inter-basin transport of mud seems to be quite limited, as the sub-basins have distinct mineralogical compositions (Miltner and Emeis, 2001). Therefore, material exchange from and toward the Gotland Basin to the east is assumed negligible.

Mass erosion rates of cliffs may be computed according to.

$$Q_{er} = \sum_i L_i \cdot Y_i \cdot H_i \cdot \rho_i \cdot S_{\text{fines},i}, \tag{1}$$

where L_i, Y_i, H_i, ρ_i, and $S_{\text{fines},\,i}$ are the width, lateral retreat rate, height, dry bulk density, and proportion by weight of fine grains of the cliff section i, respectively. Cliff widths and erosion rates are compiled from erosion maps of the Baltic coasts surrounding the Arkona and Bornholm Basins: Germany (StAuN, 1994; Ziegler and Heyen, 2004), South Sweden (Persson et al., 2014), Denmark (Kabuth et al., 2014) and Poland (Uścinowicz et al., 2004; Uścinowicz et al., 2014). Digital elevation models (GUGIK, 2019; LAIV-MV, 2019) provide cliff heights in m-scale resolution in the horizontal and vertical. Both bulk density and proportion of fines vary spatially with the local cliff lithology in the study area (Terefenko et al., 2019), but lithological data are not available for the entire coastline. Typical values for dry bulk densities are in the range of 1.6–2.0 g/cm^3 for glacial tills (Clarke et al., 2008) and 1.4–1.6 g/cm^3 for soft chalk cliffs (Mortimore et al., 2004). Lithological measurements at the Polish coast suggest that the dry bulk density of the cliffs does not exceed 1.8 g/cm^3 on average, and that the cliffs show high lithological

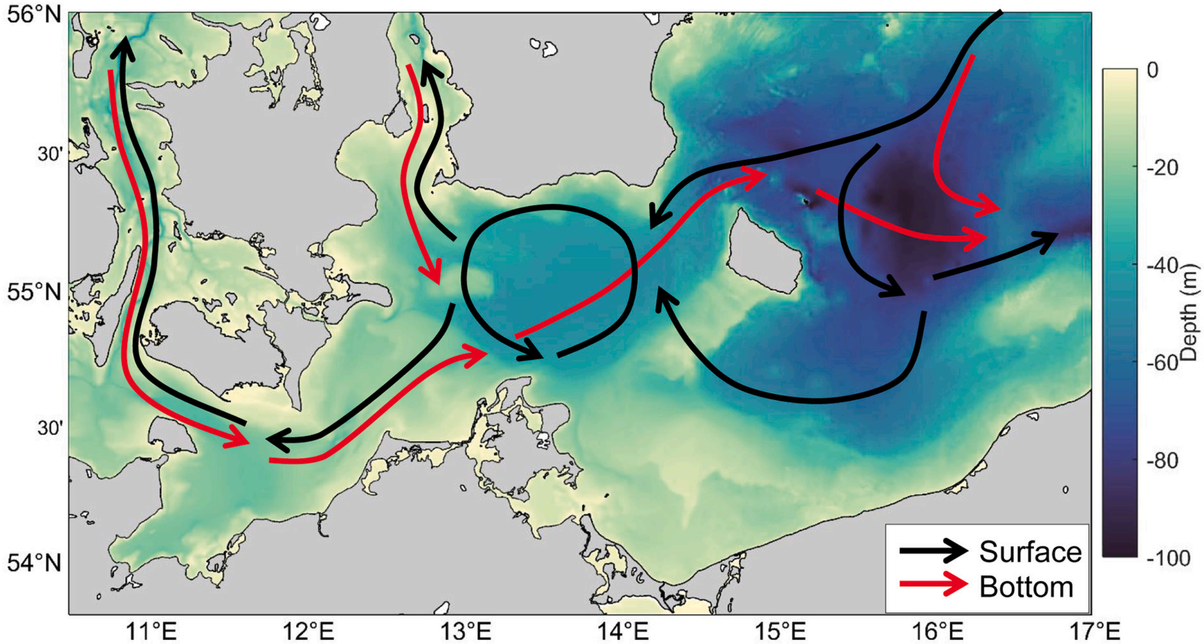

Fig. 3. Bathymetry (BSHC, 2013) and schematic illustration of mean circulation patterns in the study area in the surface (black arrows) and bottom (red arrows) after Elken and Matthäus (2008) and Meier (2007). (For interpretation of the references to colour in this figure legend, the reader is referred to the web version of this article.)

similarity along the coast (Olszak et al., 2011; Kruczkowska et al., 2019). Glacial till is known to be heterogeneous in terms of grain size composition. For the proportion of fines within the cliff rock, a range of values has been used in previous budget calculations at different sections of the German Baltic Sea coast, e.g. 33% (Lampe et al., 2007) and 70% (Emeis et al., 2002). These ranges of values for bulk densities and the proportion of fines allow an estimate of the upper and lower limits of mud supplied from cliff erosion.

Data in Emelyanov (2014) suggest that between 6 and 14% of the muddy sediment in the southwestern Baltic Sea is biogenic (organic carbon, calcium carbonate, and biogenic opal), from which an estimate for the range of biogenic sediment sources can be deduced.

The load of the Oder River, which enters the Baltic Sea at the German-Polish border (Fig. 1c), is the major riverine source of fine-grained sediment entering the study area. The Oder's discharge accounts for more than 80% of the freshwater discharge among rivers surrounding the study area, according to data compiled by Daewel and Schrum (2013). An estimate of the amount of fines exported from the Oder River was compiled by Zhang (2016) on the basis of geochemical analyses (Emeis et al., 2002) and numerical modeling (Zhang et al., 2013). According to their results, ~80% of the Oder river load is transported toward the Baltic sub-basins, amounting to 272 kt/yr. Supply by the smaller rivers is ignored for a lack of load data, but their cumulative load can be assumed to be an order of magnitude smaller than that of the Oder.

Our estimates of bulk sedimentation rates in the study area are based on published values for accumulation rates from sediment cores and total mud volumes extracted from acoustic data. Recent sedimentation in the Arkona Basin is spatially relatively uniform with a sedimentation rate of 1 mm/yr (Kostecki and Moska, 2017). Meanwhile, the Bornholm Basin experiences an elevated sedimentation rate of 2 mm/yr in local depressions (Andrén et al., 2000; Binczewska et al., 2018), and rates are three times lower in shallower parts (Christoffersen et al., 2007). Setting the culmination of the Littorina transgression to 5300 yr BP according to Kostecki and Moska (2017) results in an average accumulation rate of 0.9 mm/yr for the Arkona Basin, which agrees to within 10% with the value of 1 mm/yr reported by Kostecki and Moska (2017) based on luminescence dating. By the same argument, the spatially averaged accumulation rate in the Bornholm Basin is 0.2 mm/yr. However, the transgression in the Bornholm Basin has been dated as early as 7850 yr BP (Andrén et al., 2000), representing a sedimentation rate of only 0.14 mm/yr. In accordance with measurements by Endler (1992), we assume a grain density of 2.65 g/cm^3 and an equilibrium porosity of 70% for the mud deposit, resulting in a dry bulk density of 0.8 g/cm^3, which matches the value used by Gingele and Leipe (2001) in their calculation of total mud mass in the basins. This allows an estimate of the range of potential total accumulation rates in the Arkona and Bornholm Basins.

The long-term (multi-decadal) average volume of less saline surface waters outflowing from the Baltic Sea has been estimated from both monitoring and modeling studies between 35.000 and 90.000 m^3/s (1104–2838 km^3/yr), according to a survey of Omstedt et al. (2004). Analysis of remote sensing data by Kyryliuk and Kratzer (2019) indicates that the average near-surface SPM concentration in the study area is about 1 mg/l during summer months. In summer, surface SPM is dominated by organic matter from primary production in the inner basins, but inorganic components derived from river loads and coastal erosion are still evident in the surface waters up to 150 km offshore. Sediment transport is expected to be much higher in winter, when the southern Baltic Sea is subject to frequent wave- and current-induced resuspension in depths of up to 40 m, as shown by modeling studies (Kuhrts et al., 2004; Danielsson et al., 2007; Almroth-Rosell et al., 2011). Taking the conservative summer value of 1 mg/l as a background concentration permits an estimate of the range of total SPM advected toward the North Sea.

3.2. Numerical model

3.2.1. Hydrodynamic setup

The three-dimensional numerical modeling system SCHISM (Zhang et al., 2016b) is used to reconstruct the MBIs during the winters of 2002/2003 and 2014/2015. The hydrodynamic core of SCHISM employs a semi-implicit advection scheme for both horizontal and vertical transport. The semi-implicit formulation enhances the numerical stability of the model even for strong bathymetrical gradients, such as they appear in the study area. The model solves the discretized, Reynolds-averaged Navier-Stokes equations on unstructured horizontal grids and a flexible number of vertical layers, allowing for transitions between areas of different depth and resolution without a need for grid nesting. For turbulence closure, the generic length scale model of Umlauf and Burchard (2003) is used with a k-kl closure scheme.

The model setup encompasses the entire Baltic Sea with an open boundary at the Skagerrak-Kattegat transition (Fig. 1b). The horizontal resolution of the model is 1 km in the study area with local refinements of higher resolution in the narrow Danish Straits. Stanev et al. (2018) showed that the simulated transport through the Danish Straits is sensitive to the horizontal model resolution in that area. We follow their suggestion to adjust the resolution in the narrowest parts of the straits to 100 m. Toward the north, outside of the study area, the mesh size is increased to 10 km for computational efficiency. An average of 45 vertical layers are implemented as generalized sigma coordinates according to Song and Haidvogel (1994). The layer resolution increases from about 1 m at the surface to about 0.3 m at the bottom to ensure an adequate representation of bottom currents. The water depth at the model grid nodes is interpolated from the Baltic Sea Bathymetry Database (BSHC, 2013), which represents a composite bathymetry with a source data density of approximately 500 m in the study area. This is higher than the horizontal resolution of the model grid in the study area and is therefore considered adequate for our modeling purpose. Seabed roughness lengths are calculated from the surface grain size map of Al-Hamdani et al. (2007) by converting the grain sizes to grain roughness and form drag roughness induced by ripples according to Yalin (1977) and Nielsen (1983). The initial temperature and salinity fields and the boundary conditions at the North Sea-Baltic Sea transition are prescribed according to the monthly climatology of the World Ocean Atlas (Locarnini et al., 2013; Zweng et al., 2013). Water levels at the open boundary are prescribed according to tide gauges located at Gothenburg, Sweden (SMHI, 2020) and Frederikshavn, Denmark (DMI, 2020) using sea level data available from the European marine observation data network (EMODnet, Novellino et al., 2015). Atmospheric forcing is provided by the CoastDat2 dataset (Geyer, 2014), which represents an hourly hindcast on a 0.22° horizontal grid for Western Europe and the North Atlantic. The simulations of the inflow events are initialized at the start of December 2002 and November 2014, roughly one month before the start of the respective inflows, and three consecutive months are simulated for each inflow.

3.2.2. Sediment setup

The sediment module coupled to SCHISM, described in detail in Pinto et al. (2012), is based on the Community Sediment Transport Modeling System, which was originally developed for the Regional Ocean Modeling System (ROMS, Warner et al., 2008). Classes of suspended sediment are represented as tracer concentration values with sinking velocities depending on grain size, and their transport is handled by the implicit schemes of the hydrodynamic core.

In order to test whether the inflowing waters can lead to resuspension of fine-grained material and its subsequent advection into the Baltic Sea, an erodible layer of sediment predefined at the bottom of the Kattegat Strait at the start of the simulation (see Fig. 1b). This region is known for high near-bottom SPM concentrations, when intermittently deposited mud is resuspended during periods of high bottom shear stress (van Weering et al., 1987; Christiansen et al., 1993; Lund-Hansen and Christiansen, 2008). The initial pool in the Kattegat represents intermittent deposition from the North Sea. In the erodible layer, three sediment fractions of equal parts with the grain density of 2.65 g/cm^3 and grain diameters of 2 μm (fine silt), 20 μm (medium silt) and 63 μm (coarse silt) are initialized, reflecting the total range of expected size classes in pure muddy sediment. The erodible layer has a uniform thickness of 1 cm. Resuspension is computed according to the erosion laws of Winterwerp et al. (2012), using values typical for soft muds presented therein: a critical shear stress for erosion of 0.2 Pa and an erosion parameter of 2×10^{-4} s/m. The settling velocities of the fine, medium and coarse silt fractions are set to 10^{-3}, 10^{-1}, and 10^{0} mm/s, respectively, which correspond approximately to those given by the general formula of Benoît (2007) for the sinking speed of particles when setting the empirical coefficients to typical values for silt. The remaining seafloor is assumed hard bottom to avoid local resuspension that would bias the computation of fluxes. There is no suspended sediment in the water column at the start of the simulations and concentrations are set to zero for inflow at the open boundary.

4. Results

4.1. Mud budget

According to our budget analysis, between 1515 and 3565 kt/yr of fine-grained sediment is supplied to the study area from cliff erosion, representing the largest source contribution. The coasts of Germany and Poland contribute the vast majority, while eroded supply from Sweden and Denmark is negligible in comparison. Likely reasons for the lower erosion rates of the Scandinavian cliffs are higher resistance, as they partially comprise hard rock, and a more sheltered situation from the strong westerly winds that dominate in the study area. At 272 kt/yr, supply from the Oder River is an order of magnitude smaller than from cliff erosion. The biogenic contribution is estimated at 262–746 kt/yr. For the sinks, total sedimentation in the Arkona and Bornholm Basins is 4375–5325 kt/yr of accumulated mass. As an additional sink, the average surface outflow conditions export material toward the North Sea, the amount of which is estimated at 1104–2838 kt/yr.

Table 1 lists the estimated sources and sinks of mud in the study area according to our budget analysis. When comparing the upper (lower) limit of sources with the lower (upper) limit of sinks, the budget reveals an imbalance, wherein 896–6114 kt/yr of material is not accounted for. Inflow from the North Sea represents a possible source mechanism to partially or fully close this gap. The fluxes of fines in the study area are illustrated in Fig. 4.

Table 1
Maximum and minimum values of sources and sinks of fine-grained sediment in the southwestern Baltic Sea basins according to the budget analysis presented herein.

	Amount (kt/yr) min/max
Sources	2049/4583
Cliff erosion*	1515/3565
Germany	716/1880
Poland	445/1168
Denmark	48/125
Sweden	34/120
Riverine (Oder)	272
Biogenic production**	262/746
Sinks	5479/8163
Sedimentation	4375/5325
Arkona Basin†	3118/3464
Bornholm Basin††	1257/1861
Outflow to North Sea‡	1104/2838
Difference (Sinks-Sources)	896/6114

min (max) based on: *30 (70)% fine material and 1.6 (1.8) g/cm^3 cliff dry bulk density,
**6 (14)% biogenic sediment components,
†Sedimentation rate of 0.9 (1.0) mm/yr,
††Transgression age of 7850 (5300) yr BP,
‡ Mean outflow volume of 35.000 (90.000) m^3/s.

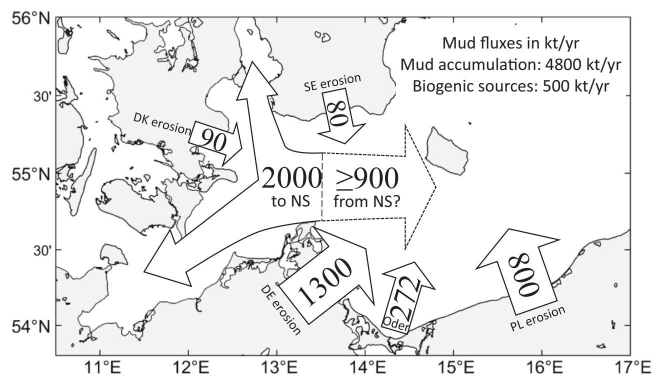

Fig. 4. Estimated fine-grained sediment fluxes in the southwestern Baltic Sea in kt/yr, including cliff erosion, riverine supply, and fluxes to and, possibly, from the North Sea (NS). See Table 1 for details and value ranges.

4.2. Numerical model results

4.2.1. Validation of model hydrodynamics

In order to validate the numerical model, we use water level and salinity as proxies for water volume flow and density gradients, respectively. The model validation is presented here in detail for the 2014/2015 MBI. Additional information on the validation of the 2002/2003 MBI can be found in the supplementary material.

After about 10 days of spin-up following the model initialization, the water level in the southwestern Baltic Sea has equilibrated, as shown in comparison with data from tide gauges in Sweden and Denmark (Fig. 5). The modeled sea level shows a near-synchronous response at both tide gauges and matches the observations well, though the small tidal oscillations are slightly underestimated by the model. After the spin-up period, the RMSE between modeled and measured water level is less than 13 cm at both tide gauges with a slight bias of −4.6 cm, and the correlation between model and observation is above 90%.

Comparison of modeled salinity to data from the mooring site located near the center of the Arkona Basin as part of the MARNET monitoring network (BSH, 2020) shows that the inflow dynamics are reproduced adequately (Fig. 6). Both the data and model show an elevation of the halocline position in mid-December following the MBI, resulting from the baroclinic flow of dense water into the basin. Both time-series show a strong oscillating signal with a period of about 14.7 h corresponding to the inertial period. Bottom salinities are slightly underestimated and the halocline depth following the inflow is somewhat shallower in the model, while surface salinities are slightly higher in the model. The correlation of modeled and measured salinities at this station during the inflow is 94%, and the RMSE is 1.8 PSU.

A comparison between simulated east-west currents during the inflow period and observation data from ADCP sensors at Darss Sill (BSH, 2020) shows a correlation of 76% over the entire water column (Fig. 7). The RMSE between modeled and measured east-west current speeds during the inflow is 6.0 cm/s, compared to a natural variability of 24.8 cm/s.

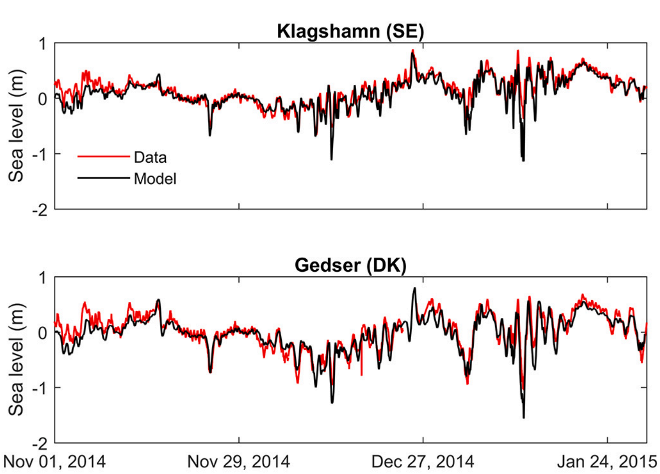

Fig. 5. Water level at tide gauge stations in Klagshamn, Sweden (top) and Gedser, Denmark (bottom) as computed by the model (black) and measured at tide gauge stations (red) for the 2014/2015 MBI. (For interpretation of the references to colour in this figure legend, the reader is referred to the web version of this article.)

4.2.2. Hydrodynamics during inflow events

In the 2014/2015 MBI, a precursor period lasting until mid-December associated with a slight decrease in water level is observed preceding the inflow (Fig. 5). This decrease is caused by easterly winds (see Fig. 6a), which push water toward the North Sea. After this precursor period follows the inflow period starting in mid-December. The inflow period is associated with strong westerly winds and an elevation in water levels.

The bottommost salinity sensor at the Arkona Basin mooring site is located in a depth of 43 m, about 2 m above seafloor. This sensor measured first signs of high-salinity, dense bottom waters on 11th December (Fig. 6b). The simulation shows this water mass entering the Baltic Sea through the Sound as saline dense plume, which is several meters in thickness and travels into the Arkona Basin as a bottom current (Fig. 8, Fig. 10b). A sharp density gradient marks the front of the gravity flow. Current velocities of close to 80 cm/s occur near the front. This is followed by a second water mass entering through the Belt Sea on 17th December (Fig. 6b, Fig. 10c), taking a longer path than the Sound water. Having entrained ambient water along its path, the Belt Sea water mass arrives later and with lower salinities. Thus, when reaching the Arkona Basin, it no longer propagates along the bottom but is wedged between the salty bottom and fresher surface waters. The inpouring saline water temporarily raises the halocline of the Arkona Basin from about 40 m to about 10 m depth. After about one month, the westerly winds abate, marking the end of the inflow event. Due to the raised halocline to about 30 m depth, the saline water continues through the Bornholm Channel into the Bornholm Basin.

The total transport of salt into the Baltic Sea computed by the model during the 2014/2015 simulation is 6.0 Gt (Fig. 9). The amount advected between the 13th and 25th December 2014 is 2.96 Gt. This is 12% lower than the 3.38 Gt calculated by Mohrholz et al. (2015) from sea level difference and salinity measurements, but matches closely the value of 3.09 Gt computed by the numerical model of Gräwe et al. (2015). It is noteworthy that the definition of an MBI employed by (Mohrholz, 2018) is based on identification of periods with continuous inward directed volume transports, causing larger inflows to be split into several minor events or to be cut off prematurely. This seems to be the case for the 2014/2015 MBI, where the simulation shows that the first inflow period is followed by a second pulse, which carries an additional 2 Gt of salt into the Baltic Sea. The reader is referred to Mohrholz et al. (2015) and Gräwe et al. (2015) for detailed analyses of the 2014/2015 MBI.

The 2002/2003 simulation shows similar dynamics as the one in 2014/2015, though only half of the amount of salt is imported during the simulation (Fig. 9). At 2.5 Gt, the simulated amount of salt imported between 1st January and 17th January 2003 exceeds the rough estimate by Feistel et al. (2003) of 2.03 Gt based on measurements, but is considerably closer than the value of 3.45 Gt computed by the model of Hofmeister et al. (2011). A noteworthy difference to the 2014/2015 MBI is that, according to our simulation, saline water reaches the Arkona Basin from the Belt Sea and the Sound at approximately the same time in mid-January 2003. The reason is that the bottom waters of the Belt Sea were already more saline during the start of the inflow than in December 2014. The dilution effect due to the longer pathway compared to the

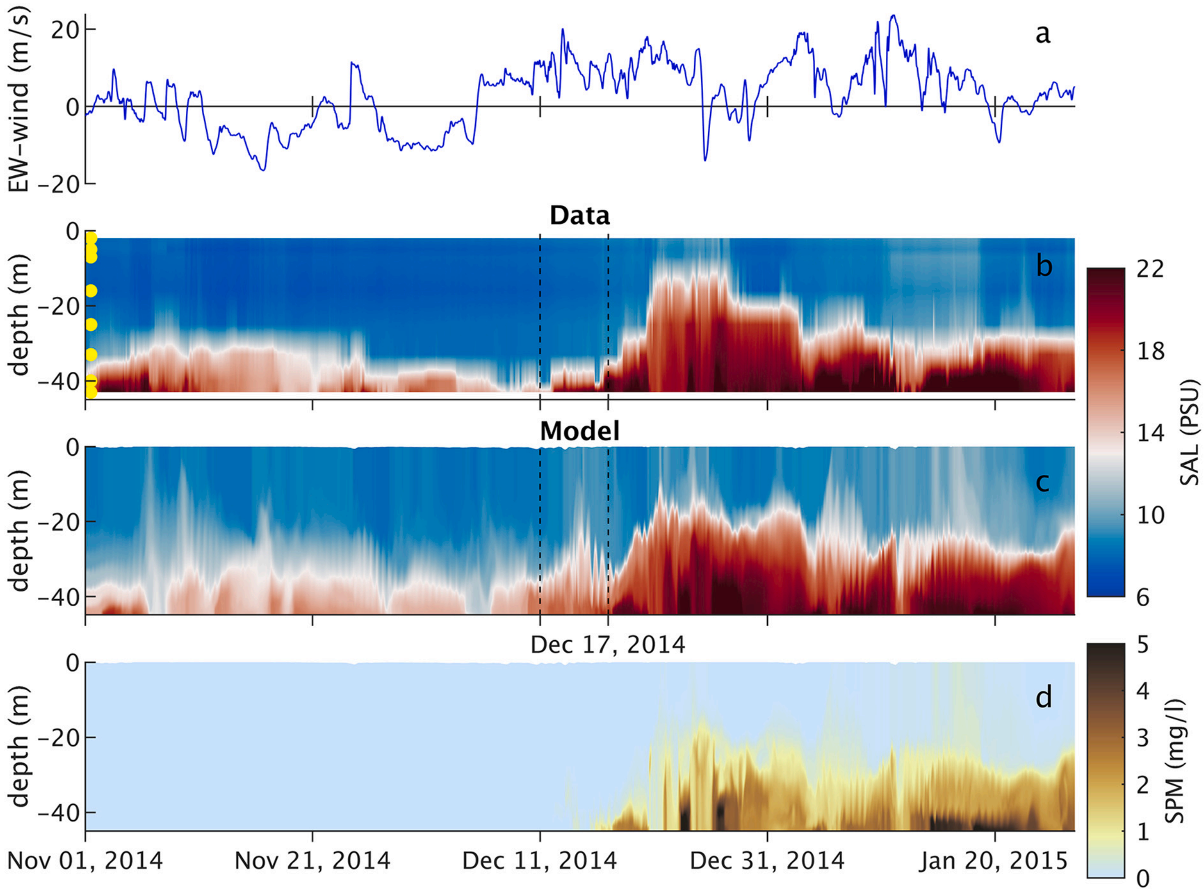

Fig. 6. Time-series of (a) EW-wind component (positive values denote eastward wind direction), (b) measured salinity, (c) modeled salinity, and (d) modeled SPM at the MARNET Arkona mooring station located near the center of the Arkona basin during the 2014/15 MBI. Yellow points denote sensor depths. (For interpretation of the references to colour in this figure legend, the reader is referred to the web version of this article.)

Sound are apparent in both MBIs.

4.2.3. Simulated sediment fluxes and upscaling

Bottom SPM concentrations of about 5–10 mg/l are maintained in the Kattegat region during the 2002/2003 MBI simulations, with occasional bursts of up to 30 mg/l during strong wind gusts. These values compare favorably with those measured by Lund-Hansen and Christiansen (2008) during autumn 2002 of 8–22 mg/l. During the 2014/2015 MBI, modeled bottom concentrations in this region are higher at 10–15 mg/l, occasionally reaching up to 70 mg/l locally.

In the model experiments, fine and medium silt are advected into the Arkona and Bornholm Basins along with the high-salinity dense water from the Kattegat during the inflows (Fig. 6d and Fig. 10), while the coarse silt fraction (not shown) remains near the initial pool. Carried by the dense plume, silt enters the study area as a dilute suspension (<10 mg/l) within the bottom layers, and is kept in suspension due to enhanced turbulence at the plume front (Fig. 8). Although the model accounts for the effect of suspended sediment on water density, the suspension does not add to the negative buoyancy of the flow significantly in this case. At the end of the simulations, 126 kt and 630 kt of silt-like sediment have been advected into the study area via the Darss and Drogden Sills during the 2002/2003 and 2014/2015 MBIs, respectively (Fig. 9). The fine silt fraction makes up the vast majority of the SPM, while the medium silt fraction is minimal. For the 2014/2015 MBI, about 95% of the transported sediment is fine silt, and this portion is even higher at 99% in the 2002 MBI. The spatial extent of the modeled deposit about one month after the end of the inflow event roughly matches the area where surface mud is located in reality (Fig. 11).

We apply the dataset of historical MBI intensities compiled by Mohrholz (2018) in order to upscale our model results in time (Fig. 12). The dataset contains dates and amounts of salt advected into the Baltic Sea for 1426 MBIs. According to a linear scaling of advected sediment with advected salt, 116 kt of sediment per Gt of salt are advected during an MBI, on average. Applying this to the entire MBI time series results in an average sediment inflow of 467 kt/yr. Extending this relationship to the total average salt flux to the Baltic Sea (8.2 Gt/yr according to Mohrholz, 2018) brings the advected sediment to 950 kt/yr.

In-situ monitoring during a small MBI during October 2002 showed elevated SPM bottom concentrations in the northern Kattegat, but no signs of higher concentrations in the Arkona Basin (Lund-Hansen and Christiansen, 2008). This observation suggests that only events above a certain intensity can transport a significant amount of SPM into the study area, such that there exists a non-linear relationship between salt and sediment inflow. Considering this information, a scaling relationship using an exponential fit is applied, which brings the average amount of sediment advected during MBIs to 108 kt/yr.

5. Discussion

5.1. Implications

Our sediment budget analysis indicates that the major source of fine-grained sediment in the study area are the cliffs located on the Baltic Sea coasts of Germany and Poland. Contrasting the sediment sinks with the upper limit of sources from cliff erosion, riverine supply and biogenic production reveals that additional input on the order of 1000 kt/yr is

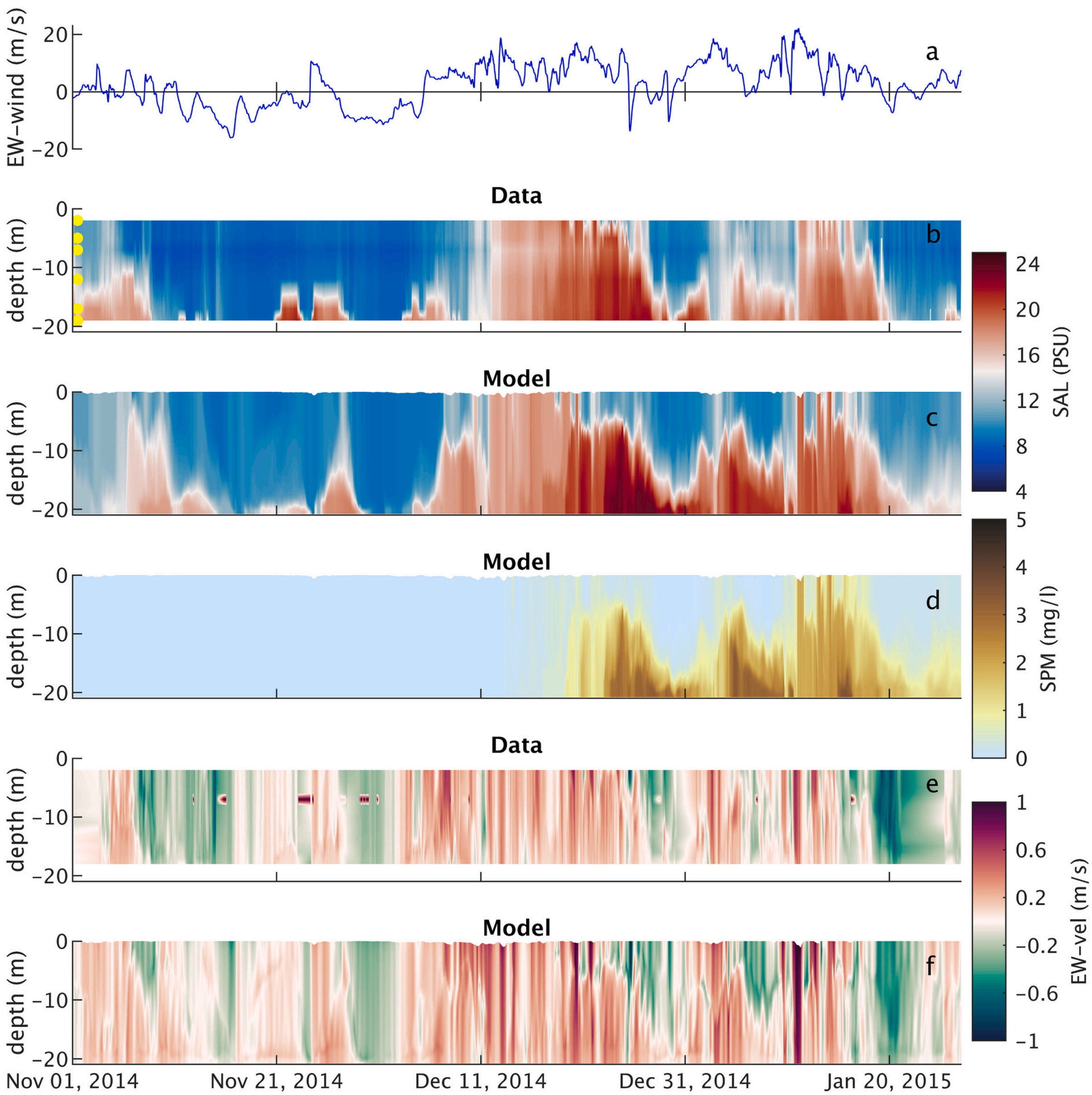

Fig. 7. Time-series of (a) EW-wind component, (b) measured salinity, (c) modeled salinity, (d) modeled SPM, (e) measured EW-current speed, and (f) modeled EW-current speed at the MARNET Darss Sill mooring station during the 2014/15 MBI. Yellow points denote sensor depths. Positive values in (a, e, f) denote eastward flow directions. (For interpretation of the references to colour in this figure legend, the reader is referred to the web version of this article.)

needed to close the fine-grained sediment budget in the study area. Dense water inflows from the North Sea may present a missing source mechanism to close this gap. This result supports the original hypothesis of Gingele and Leipe (2001), who estimated the amount to 1000–5500 kt/yr based on the average inflow volume to the Baltic Sea and a range of possible average suspended loads.

One may expect the imported sediment to scale linearly with imported salt, as both behave like tracers in the water column and are treated as such in the numerical model. Applying such linear upscaling to our model results, the amount of 951 kt/yr of advected sediment is in fair agreement with the total lower limit of 900 kt/yr in our budget calculation. It is also close to the lower estimate of 1000 kt/yr by Gingele and Leipe (2001) when assuming average suspended load of 1 mg/l in the inflowing bottom waters. However, the simulations and measurement data indicate a non-linear relationship of salt and sediment flux, such that an event of higher intensity contributes a disproportionately larger amount. A natural explanation for such a non-linearity is that the critical shear stress for erosion of the sediment pool in the Kattegat is reached more frequently during events of higher intensity, while total transport can be quite low during small events. According to an exponential scaling relationship, sediment transport by MBIs is 108 kt/yr, which is lower than indicated by our budget analysis. A lack of in-situ observation of near-bottom SPM transport during MBIs impedes a precise estimate of transport in the model, and more data points of SPM measurements during MBIs would improve the quality of such a scaling relationship. Nevertheless, the exponential fit explains both the model results and the lack of increased bottom SPM concentrations during the October 2002 MBI measurements. This non-linearity should hold for other sediment transport parameterizations as well. The model results give a strong indication that MBIs introduce a significant amount (on the order of 100 kt/yr) of fine-grained sediment into the Baltic Sea.

It is possible that the supply of sediment to the mud depocenters has changed along with environmental conditions since the end of the Littorina transgression. In this case, the sources given in Table 1 are

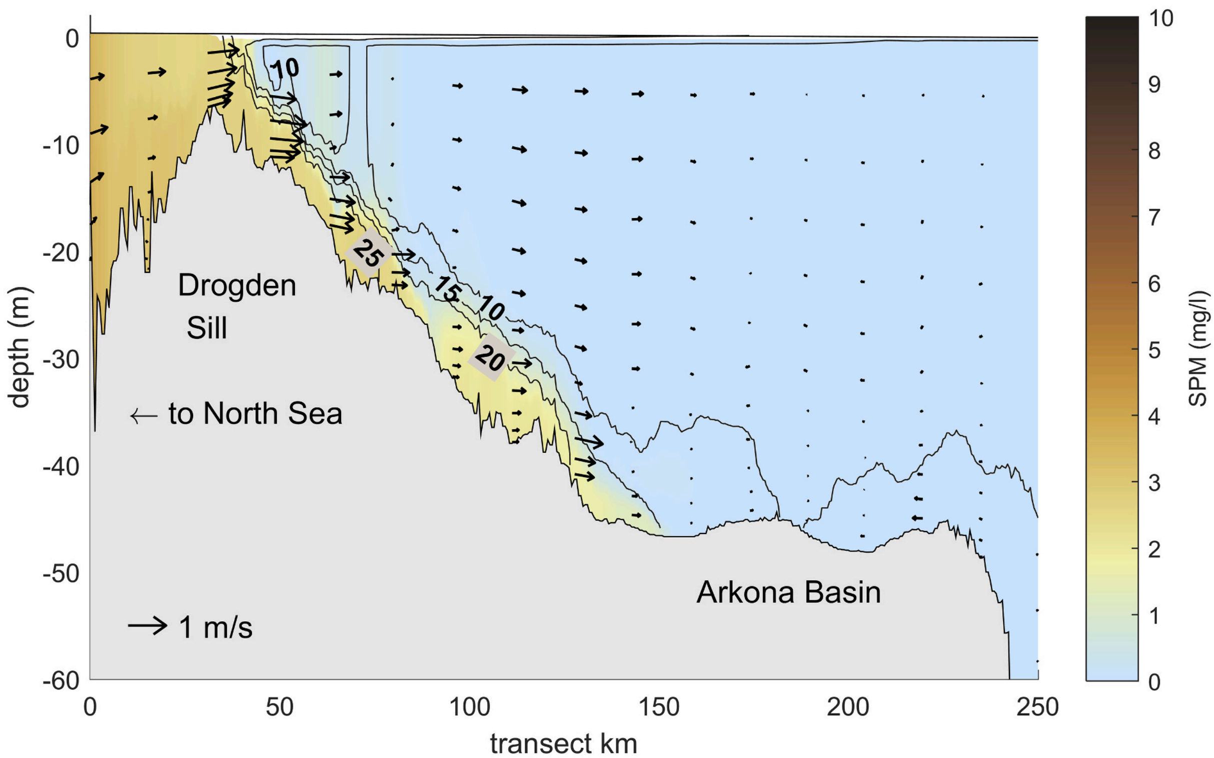

Fig. 8. Transect snapshot of modeled SPM, current velocity and labeled salinity contours during the 2014/2015 MBI (11. Dec. 2014, 6:00:00). See Fig. 1c for the location of the transect (T1). Velocity arrows of the model output are drawn for every fifth and every 30th element in the vertical and horizontal, respectively.

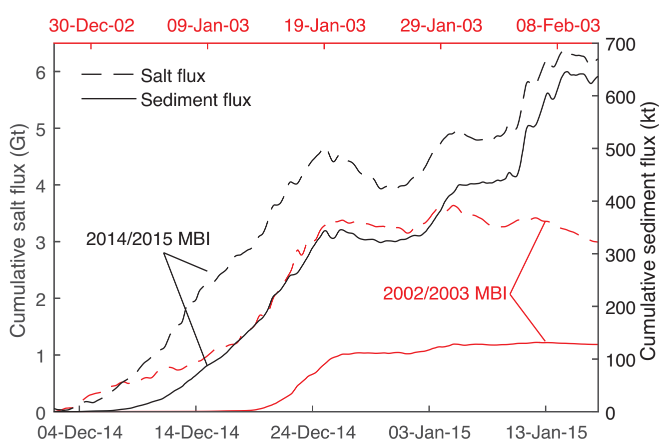

Fig. 9. Time evolution of simulated salt and sediment transport into the study area during the 2002/2003 and 2014/2015 MBIs. Fluxes are calculated across the transects shown in Fig. 1c. A duration of 47 days is shown for both MBIs.

representative of recent supply only. Several studies have correlated changes in muddy sedimentation in the Baltic Sea with changes in climatic conditions and relative sea level in the mid- to late-Holocene, including those related to North Atlantic Oscillation, Medieval Warm Period, and Little Ice Age (e.g. Andrén et al., 2000; Emeis et al., 2003; Zillén et al., 2008; Harff et al., 2011; van Wirdum et al., 2019). Though the overall climate in the Baltic Sea region has shown some variation in the mid- to late-Holocene, there is no indication of strong trends from which one could deduce major changes in sediment supply. This notion is supported by the apparent consistency of sedimentation rates and patterns in the study area following the Littorina transgression. Moreover, the fossil and geochemical proxies utilized in those studies do not allow inferences about changes in MBI statistics. For example, while MBIs do promote bioturbation by ventilation, they are also the source of permanent stratification, which allows hypoxia to develop in the first place, and temperature may have a stronger effect on hypoxia than inflow frequency. Similarly, salinity changes may be attributed to changes in precipitation and river runoff rather than exchange with the North Sea. The amount of terrigenous sources may also have varied since the Littorina transgression. Reconstructions of relative sea level from the German and Polish Baltic coasts show a rapid rise during the transgression (ca. 8–5 kyr BP), after which the rate of sea level rise slowed to the current rate of about 1 mm/yr (Lampe, 2005; Uścinowicz, 2006). It is conceivable that terrigenous supply to the mud depocenters was significantly higher during the earlier part of their development, when more rapid sea level rise caused higher coastal erosion rates.

It cannot be ruled out that additional sources, such as erosion of subaqueous relict deposits in the nearshore or aeolian input, including volcanic dust, also contribute to the fine-grained sediment budget of the study area. Such figures are exceptionally difficult to estimate. At 1600 kt/yr, aeolian input makes up a surprisingly large portion of the North Sea mud budget according to McCave (1973). There are no significant sources of dust within northern Europe, but silt-sized particles are known to travel over remarkably long distances in the atmosphere (van der Does et al., 2018). For example, simulations by Dobricic (1997) show dust deposition as high as 2 g/m^2 in our study area within one week following a single Saharan dust event. However, such events are considered rare and each one would amount to less than 1 kt of deposition for the entire study area.

Even though no surface waves are considered in the model, which would prevent mud deposition in shallow areas, mud deposition simulated by the model is limited in the nearshore and occurs primarily in the basins. In the Arkona Basin, the patchy deposition caused by individual events is likely to be flattened by following events, and deposition on shallow nearshore areas is expected to be reworked by surface gravity waves which penetrate to 20–30 m water depth during storms (Zhang et al., 2010). Previous modeling efforts of fines in the study area suffered the deficiency that sediment originating from the shallow coasts

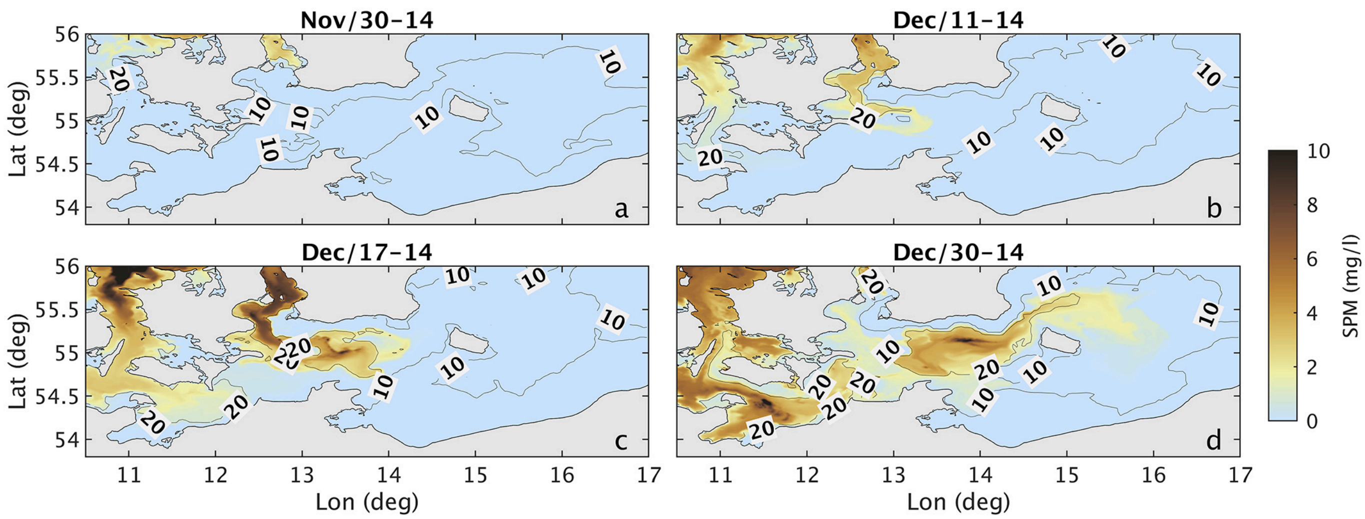

Fig. 10. Modeled bottom SPM and salinity contours at 10 and 20 PSU in the bottom model layer during the 2014/2015 MBI (a) shortly before the start of inflow, (b) during inflow via Drogden Sill, (c) during inflow via Darss Sill, and (d) after the inflow.

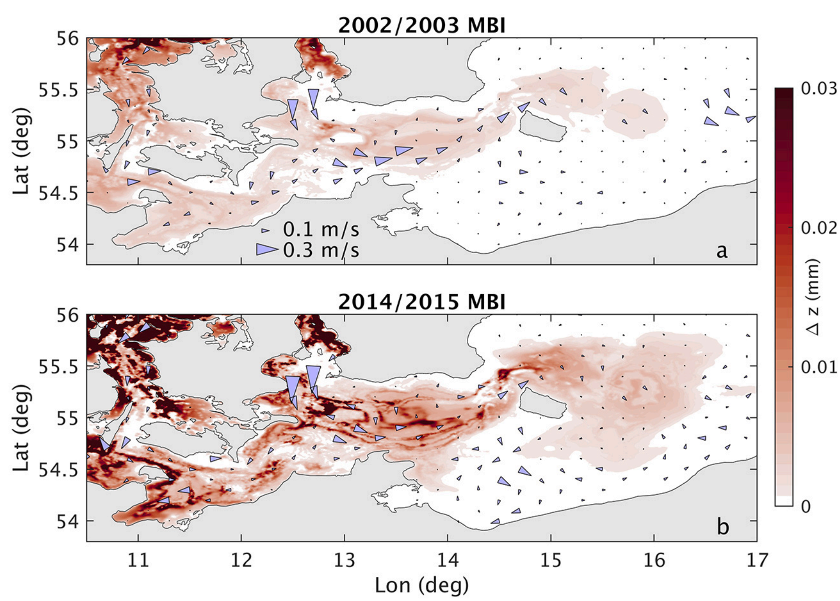

Fig. 11. Modeled deposit thicknesses induced by the dense water inflow about one month after the inflow events and mean bottom current speeds (arrows) during the inflow periods for (a) the 2002/2003 MBI and (b) the 2014/2015 MBI. Modeled current speeds are interpolated to a 0.4° × 0.2°-grid for the purpose of presentation. Note that at this stage, the majority of the advected silt is still in suspension within the water column.

deposited primarily on the slopes of the basins instead of in their centers, and an underestimation of shear stresses was suggested as a likely reason (cf. Kuhrts et al., 2004; Seifert et al., 2009). Our model results suggest that inflow events exert the necessary shear stress to redistribute mud in the deeper parts of the basins rarely impacted by surface waves and transport fines toward the basin centers. While erosion and resuspension by storm waves is the mechanism responsible for delivering suspended matter to the coastal area, transport and shaping by bottom currents during MBIs determine its ultimate fate. This is especially evident in the Bornholm Basin, where model studies show no influence of surface waves on the seafloor (Danielsson et al., 2007; Almroth-Rosell et al., 2011), and bottom currents have produced a muddy contourite depositional system as evidenced in Fig. 2 (bottom).

5.2. Uncertainties and limitations

In absence of more accurate field data, assumptions are needed in the calculation of mud sources and sinks. On those quantities for which insufficient field data are available, we have been careful to select reasonable lower and upper limits. Therefore, we are confident of the estimated gap in sources revealed by the budget analysis.

Despite the fact that a small amount of fines is also deposited in the nearshore areas such as the Mecklenburg Bight and Pomeranian Bight, all of the fine source material is assumed to end up in the Arkona and Bornholm Basin depocenters. Deposition in the bights would only increase the need for additional sources to close the budget.

A quantification of biogenic particulates in the sediment budget in terms of total mass proves challenging, because carbon and nutrients may be cyclically regenerated as long as they are bioavailable. In a study of mass fluxes in the Pomeranian Bight between Germany and Poland, Emeis et al. (2002) suggested that primary production of diatoms in the bight delivers around 120 kt/yr of biomass to the Arkona and Bornholm Basins. However, their biological mass balance estimates suggest that all pelagic biomass produced in the surface layer of the bight should be

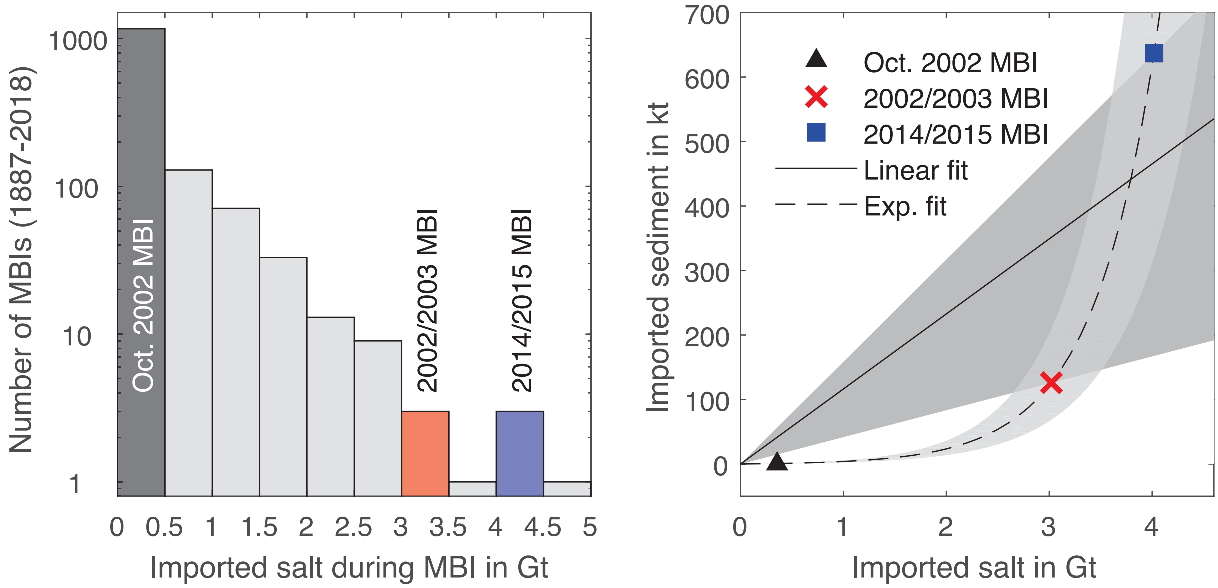

Fig. 12. Left: Histogram of MBI intensity according to the time-series of MBI activity between 1887 and 2018, as compiled by Mohrholz (2018). Colored bars indicate the intensities of the MBIs used to upscale the sediment fluxes: the Oct. 2002 MBI (as measured by Lund-Hansen and Christiansen, 2008), and the 2002/2003 and 2014/2015 MBIs (modeled in this study). Right: Upscaling of sediment fluxes with salt fluxes during MBIs using a linear scaling law (solid) and an exponential law (dashed). For the linear scaling, only the 2002/2003 and 2014/2015 MBIs are considered. Shaded areas indicate the uncertainty of the scaling, given by individual data points in the case of the linear model and by the 95% confidence interval of the fit in the case of the exponential model. The exponential fit of the form sediment $= a(\exp(b\ \text{salt}) - 1)$, with sediment given in kt and salt given in Gt, yields $a = 0.96$ and $b = 1.62$.

respired within the bight by pelagic and benthic processes, and thus no net export of organic carbon out of the bight should take place. A more reliable estimate of buried biogenic particulates may be obtained from analyses of the sediment itself. According to Leipe et al. (2011), who measured the organic carbon content in Baltic Sea surface sediments, organic carbon burial in the entire Baltic Proper reaches the order of 1000 kt/yr, albeit with considerable uncertainty (1840 ± 1470 kt/yr). However, the provenance of this organic matter remains unclear. For example, geochemical analysis of surface sediments yielded that up to 30% of organic carbon in the Baltic Sea is of terrestrial origin (Miltner and Emeis, 2001). Therefore, to consider all biogenic particulates as independent, autochthonous sources amounts to double billing of some constituents, as they may be included in the terrigenous source terms as well. Given this, autochthonous sedimentation should not exceed our upper limit of 746 kt/yr based on sediment compositional maps of Emelyanov (2014).

An important uncertainty in our mass balance concerns the sedimentation rates as computed by the total mass and age of the depocenters. The uniform value of 1 mm/yr applied for the Arkona Basin depocenter is supported by core analyses and is thus deemed as representative of modern sedimentation rates. By contrast, total sedimentation rates in the Bornholm Basin are more difficult to estimate due to a strong spatial inhomogeneity. Here, our values are based solely on published isopach maps of the depocenter and its age, i.e. the timing of the transgression to brackish conditions. It is widely accepted that this transgression was complex and was recorded at different times in different sub-basins (e.g. Andrén et al., 2000; Kortekaas et al., 2007; Rößler et al., 2011). Proposed datings of the transgression span a few thousand years depending on core location, dating method, and age calibration model. Setting the transgression in the Bornholm Basin at 7850 yr BP instead of 5300 yrs. BP, as suggested by Andrén et al. (2000) based on dating of bulk sediment samples, decreases the sinks in our budget by about 500 kt/y. However, we consider it unlikely that the transgressions in the adjacent sub-basins manifested that far apart in time. If anything, the Bornholm Basin should have reached brackish conditions after the Arkona Basin had. Dating of bulk material is known to overestimate ages due to vertical mixing of material within the sediment column (Rößler et al., 2011), which is another argument in favor of a younger transgression age.

Though the numerical model is able to recreate the hydrodynamics of MBIs adequately, the choice of sediment properties in the model such as sinking speed remains a first-order approximation. The simulated fluxes are highly sensitive to the sinking speed of the sediment tracers. Most of the sediment advected into the study area during the simulations has a sinking speed equivalent to that of individual fine silt particles, and the amount of medium silt-equivalent sediment advected increases with higher inflow intensity. Modeled SPM concentrations in the Kattegat of around 10 mg/l are nevertheless close to the lower limit of the measurements (8–22 mg/l) by Lund-Hansen and Christiansen (2008) during autumn 2002, indicating that SPM fluxes may be under- rather than overestimated by the model.

Our model runs terminate after the inflows have reached Bornholm Basin. At about 60 m depth, the Stolpe Sill represents a major barrier for the eastward passage of bottom waters from the Bornholm Basin with 90 m depth. It is possible that part of the SPM continues eastward toward the Eastern Gotland Basin via the Stolpe Sill as bottom waters of Bornholm Basin spill over, a phenomenon exhibited in simulations of Gräwe et al. (2015) for the 2014/2015 MBI. Our simulations can provide only a rough estimate of transport to the Eastern Gotland Basin due to a coarse resolution (10 km) outside of the study area. However, the intensity of bottom currents generally decreases after the inflow reaches Bornholm Basin, as the dense water is continually mixed during its transit (Stanev et al., 2018). Furthermore, the depocenter of the Eastern Gotland Basin has a small average mud thickness (~1 m, Gingele and Leipe, 2001), even though it is much deeper, which generally facilitates deposition. This provides evidence that transport toward the Eastern Gotland Basin is quite limited during MBIs compared to the Arkona and Bornholm Basins.

A cohesive behavior of the suspended mud could significantly alter the modeled sediment fluxes. For example, aggregation of silt and clay particles into large aggregates would increase the effective settling rates, leading to lower lateral fluxes. On the other hand, hindered settling effects within high-concentration layers in the near-bottom could decrease effective settling speeds. High organic contents may even allow the development of high-porosity fluff layers. Such fluffy layers have been observed by Emeis et al. (2002) en route from the Mecklenburg Bight to the Arkona Basin. However, organic-mediated phenomena such as flocculation and fluffy layers can be expected to lessen in winter, when primary production is reduced, and when MBIs usually occur.

6. Summary and outlook

The Baltic Sea represents an example of a tide-less, semi-enclosed depositional shelf system, in which muddy depocenters develop under typically near-stagnant hydrodynamic conditions. This study aims to quantify the role of episodic sedimentation events on the long-term development of muddy depocenters using budget analysis and numerical sediment transport modeling.

In the southwestern Baltic Sea, seismo-acoustic data show contouritic mud deposits, indicating a significant influence of episodic dense-water inflow events from the North Sea. Our budget analysis of mud in the southwestern Baltic Sea reveals a shortage of mud sources when compared to mud sinks. The gap in the budget is on the order of 1000 kt/yr, comparable in magnitude to supply by coastal erosion and biogenic production, and exceeds the material supply by riverine input. Sediment-laden inflows from the North Sea represent a possible source mechanism to partially close this gap. We perform a set of numerical model experiments in order to quantify this potential contribution. The numerical model experiments demonstrate that individual MBIs are capable of resuspending and advecting fine-grained material into the study area from the Kattegat Strait. We argue that because the general eastward direction of transport is the same for all MBIs, it is feasible to upscale these model results to timescales during which mean sedimentation conditions have remained stable. We use a 130 yr time-series of hydrographic inflow measurements for the upscaling, resulting in an estimated sediment input of 100–900 kt/yr from the Kattegat, which is at the lower end of the amount indicated by the budget analysis.

Our results indicate that episodic, wind-driven inflow events shape the muddy basins of the southwestern Baltic Sea, both by advection of sediment from the North Sea and by action of near-bottom currents. In an effort to improve the upscaling of individual inflow events, further studies should focus on the role of minor inflows as part of the general background circulation, including baroclinic inflows during summer months. Indeed, wind-driven inflows only account for approximately half of the total salt import to the Baltic Sea (Mohrholz, 2018). Smaller inflows may advect much less sediment individually but occur far more frequently than the large inflow events studied herein. More information on the physical sediment properties is needed in order to constrain parameterizations used in the sediment transport model, and to lower uncertainties in the budget estimation. Furthermore, the mechanisms behind the formation of local contouritic deposits, which are a common feature in the Baltic Sea basins, deserve further investigation.

The methodology of combining budget analysis, numerical modeling of high-energy events, and upscaling of the simulation results to a longer timescale proves useful in advancing our understanding of the processes controlling large-scale sedimentary systems.

Declaration of Competing Interest

The authors declare that they have no known competing financial interests or personal relationships that could have appeared to influence the work reported in this paper.

Acknowledgements

This study is a contribution by the Helmholtz Society through the PoF IV program, Topic 4 „Coastal Zones at a time of global change". W. Zhang acknowledges the support from the I2B project "Unravelling the linkages between benthic biological functioning, biogeochemistry and coastal morphodynamics – from big data to mechanistic modeling" funded by Helmholtz-Zentrum Hereon. Two anonymous reviewers and the associate editor provided highly valuable comments for improving the manuscript. We thank Beate Geyer for supplying the extended CoastDat2 atmospheric hindcast through 2015. Fabian Werner is thanked for supplying a dataset of freshwater discharge in the Baltic Sea region from 1950 to 2014. We further thank Peter Feldens of the Leibniz-Institute for Baltic Sea Research (IOW) for the sediment acoustic data from the Baltic Sea.

Data statement

There is no restriction on the data used in this study. Model code and data used in this study is in the public domain and all resources used have been cited in the article.

Appendix A. Supplementary data

Supplementary data to this article can be found online at https://doi.org/10.1016/j.margeo.2021.106523.

References

Al-Hamdani, Z.K., Reker, J., Leth, J.O., Reijonen, A., Kotilainen, A.T., Dinesen, G.E., 2007. Development of marine landscape maps for the Baltic Sea and the Kattegat using geophysical and hydrographical parameters. Geol. Surv. Denm. Greenl. Bull. 13, 61–64.

Almroth-Rosell, E., Eilola, K., Hordoir, R., Meier, H.E.M., Hall, P.O., 2011. Transport of fresh and resuspended particulate organic material in the Baltic Sea — a model study. J. Mar. Sys. 87, 1–12. https://doi.org/10.1016/j.jmarsys.2011.02.005.

Andrén, E., Andrén, T., Sohlenius, G., 2000. The Holocene history of the southwestern Baltic Sea as reflected in a sediment core from the Bornholm Basin. Boreas 29, 233–250.

Baltic Sea Hydrographic Commission, 2013. Baltic Sea Bathymetry Database version 0.9.3. http://data.bshc.pro/ (Accessed 20 April 2020).

Benoît, C., 2007. Simple and general formula for the settling velocity of particles. J. Hydraul. Eng. 133, 229–233. https://doi.org/10.1061/(ASCE)0733-9429(2007)133:2(229).

Binczewska, A., Moros, M., Polovodova Asteman, I., Sławińska, J., Bąk, M., 2018. Changes in the inflow of saline water into the Bornholm Basin (SW Baltic Sea) during the past 7100 years - evidence from benthic foraminifera record. Boreas 47, 297–310. https://doi.org/10.1111/bor.12267.

Bonacker, P., 1996. Massenbilanzmodell holozäner Ostseesedimente [Research Report]. Institut für Ostseeforschung Warnemünde.

Bundesamt für Seeschifffahrt und Hydrographie, 2020. Marine Environmental Monitoring Network in the North Sea and Baltic Sea. https://www.bsh.de/EN/TOPICS/Monitoring_systems/MARNET_monitoring_network/marnet_monitoring_network_node.html. (Accessed 11 November 2020).

Burchard, H., Bolding, K., Feistel, R., Gräwe, U., Klingbeil, K., MacCready, P., Mohrholz, V., Umlauf, L., van der Lee, E.M., 2018. The Knudsen theorem and the Total Exchange Flow analysis framework applied to the Baltic Sea. Prog. Oceanogr. 165, 268–286. https://doi.org/10.1016/j.pocean.2018.04.004.

Carstensen, J., Andersen, J.H., Gustafsson, B.G., Conley, D.J., 2014. Deoxygenation of the Baltic Sea during the last century. Proc. Natl. Acad. Sci. U. S. A. 111, 5628. https://doi.org/10.1073/pnas.1323156111.

Christiansen, C., Kunzendorf, H., Otto, C., Senstius, J., 1993. Recent and subrecent sedimentary conditions in the southern part of the North Sea–Baltic Sea transition. Boreas 22, 357–366. https://doi.org/10.1111/j.1502-3885.1993.tb00199.x.

Christoffersen, P.L., Christiansen, C., Jensen, J.B., Leipe, T., Hille, S., 2007. Depositional conditions and organic matter distribution in the Bornholm Basin, Baltic Sea. Geo-Mar. Lett. 27, 325–338. https://doi.org/10.1007/s00367-007-0054-6.

Clarke, B.G., Hughes, D.B., Hashemi, S., 2008. Physical characteristics of subglacial tills. Géotechnique 58, 67–76. https://doi.org/10.1680/geot.2008.58.1.67.

Daewel, U., Schrum, C., 2013. Simulating long-term dynamics of the coupled North Sea and Baltic Sea ecosystem with ECOSMO II: Model description and validation. J. Mar. Syst. 119-120, 30–49. https://doi.org/10.1016/j.jmarsys.2013.03.008.

Danielsson, Å., Jönsson, A., Rahm, L., 2007. Resuspension patterns in the Baltic proper. J. Sea Res. 57, 257–269. https://doi.org/10.1016/j.seares.2006.07.005.

Danish Meteorological Institute, Oceanographic Section, 2020. Time Series of Sea Level at Frederikshavn, Denmark. http://www.emodnet-physics.eu/Map/platinfo/piroosplot.aspx?platformid=8569. Accessed 28 May 2020.

Dobricic, S., 1997. Atmospheric transport of desert dust toward European seas: model parameterisation and a simulated case. In: Özsoy, E., Mikaelyan, A. (Eds.), Sensitivity to Change: Black Sea, Baltic Sea and North Sea. Springer Netherlands, Dordrecht, pp. 501–507.

Dott, R.H., 1983. Episodic sedimentation - how normal is average? How rare is rare? Does it matter? 1982 SEPM presidential address. J. Sediment. Petrol. 53, 5–23.

Dott, R.H., 1996. Episodic event deposits versus stratigraphic sequences—shall the twain never meet? Sediment. Geol. 104, 243–247. https://doi.org/10.1016/0037-0738(95)00131-X.
Elken, J., Matthäus, W., 2008. Baltic Sea oceanography. In: BACC Author Team (Ed.), Assessment of Climate Change for the Baltic Sea Basin. Springer, Berlin, pp. 379–386.
Emeis, K.-C., Christiansen, C., Edelvang, K., Jähmlich, S., Kozuch, J., Laima, M., Leipe, T., Löffler, A., Lund-Hansen, L.C., Miltner, A., Pazdro, K., Pempkowiak, J., Pollehne, F., Shimmield, T., Voss, M., Witt, G., 2002. Material transport from the near shore to the basinal environment in the southern Baltic Sea: II: synthesis of data on origin and properties of material. J. Mar. Sys. 35, 151–168. https://doi.org/10.1016/S0924-7963(02)00127-6.
Emeis, K.-C., Struck, U., Blanz, T., Kohly, A., Voss, M., 2003. Salinity changes in the central Baltic Sea (NW Europe) over the last 10000 years. The Holocene 13, 411–421. https://doi.org/10.1191/0959683603hl634rp.
Emelyanov, E.M., 2014. Biogenic components of the Baltic Sea sediments. Russ. Geol. Geophys. 55, 1404–1417. https://doi.org/10.1016/j.rgg.2014.11.005.
Endler, R., 1992. Physikalische Eigenschaften rezenter Schlickablagerungen des Arkonabeckens, Ostsee. Beiträge zur Meereskunde 63, 19–28.
Feistel, R., Nausch, G., Matthäus, W., Hagen, E., 2003. Temporal and spatial evolution of the Baltic deep water renewal in spring 2003. Oceanologia 45.
Friedrichs, C.T., Scully, M.E., 2007. Modeling deposition by wave-supported gravity flows on the Po River prodelta: from seasonal floods to prograding clinoforms. Cont. Shelf Res. 27, 322–337. https://doi.org/10.1016/j.csr.2006.11.002.
Geyer, B., 2014. High-resolution atmospheric reconstruction for Europe 1948-2012: coastDat2. Earth Syst. Sci. Data 6, 147.
Giesse, C., Meier, H.E.M., Neumann, T., Moros, M., 2020. Revisiting the role of convective deep water formation in northern Baltic Sea bottom water renewal. J. Geophys. Res. Oceans 125. https://doi.org/10.1029/2020JC016114 e2020JC016114.
Gingele, F.X., Leipe, T., 2001. Southwestern Baltic Sea—a sink for suspended matter from the North Sea? Geology 29, 215. https://doi.org/10.1130/0091-7613(2001)029<0215:SBSASF>2.0.CO;2.
Główny Urząd Geodezji i Kartografii, Poland, 2019. Digital terrain model in a uniform standard for the total development of 137 167 km2 - GRID mesh 1m. www.geoportal.gov.pl. (Accessed 18 July 2019).
Gräwe, U., Naumann, M., Mohrholz, V., Burchard, H., 2015. Anatomizing one of the largest saltwater inflows into the Baltic Sea in December 2014. J. Geophys. Res. Oceans 120, 7676–7697. https://doi.org/10.1002/2015JC011269.
Harff, J., Endler, R., Emelyanov, E., Kotov, S., Leipe, T., Moros, M., Olea, R., Tomczak, M., Witkowski, A., 2011. Late quaternary climate variations reflected in baltic sea sediments. In: Harff, J., Björck, S., Hoth, P. (Eds.), The Baltic Sea Basin. Springer, Berlin Heidelberg, Berlin, Heidelberg, pp. 99–132.
Harff, J., Deng, J., Dudzińska-Nowak, J., Fröhle, P., Groh, A., Hünicke, B., Soomere, T., Zhang, W., 2017. What Determines the Change of Coastlines in the Baltic Sea? In: Harff, J., Furmańczyk, K., von Storch, H. (Eds.), Coastline Changes of the Baltic Sea from South to East: Past and Future Projection. Springer International Publishing, Cham, pp. 15–35.
Hofmeister, R., Beckers, J.-M., Burchard, H., 2011. Realistic modelling of the exceptional inflows into the Central Baltic Sea in 2003 using terrain-following coordinates. Ocean Model. 39, 233–247. https://doi.org/10.1016/j.ocemod.2011.04.007.
Holtermann, P.L., Prien, R., Naumann, M., Mohrholz, V., Umlauf, L., 2017. Deepwater dynamics and mixing processes during a major inflow event in the central Baltic Sea. J. Geophys. Res. Oceans 122, 6648–6667. https://doi.org/10.1002/2017JC013050.
Jensen, J.B., Moros, M., Endler, R., IODP Expedition 347 Members, 2017. The Bornholm Basin, southern Scandinavia: a complex history from Late Cretaceous structural developments to recent sedimentation. Boreas 46, 3–17. https://doi.org/10.1111/bor.12194.
Kabuth, A.K., Kroon, A., Pedersen, J.B., 2014. Multidecadal shoreline changes in Denmark. J. Coast. Res. 296, 714–728. https://doi.org/10.2112/JCOASTRES-D-13-00139.1.
Kortekaas, M., Murray, A.S., Sandgren, P., Björck, S., 2007. OSL chronology for a sediment core from the southern Baltic Sea: a continuous sedimentation record since deglaciation. Quat. Geochronol. 2, 95–101. https://doi.org/10.1016/j.quageo.2006.05.036.
Kostecki, R., Janczak-Kostecka, B., 2012. Holocene environmental changes in the southwestern Baltic Sea reflected by the geochemical data and diatoms of the sediment cores. J. Mar. Sys. 105-108, 106–114. https://doi.org/10.1016/j.jmarsys.2012.06.005.
Kostecki, R., Moska, P., 2017. Baltic Sea Holocene evolution based on OSL and radiocarbon dating: evidence from a sediment core from the Arkona Basin (the southwestern Baltic Sea). Oceanol. Hydrobiol. Stud. 46, 48. https://doi.org/10.1515/ohs-2017-0031.
Kruczkowska, B., Jonczak, J., Gadziszewska, J., Niska, M., Florek, W., Degórski, M., 2019. The record of postglacial environmental changes of the southern Baltic coastal zone in the sequence of fossil soils. J. Soils Sediments 19, 848–861. https://doi.org/10.1007/s11368-018-2058-4.
Kuhrts, C., Fennel, W., Seifert, T., 2004. Model studies of transport of sedimentary material in the western Baltic. J. Mar. Sys. 52, 167–190. https://doi.org/10.1016/j.jmarsys.2004.03.005.
Kyryliuk, D., Kratzer, S., 2019. Summer distribution of total suspended matter across the Baltic Sea. Front. Mar. Sci. 5, 504. https://doi.org/10.3389/fmars.2018.00504.
Lampe, R., 2005. Lateglacial and Holocene water-level variations along the NE German Baltic Sea coast: review and new results. Quat. Int. 133-134, 121–136. https://doi.org/10.1016/j.quaint.2004.10.005.
Lampe, R., Meyer, H., Ziekur, R., Janke, W., Endtmann, E., 2007. Holocene evolution of the irregularly sinking southern Baltic Sea coast and the interactions of sea-level rise, accumulation space and sediment supply. Bericht der Römisch-Germanischen Kommission 88, 14–46.
Landesamt für innere Verwaltung M-V, Amt für Geoinformation, Vermessung und Katasterwesen, 2019. Digitale Topographische Karte 1:10 000 (DTK10). https://www.geoportal-mv.de/gaia/gaia.php. (Accessed 18 July 2019).
Leipe, T., Tauber, F., Vallius, H., Virtasalo, J.J., Uścinowicz, S., Kowalski, N., Hille, S., Lindgren, S., Myllyvirta, T., 2011. Particulate organic carbon (POC) in surface sediments of the Baltic Sea. Geo-Mar. Lett. 31, 175–188. https://doi.org/10.1007/s00367-010-0223-x.
Lemke, W., 1998. Sedimentation und paläogeographische Entwicklung im westlichen Ostseeraum (Mecklenburger Bucht bis Arkonabecken) vom Ende der Weichselvereisung bis zur Litorinatransgression. Marine Science Reports, 31. Institut für Ostseeforschung Warnemünde.
Locarnini, R.A., Mishonov, A.V., Antonov, J.I., Boyer, T.P., Garcia, H.E., Baranova, O.K., Zweng, M.M., Paver, C.R., Reagan, J.R., Johnson, D.R., 2013. World Ocean Atlas 2013, Volume 1: Temperature. In: Levitus, S., Mishonov, A. (Eds.), NOAA Atlas NESDIS, 73. NOAA National Centers for Environmental Information. https://doi.org/10.7289/v5f769gt.
Lund-Hansen, L.C., Christiansen, C., 2008. Suspended particulate matter (SPM) in the North Sea-Baltic Sea transition: Distributions, inventories, and the autumn 2002 inflows. Geografisk Tidsskrift-Danish J. Geogr. 108, 37–47. https://doi.org/10.1080/00167223.2008.10649587.
Matthäus, W., Franck, H., 1992. Characteristics of major Baltic inflows—a statistical analysis. Cont. Shelf Res. 12, 1375–1400. https://doi.org/10.1016/0278-4343(92)90060-W.
McCave, I.N., 1973. Mud in the North Sea. In: Goldberg, E.D. (Ed.), North Sea Science. MIT Press, Cambridge, Mass, pp. 75–100.
Meier, H.E.M., 2007. Modeling the pathways and ages of inflowing salt- and freshwater in the Baltic Sea. Estuar. Coast. Shelf Sci. 74, 610–627. https://doi.org/10.1016/j.ecss.2007.05.019.
Meier, H.E.M., Feistel, R., Jan, P., Arneborg, L., Burchard, H., Volker, F., Nikolay, G., Natalia, K., Mohrholz, V., Christian, N., Paka, V., Stips, A., Victor, Z., 2006. Ventilation of the Baltic Sea deep water: a brief review of present knowledge from observations and models. Oceanologia 48.
Miall, A.D., 2015. Updating uniformitarianism: Stratigraphy as just a set of 'frozen accidents'. Geol. Soc. Lond., Spec. Publ. 404, 11–36. https://doi.org/10.1144/SP404.4.
Miltner, A., Emeis, K.-C., 2001. Terrestrial organic matter in surface sediments of the Baltic Sea, Northwest Europe, as determined by CuO oxidation. Geochim. Cosmochim. Acta 65, 1285–1299. https://doi.org/10.1016/S0016-7037(00)00603-7.
Mohrholz, V., 2018. Major Baltic Inflow Statistics – revised. Front. Mar. Sci. 5, 384. https://doi.org/10.3389/fmars.2018.00384.
Mohrholz, V., Naumann, M., Nausch, G., Krüger, S., Gräwe, U., 2015. Fresh oxygen for the Baltic Sea — an exceptional saline inflow after a decade of stagnation. J. Mar. Sys. 148, 152–166. https://doi.org/10.1016/j.jmarsys.2015.03.005.
Moros, M., Andersen, T.J., Schulz-Bull, D., Häusler, K., Bunke, D., Snowball, I., Kotilainen, A., Zillén, L., Jensen, J.B., Kabel, K., Hand, I., Leipe, T., Lougheed, B.C., Wagner, B., Arz, H.W., 2017. Towards an event stratigraphy for Baltic Sea sediments deposited since AD 1900: approaches and challenges. Boreas 46, 129–142. https://doi.org/10.1111/bor.12193.
Moros, M., Kotilainen, A.T., Snowball, I., Neumann, T., Perner, K., Meier, H.E.M., Leipe, T., Zillén, L., Sinninghe Damsté, J.S., Schneider, R., 2020. Is 'deep-water formation' in the Baltic Sea a key to understanding seabed dynamics and ventilation changes over the past 7,000 years? Quat. Int. 550, 55–65. https://doi.org/10.1016/j.quaint.2020.03.031.
Mortimore, R.N., Stone, K.J., Lawrence, J., Duperret, A., 2004. Chalk Physical Properties and Cliff Instability, 20. Geological Society, London, Engineering Geology Special Publications, p. 75. https://doi.org/10.1144/GSL.ENG.2004.020.01.05.
Nielsen, P., 1983. Analytical determination of nearshore wave height variation due to refraction shoaling and friction. Coast. Eng. 7, 233–251. https://doi.org/10.1016/0378-3839(83)90019-4.
Nittrouer, C.A., Sternberg, R.W., 1981. The formation of sedimentary strata in an allochthonous shelf environment: the Washington continental shelf. Mar. Geol. 42, 201–232. https://doi.org/10.1016/0025-3227(81)90164-X.
European marine observation data network — EMODnet physics. In: Novellino, A., D'Angelo, P., Benedetti, G., Manzella, G., Gorringe, P., Schaap, D., Pouliquen, S., Rickards, L. (Eds.), 2015. OCEANS 2015 - Genova, pp. 1–6.
Olszak, I., Florek, W., Seul, C., Majewski, M., 2011. Lithology of sediments and stratigraphy of glacial layers of some cliff sections on Central and Western Polish Coast. Geologija 53. https://doi.org/10.6001/geologija.v53i1.1612.
Omstedt, A., Elken, J., Lehmann, A., Piechura, J., 2004. Knowledge of the Baltic Sea physics gained during the BALTEX and related programmes. Prog. Oceanogr. 63, 1–28. https://doi.org/10.1016/j.pocean.2004.09.001.
Persson, K.M., Nyberg, J., Ising, J., Persson, M., 2014. Skånes känsliga stränder–ett geologiskt underlag för kustzonsplanering och erosionsbedömning. SGU-Rapport 20, 30.
Pinto, L., Fortunato, A.B., Zhang, Y.J., Oliveira, A., Sancho, F.E., 2012. Development and validation of a three-dimensional morphodynamic modelling system for non-cohesive sediments. Ocean Model. 57, 1–14.
Plint, G.A., 2014. Mud dispersal across a cretaceous prodelta: Storm-generated, wave-enhanced sediment gravity flows inferred from mudstone microtexture and microfacies. Sedimentology 61, 609–647. https://doi.org/10.1111/sed.12068.

Qiao, S., Shi, X., Wang, G., Zhou, L., Hu, B., Hu, L., Yang, G., Liu, Y., Yao, Z., Liu, S., 2017. Sediment accumulation and budget in the Bohai Sea, Yellow Sea and East China Sea. Mar. Geol. 390, 270–281. https://doi.org/10.1016/j.margeo.2017.06.004.

Rößler, D., Moros, M., Lemke, W., 2011. The Littorina transgression in the southwestern Baltic Sea: new insights based on proxy methods and radiocarbon dating of sediment cores. Boreas 40, 231–241. https://doi.org/10.1111/j.1502-3885.2010.00180.x.

Schimmelmann, A., Lange, C.B., Schieber, J., Francus, P., Ojala, A.E., Zolitschka, B., 2016. Varves in marine sediments: a review. Earth Sci. Rev. 159, 215–246. https://doi.org/10.1016/j.earscirev.2016.04.009.

Seifert, T., Fennel, W., Kuhrts, C., 2009. High resolution model studies of transport of sedimentary material in the south-western Baltic. J. Mar. Sys. 75, 382–396. https://doi.org/10.1016/j.jmarsys.2007.01.017.

Sivkov, V., Gorbatskiy, V., Kuleshov, A., Zhurov, Y., 2002. Muddy contourites in the Baltic Sea: an example of a shallow-water contourite system. In: Geological Society, London, Memoirs, 22, pp. 121–136. https://doi.org/10.1144/GSL.MEM.2002.022.01.10.

Song, Y., Haidvogel, D., 1994. A Semi-implicit ocean circulation model using a generalized topography-following coordinate system. J. Comput. Phys. 115, 228–244. https://doi.org/10.1006/jcph.1994.1189.

Staatliches Amt für Umwelt und Natur Rostock, 1994. Generalplan Küsten- und Hochwasserschutz Mecklenburg-Vorpommern.

Stanev, E.V., Pein, J., Grashorn, S., Zhang, Y.J., Schrum, C., 2018. Dynamics of the Baltic Sea straits via numerical simulation of exchange flows. Ocean Model. 131, 40–58. https://doi.org/10.1016/j.ocemod.2018.08.009.

Stow, D.A.V., Faugères, J.-C., Howe, J.A., Pudsey, C.J., Viana, A.R., 2002. Bottom currents, contourites and deep-sea sediment drifts: current state-of-the-art. In: Geological Society, London, Memoirs, 22, pp. 7–20. https://doi.org/10.1144/GSL.MEM.2002.022.01.02.

Swedish Meteorological and Hydrological Institute, 2020. Time Series of Sea Level at Gothenburg-Larjeholm, Sweden. http://www.emodnet-physics.eu/Map/platinfo/piroosplot.aspx?platformid=26826. (Accessed 28 May 2020).

Terefenko, P., Paprotny, D., Giza, A., Morales-Nápoles, O., Kubicki, A., Walczakiewicz, S., 2019. Monitoring cliff erosion with LiDAR surveys and Bayesian network-based data analysis. Remote Sens. 11, 843.

Umlauf, L., Burchard, H., 2003. A generic length-scale equation for geophysical turbulence models. J. Mar. Res. 61, 235–265. https://doi.org/10.1357/002224003322005087.

Uścinowicz, G., Kramarska, R., Kaulbarsz, D., Jurys, L., Frydel, J., Przezdziecki, P., Jegliński, W., 2014. Baltic Sea coastal erosion; a case study from the Jastrzębia Góra region. Geologos 20, 259–268. https://doi.org/10.2478/logos-2014-0018.

Uścinowicz, S., 2006. A relative sea-level curve for the Polish Southern Baltic Sea. Quat. Int. 145-146, 86–105. https://doi.org/10.1016/j.quaint.2005.07.007.

Uścinowicz, S., Zachowicz, J., Graniczny, M., Dobracki, R., 2004. Geological structure of the southern Baltic coast and related hazards. Pol. Geol. Inst. Sp. Pap. 15, 61–68.

Van der Does, M., Knippertz, P., Zschenderlein, P., Giles Harrison, R., Stuut, J.-B.W., 2018. The mysterious long-range transport of giant mineral dust particles. Sci. Adv. 4, eaau2768. https://doi.org/10.1126/sciadv.aau2768.

Van Weering, T., Berger, G.W., Kalf, J., 1987. Recent sediment accumulation in the Skagerrak, Northeastern North Sea. Neth. J. Sea Res. 21, 177–189. https://doi.org/10.1016/0077-7579(87)90011-1.

Van Wirdum, F., Andrén, E., Wienholz, D., Kotthoff, U., Moros, M., Fanget, A.-S., Seidenkrantz, M.-S., Andrén, T., 2019. Middle to late holocene variations in salinity and primary productivity in the Central Baltic Sea: a multiproxy study from the landsort deep. Front. Mar. Sci. 6, 51.

Virtasalo, J.J., Endler, M., Moros, M., Jokinen, S.A., Hämäläinen, J., Kotilainen, A.T., 2016. Base of brackish-water mud as key regional stratigraphic marker of mid-Holocene marine flooding of the Baltic Sea Basin. Geo-Mar. Lett. 36, 445–456. https://doi.org/10.1007/s00367-016-0464-4.

Warner, J.C., Sherwood, C.R., Signell, R.P., Harris, C.K., Arango, H.G., 2008. Development of a three-dimensional, regional, coupled wave, current, and sediment-transport model. Comput. Geosci. 34, 1284–1306. https://doi.org/10.1016/j.cageo.2008.02.012.

Weltje, G.J., Brommer, M.B., 2011. Sediment-budget modelling of multi-sourced basin fills: application to recent deposits of the western Adriatic mud wedge (Italy). Basin Res. 23, 291–308. https://doi.org/10.1111/j.1365-2117.2010.00484.x.

Winterhalter, B., Flodén, T., Ignatius, H., Axberg, S., Niemistö, L., 1981. Chapter 1 Geology of the Baltic Sea. In: Voipio, A. (Ed.), Elsevier Oceanography Series: The Baltic Sea, vol. 30. Elsevier, pp. 1–121.

Winterwerp, J.C., van Kesteren, W.G.M., van Prooijen, B., Jacobs, W., 2012. A conceptual framework for shear flow–induced erosion of soft cohesive sediment beds. J. Geophys. Res. Oceans 117. https://doi.org/10.1029/2012JC008072.

Yalin, M.S., 1977. Mechanics of Sediment Transport. Pergamon Press, New York.

Zhang, W., 2016. Sediment budgets. In: Kennish, M.J. (Ed.), Encyclopedia of Estuaries. Springer Netherlands, Dordrecht, pp. 550–553.

Zhang, W., Harff, J., Schneider, R., Wu, C., 2010. Development of a modelling methodology for simulation of long-term morphological evolution of the southern Baltic coast. Ocean Dyn. 60, 1085–1114. https://doi.org/10.1007/s10236-010-0311-5.

Zhang, W., Deng, J., Harff, J., Schneider, R., Dudzinska-Nowak, J., 2013. A coupled modeling scheme for longshore sediment transport of wave-dominated coasts—a case study from the southern Baltic Sea. Coast. Eng. 72, 39–55. https://doi.org/10.1016/j.coastaleng.2012.09.003.

Zhang, W., Cui, Y., Santos, A.I., Hanebuth, T.J., 2016a. Storm-driven bottom sediment transport on a high-energy narrow shelf (NW Iberia) and development of mud depocenters. J. Geophys. Res. Oceans 121, 5751–5772. https://doi.org/10.1002/2015JC011526.

Zhang, Y.J., Ye, F., Stanev, E.V., Grashorn, S., 2016b. Seamless cross-scale modeling with SCHISM. Ocean Model. 102, 64–81. https://doi.org/10.1016/j.ocemod.2016.05.002.

Ziegler, B., Heyen, A., 2004. Rückgang der Steilufer an der schleswig-holsteinischen Ostseeküste. Landesamt für Natur und Umwelt des Landes Schleswig-Holstein–Abteilung Gewässer.

Zillén, L., Conley, D.J., Andrén, T., Andrén, E., Björck, S., 2008. Past occurrences of hypoxia in the Baltic Sea and the role of climate variability, environmental change and human impact. Earth Sci. Rev. 91, 77–92. https://doi.org/10.1016/j.earscirev.2008.10.001.

Zweng, M.M., Reagan, J.R., Antonov, J.I., Locarnini, R.A., Mishonov, A.V., Boyer, T.P., Garcia, H.E., Baranova, O.K., Johnson, D.R., Seidov, D., 2013. World Ocean Atlas 2013, Volume 2: Salinity. In: Levitus, S., Mishonov, A. (Eds.), NOAA Atlas NESDIS, 74. NOAA National Centers for Environmental Information. https://doi.org/10.7289/v5f769gt.

4. On the development of two mud depocenters in the southwestern Baltic Sea

This chapter contains a paper, parts of which have been submitted to Oceanologia as:

Porz, L., Zhang, W., Schrum, C., 2021. Natural and anthropogenic influences on the development of mud depocenters in the southwestern Baltic Sea (under review).

The contribution of Lucas Porz and the other authors to this paper is as follows:

LP and WZ conceived the study. LP set up and ran the numerical model and processed the results. LP, WZ and CS discussed the results. LP wrote the manuscript.

On the development of two mud depocenters in the southwestern Baltic Sea

Lucas Porz[1,*], Wenyan Zhang[1], Corinna Schrum[1,2]

[1]Institute of Coastal Systems, Helmholtz-Zentrum Hereon, Max-Planck-Strasse 1, 21502 Geesthacht, Germany

[2]Institute of Oceanography, Center for Earth System Research and Sustainability, Universität Hamburg, Bundesstrasse 53, 20146 Hamburg, Germany

*Corresponding author. E-mail address: lucas.porz@hereon.de

Abstract

The morphological evolution of two muddy depocenters in the southwestern Baltic Sea is investigated by comparison of numerical model results to geological data. The pathways of dense currents during episodically occurring dense-water inflows from the North Sea are shown to correspond to current pathways inferred from contouritic depositional geometries in the flow-confining channels within the study area. Favorable comparison of model results to published current speed observations indicate that the dynamics of each individual inflow event are deterministic in the sense that water flow is guided by bathymetry. The bottom current directions during inflows show high stability in the flow-confining channels, which explains the contouritic depositional geometries. Asymmetric depositional features in the channels are qualitatively reproduced in the model. Low bottom current stability occurs in areas without contouritic features, possibly resulting in an overall diffusive effect on sediment distribution in those areas. The results give a strong indication that rather than hemi-pelagic background sedimentation, episodic events with high bottom current velocities are responsible for the morphological configuration of the mud depocenters in the southwestern Baltic Sea.

Introduction

Ocean currents can give rise to impressive bathymetric features. Among them are moat-levee structures termed contourites, which develop as a result of sustained or recurring bottom currents strong enough to resuspend sediment from the seabed (Rebesco et al., 2014b). Contourites occur in a wide range of spatial scales, depths, and oceanographic settings, and they are often recognizable in seismic reflection data as slope-parallel, mounded sediment drifts (Stow et al., 2002). However, distinguishing between different forcing mechanisms, such as wind-, tide-, or density-driven bottom currents, based solely on sedimentological criteria remains challenging, because contourites may exhibit greater variation than the established facies models (Mulder et al., 2013; Shanmugam, 2017; Stow and Smillie, 2020). This has prompted the need for a multi-disciplinary approach to understand the process-product relationship between bottom-current reworked submarine geometries and their driving forces. A combination of geological data, numerical modelling and oceanographic measurements has proved useful in this regard (e.g. Hernández-Molina et al., 2016; Zhang et al., 2016b).

The Baltic Sea (Figure 1) exhibits a set of diverse depositional environments due to spatially varying bathymetry, oceanographic conditions, and sediment sources. Muddy, bottom-current-reworked sediment deposits in the southwestern Baltic Sea have previously been classified as shallow-water contourites based on seismo-acoustic data (Sivkov et al., 2002; Christoffersen et al., 2007). In particular, bottom currents associated with episodic dense inflows from the North Sea have long been hypothesized as a forcing mechanism for small-scale contourites within the Bornholm Basin (Larsen and Kögler, 1975; Sivkov and Sviridov, 1994; Sivkov et al., 2002). In contrast, no such features are found in the Arkona Basin, which exhibits a homogenous sediment fill, even though it is where density gradients and bottom currents are expected to be greatest during inflow events. The Arkona Basin has alternatively been described both as an accumulation bottom due to its muddy surface (Carman and Cederwall, 2001), or as a transport bottom due to frequent resuspension by surface waves (Almroth-Rosell et al., 2011).

In this study, we analyze results of numerical modelling of currents and sediment transport in order to connect the hydrodynamics of inflow events to morphological features. We contrast the results in the Bornholm Channel and the Bornholm Basin with those of the shallower Arkona Basin, where no obvious contouritic features are found, in order to compose a conceptual model for the recent development of the southwestern Baltic Sea basins.

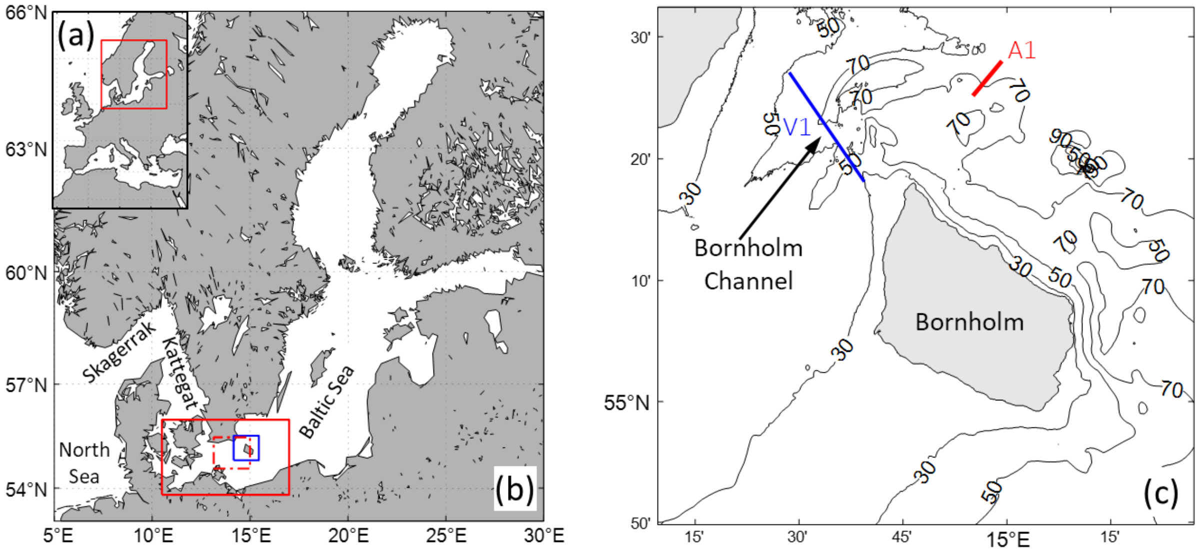

Figure 1. (a) Location of the Baltic Sea (red box) within the European context. (b) Location of the study area (red box) within the Baltic Sea, the Bornholm sub-regoin (blue box), and the Arkona Sea sub-region (dash-dotted red box). (c) Bornholm area with virtual transect V1 used in the analysis of model results and seismo-acoustic track line A1.

Methods

The unstructured, semi-implicit hydrodynamic modelling system SCHISM (Zhang et al., 2016c) is used to reproduce hydrodynamics during the Major Baltic Inflows (MBIs) of 2002/2003 and 2014/2015. The model encompasses the entire Baltic Sea and Kattegat, with special focus on the southwestern Baltic Sea, where the horizontal resolution is about 1 km. The setup is described in detail in Porz et al. (2021b), and validation of inflow hydrodynamics may be found therein. A notable feature of this setup is the increase of vertical resolution from 1 m at the surface to about 30 cm towards the bottom, which has been shown to be sufficient for the correct representation of gravity currents (Laanaia et al., 2010). Furthermore, the implicit numerical implementation means that no bathymetry smoothing is necessary, making it possible to utilize a high-resolution bathymetric dataset available for the study area (BSHC, 2013, horizontal grid resolution 500 m). For the purpose of this study, the resolution in the area of the Bornholm Channel and the northwestern part of Bornholm Basin is further increased to a minimum distance between grid nodes of 200 m. As the Bornholm Channel is a few km in width, we consider a node distance of 200 m is considered sufficient to capture the flow through the channel. In order to avoid numerical issues due to strong gradients in grid resolution, node-distance is varied smoothly from the high-resolution area to the surrounding area as a function of depth, with highest resolution in the deepest parts of the channel system. In order to ensure numerical stability, the model timestep is reduced from 150 s to 75 s, keeping within the operational range of the numerical scheme. Transport, erosion and deposition of sediment as well as bed level changes are included through the model described in Pinto et al. (2012). Initial sediment bed conditions are prescribed according to surface sediment maps of Al-Hamdani et al. (2007) using a constant thickness of 10 cm in the muddy areas.

In order to relate the model results to the geological record, we compare them to the findings of Sivkov and Sviridov (1994). Their analysis is based on the interpretation of seismo-acoustic transects in the Bornholm Channel and Bornholm Basin, which show symmetric and asymmetric depositional geometries in areas of confined flow. Referring to analytical solutions of Bowden (1960) for two-layer flows on a sloping bottom, those authors argue that symmetric deposition occurs when the flow is dominated by gravity, whereas asymmetric deposition points toward geostrophic control. In the latter case, flow is concentrated to the right in the northern hemisphere, allowing more net deposition on the left flank of the channel (Figure 2).

As a measure of directional stability of bottom currents during inflow events, we compute the ratio of vector mean to scalar mean velocities:

$$S = \frac{\sqrt{\overline{v_x}^2 + \overline{v_y}^2}}{\overline{|\boldsymbol{v}|}} \in [0,1], \tag{1}$$

where v_x and v_y are the east-west and north-south components of the current vector $\boldsymbol{v}$, respectively, and an overbar denotes temporal averages. This parameter has been proposed by Ramster et al. (1978) as a measure of current steadiness in processing of current meter

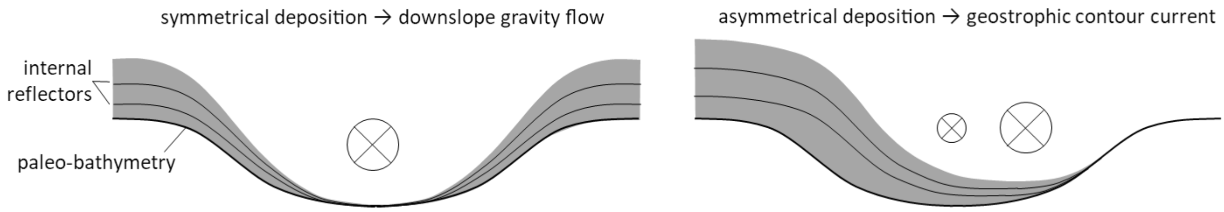

Figure 2. Conceptual illustration indicating the cross-sectional development of channel-related contourite drifts as seen in seismo-acoustic reflection data. Left: gravity-driven, fully non-geostrophic flow producing symmetrical deposition. Right: geostrophic contour-following flow producing asymmetrical deposits. Isochronic internal reflectors can be interpreted as time slices of relief evolution. The paleo-bathymetry is considered non-erodible.

records and has occasionally been used in morphodynamic studies (e.g. Pattiaratchi and Collins, 1987; Harris et al., 1992; Poulos, 2001). Values close to unity denote high directional current stability, whereas values close to zero denote essentially random current directions.

Results

The model result shows several basin-scale, deep reaching and short-lived eddies associated with the passage of inflowing waters in the Arkona Basin. During the 2002/2003 MBI, the model shows a cyclonic gyre in the Arkona Basin (Figure 3a), which lasts for only a few days before dissipating. Measurements by Piechura and Beszczynska-Möller (2004) during this inflow show a similar structure (Figure 3b). This transect was observed at the northeastern edge of the Arkona Basin as the dense water reached the Bornholm Channel. Those authors interpreted a strong shear in the flow as a basin-scale cyclonic eddy in the upper 30 m. They showed that this feature is directly related to the dense inflow, as the velocity structure closely matches the baroclinic velocities computed from measured density. Along with the cyclonic motion of the upper water column, the model shows a weaker anticyclonic motion toward the bottom (Figure 3c), which can be neither confirmed nor refuted by the measurements. Nevertheless, the data confirms the generation of a strong, basin-scale cyclonic eddy in the upper 30 m of the central Arkona Basin during this inflow. This shows that the hydrodynamic model is able to reproduce the mesoscale dynamics of inflow events in the southwestern Baltic Sea realistically. A snapshot of vorticity during passage of dense waters through the Arkona Basin in December 2014 paints a different picture: Here, a strong and deep-reaching anti-cyclonic eddy develops as part of a dipole structure, with a cyclonic eddy developing in the northwestern part of the basin (Figure 4). A model run with the baroclinic force turned off shows no such feature, confirming that this eddy is also related to the baroclinic inflow, as opposed to wind or sea level forcing. Similar to the 2003 cyclonic gyre, this gyre also dissipates after a few days.

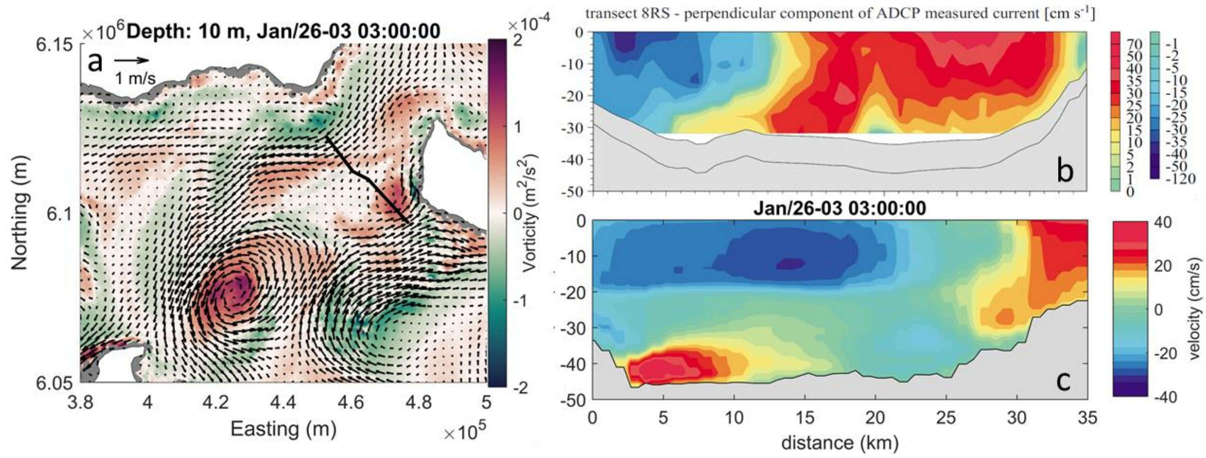

Figure 3. (a) Snapshot of vorticity and velocity in 10 m depth in the Arkona Basin during the 2002/2003 MBI. The black line denotes the transect of perpendicular velocity component of ADCP measurements shown in (b) by Piechura and Beszczynska-Möller (2004, transect 8YRSL) and of that produced by the numerical model (c). Positive velocities in (b-c) are directed into the plane of view.

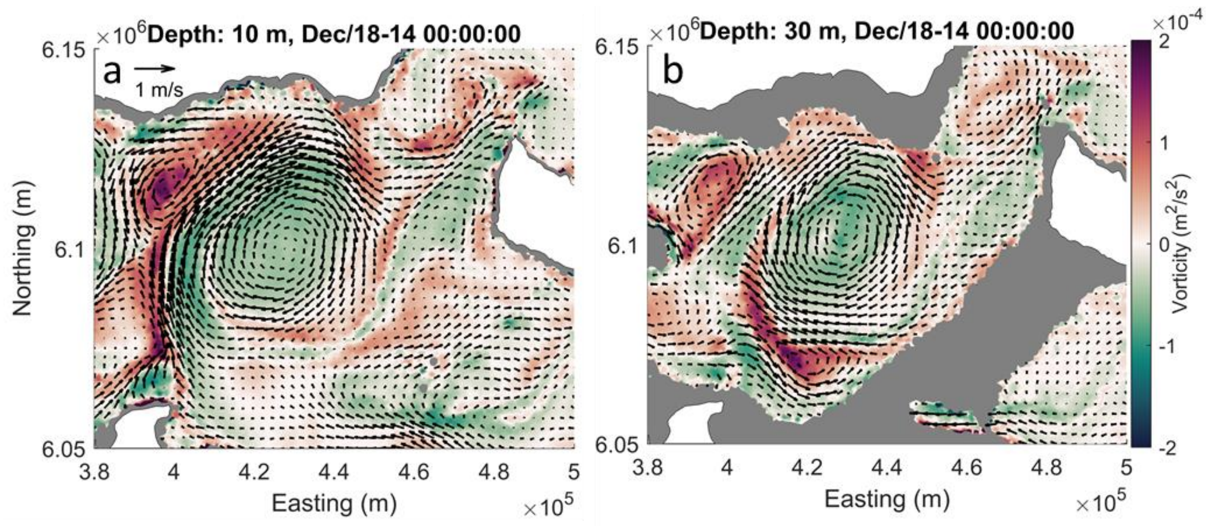

Figure 4. Snapshots of modeled vorticity and velocity in the Arkona Basin during the 2014/2015 MBI in (a) 10 m depth and (b) 30 m depth showing an basin-scale, anticyclonic eddy.

Figure 5 shows the proposed current pathways of Sivkov and Sviridov (1994) and the mean current directions and strengths during the inflow phase in the Bornholm Channel for the high-resolution model. A comparison shows overall agreement, with downslope gravity flow at the entrances of the Bornholm Channel and a transition to an alongslope, geostrophic current At a depth of ~70 m. Nevertheless, some differences between the model and proposed mean current pathways are apparent. The current pathways of Sivkov and Sviridov

(1994) show one southeasterly branch of flow in the northeastern part of the study area, which is missing in the simulations. The most jarring difference, however, is seen in a channel north of Bornholm, where the sediment-acoustic data predict a north-west directed current, while the model shows a southeast directed current. Indeed, a sediment-acoustic line across this channel branch (Figure 6) shows a channel-related contourite (sensu Stow et al., 2002) in the form of an asymmetric sediment drape on the southwestern channel flank, indicating northwest-directed currents (Figure 2). Both of these discrepancies can be explained by the fact that these particular channel structures are not represented in the model bathymetry used, nor in any other bathymetric datasets (cf. Seifert et al., 2001; BSHC, 2013; EMODnet, 2020). A transect across the Bornholm Channel (Figure 7) shows the development of a contouritic feature in the channel related to an asymmetric flow structure in the model, with erosion to right of the flow and deposition to the left.

Figure 8 shows the steadiness factor of modeled bottom velocities computed according to Eq. (1) in order to gauge the spatio-temporal variability of bottom currents during the inflow events. Both events show a similar pattern, where steadiness is highest at the flow-confining channels at the entrance to Arkona Basin, north and south of the sandy shoal Kriegers Flak, as well as in the Bornholm Channel and parts of Bornholm Basin. High values are also seen at the southern rim of the Arkona Basin. However, in the central Arkona Basin, steadiness is quite low, indicating essentially random current directions.

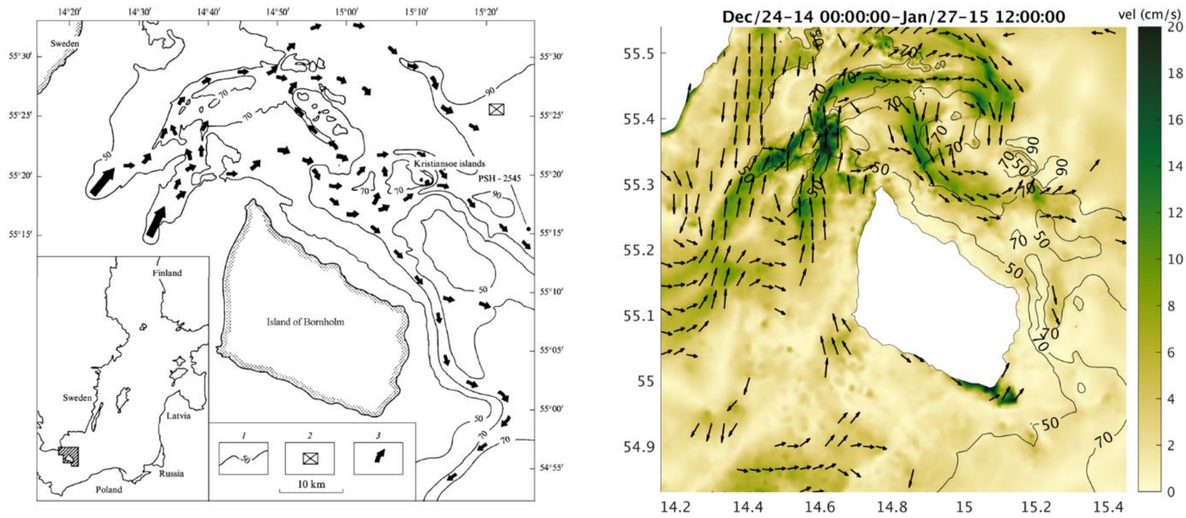

Figure 5. Left: Current directions inferred from seismic data from Sivkov and Sviridov (1994). Right: Average modeled bottom current directions (arrows) and speeds (color) during the 2014/2015 MBI. Arrows are only shown for average speeds larger than 4 cm/s.

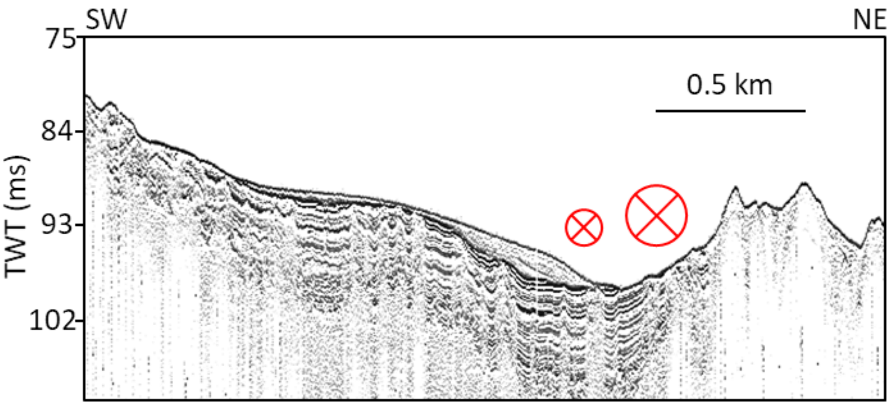

Figure 6. Sediment acoustic profiles (15 kHz) across the end of Bornholm Channel leading into Bornholm Basin (see Figure 1c for location). A muddy contourite drift on the southwestern channel levee indicates northwestward, geostrophic bottom currents. Modified from Porz et al. (2021b).

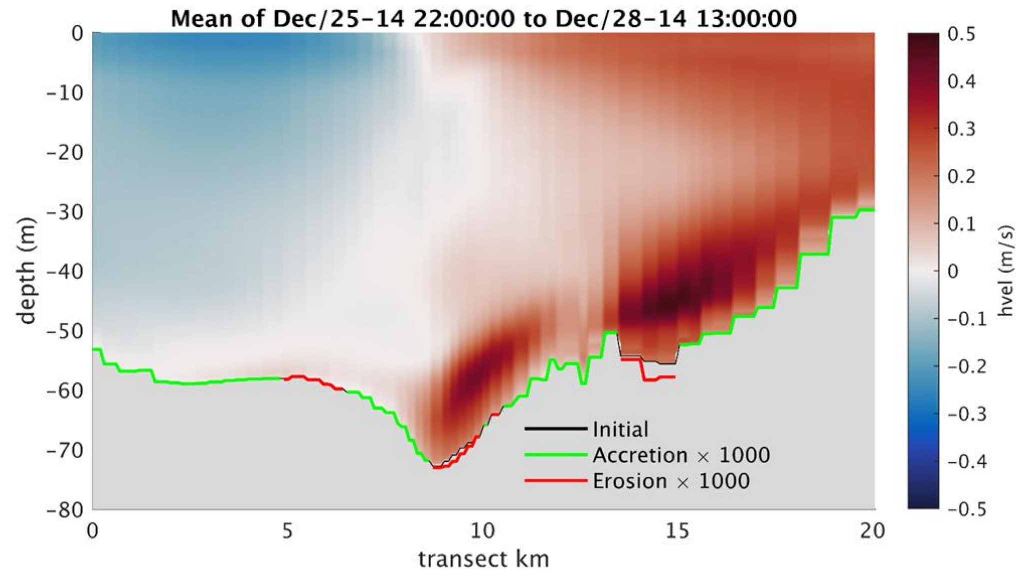

Figure 7. Time-averaged perpendicular current velocity and bed elevation changes at a transect across the Bornholm Channel during the passage of dense water of the 2014/2015 MBI. Positive values are directed into the plane of view. Bed elevation changes in terms of accretion (green) and erosion (red) are enhanced by a factor of 1000 for presentation. See Figure 1c for the location of the transect.

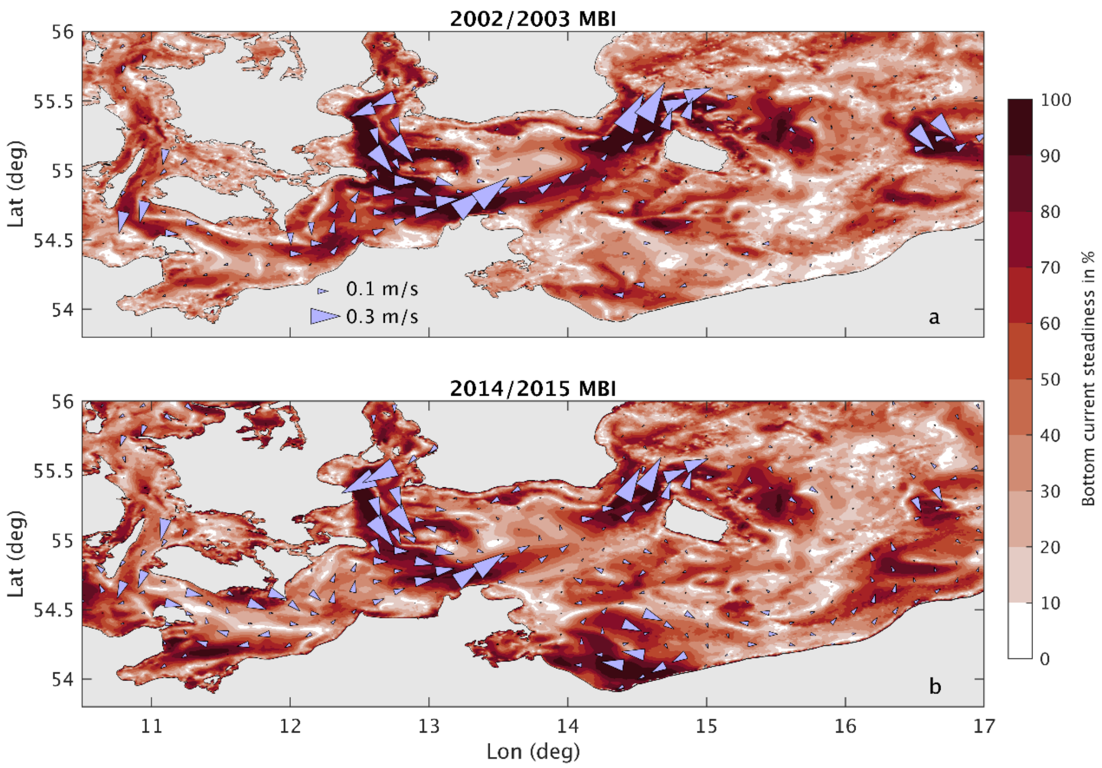

Figure 8. Average bottom current speeds (arrows) and bottom current steadiness (color) for the inflow period of the 2002/2003 MBI (top) and the 2014/2015 MBI (bottom).

Discussion and Conclusion

This study links the hydrodynamics of episodic bottom currents to the morphologies of two different depositional environments. The Bornholm Basin is actively shaped by bottom currents, which are locally enhanced due to outcropping obstacles that confine the flow, leading to contouritic deposits. The modeled bottom current direction in the Bornholm Channel is very stable during the passage of bottom waters. A comparison of model results to proposed flow directions based on seismo-acoustic data show overall agreement, which is an indication that the contouritic features in the Bornholm Basin are controlled by MBI currents. Vice versa, this means that symmetries (asymmetries) in the depositional architecture of channelized flows may be used to designate gravity-driven (geostrophic) flows as their driving forces. However, such interpretation should be exercised with caution, as entirely symmetric deposition is unlikely to occur in reality, both because the Coriolis force will have an effect even for gravitational currents, and because the paleo-bottom of a channel itself is generally not entirely symmetric, potentially favoring deposition on one channel flank regardless of flow structure.

In the Arkona Basin, the situation is complicated by the homogeneity of its modern sea bottom, indicating a type of equilibrium where any previous channels have been infilled. Here, the morphology alone does not permit inferences about bottom current strength or direction. Model studies indicate that resuspension and mixing by waves and bottom trawling are common in the Arkona Basin, making it a more dynamic environment than its muddy bottom suggests (Jönsson et al., 2005; Almroth-Rosell et al., 2011; Bunke et al., 2019). However, waves and bottom trawling alone generate little lateral transport. Bottom currents are additionally required for net transport to occur. MBIs are able to fill that role. Our numerical model results indicate that the mesoscale dynamics of an inflow traversing the Arkona Basin are guided along the rim of the basin, but the two events modeled show different short-term flow patterns, with both cyclonic and anticyclonic eddies developing. Though the overall circulation in the Arkona Basin has the appearance of a cyclonic gyre (Meier, 2007), the basin-scale eddies observed and shown in the model are short-lived and therefore should not be interpreted as characteristics of overall circulation. Mesoscale eddies in the Arkona Basin associated with saltwater plumes during MBIs have also been reported by Lass and Mohrholz (2003). According to Sayin and Krauss (1996), the inflowing water piles up in the Arkona Basin under geostrophic control, preventing the inflow from reaching the Bornholm Channel quickly. This phenomenon is confirmed by our simulations. During MBIs, these pulsating eddies produce a patchy sediment distribution in the Arkona Basin (Porz et al., 2021b). It is likely that the integrated effect of many such events, along with surface waves during storms and bottom trawling, have an overall diffusive effect on the lateral deposit thickness, which would explain the homogeneity of the Arkona Basin fill.

At about 110 m below modern sea level, the Bornholm Basin's paleo-surface is much deeper compared to the Arkona-Basin's at 55 m. From a sedimentological perspective, greater depths are equivalent to more accommodation space and thus promote the deposition of mud. Why then is the average mud thickness in the Arkona Basin much greater than in the Bornholm Basin, or any of the other deep Basins in the Baltic Sea? Two possible explanations are the ample supply of soft moraine material from the erodible landscape surrounding the Arkona Basin, and introduction of mud from the North Sea/Kattegat during MBIs (Gingele and Leipe, 2001; Porz et al., 2021b). After its infilling, the modern Arkona Basin seems to have developed from a depositional into a transitional zone for sediment, similar to the Mecklenburg Bight, where net accumulation appears to have already ceased (Bunke et al., 2019). Mud entrained by the dense water inflows could eventually bypass the Arkona Basin depocenter and deposit instead in the Bornholm Basin. In fact, sedimentation rates in the Bornholm Basin have increased slightly during the past centuries (Kunzendorf and Larsen, 2009). Bottom currents during MBIs represent the likely mechanism for this eastward transport. This notion is further supported by Hg-concentrations in the surface sediments of the Arkona Basin, which point to eastward spreading of from a military dumping site near the center of the basin (Leipe et al., 2013). Similarly, repeated grain size measurements have shown a coarsening trend in the West and a fining trend in the East (Leipe et al., 2008), further indicating an eastward migration of fines on sub-recent time-scales. In this sense, the basins of the southwestern Baltic Sea seem to have developed in a cascading manner from west to east (Figure 9).

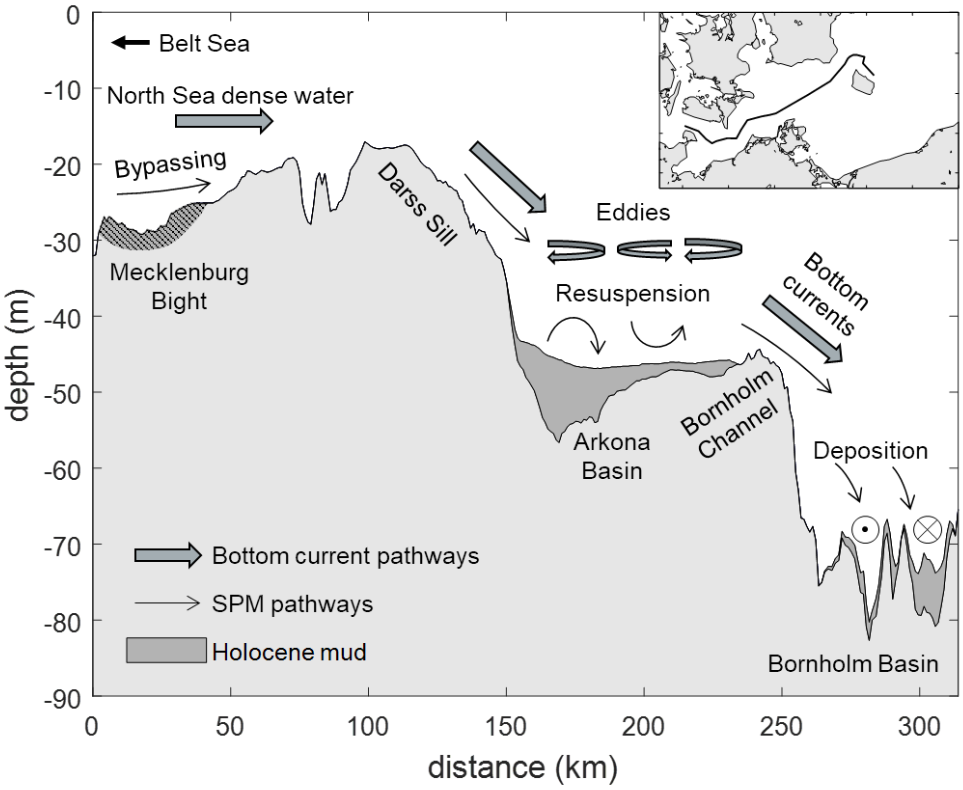

Figure 9. Conceptual illustration of SPM cascading and associated development of mud depocenters (dark areas) in the southwestern Baltic Sea.

Acknowledgements

This study is a contribution by the Helmholtz Association through the PoF IV program, Topic 4 „Coastal Zones at a time of global change". W. Zhang acknowledges the support from the I2B project "Unravelling the linkages between benthic biological functioning, biogeochemistry and coastal morphodynamics – from big data to mechanistic modeling" funded by Helmholtz-Zentrum Hereon.

Data statement

There is no restriction on the data used in this study. All code and data used in this study is in the public domain and all resources used have been cited in the article.

References

Al-Hamdani, Z.K., Reker, J., Leth, J.O., Reijonen, A., Kotilainen, A.T., Dinesen, G.E., 2007. Development of marine landscape maps for the Baltic Sea and the Kattegat using geophysical and hydrographical parameters. Geological Survey of Denmark and Greenland Bulletin 13, 61–64.

Almroth-Rosell, E., Eilola, K., Hordoir, R., Meier, H.E.M., Hall, P.O., 2011. Transport of fresh and resuspended particulate organic material in the Baltic Sea — a model study. J. Mar. Sys. 87, 1–12. 10.1016/j.jmarsys.2011.02.005.

Baltic Sea Hydrographic Commission, 2013. Baltic Sea Bathymetry Database version 0.9.3. http://data.bshc.pro/. Accessed 20 April 2020.

Bowden, K.F., 1960. The Dynamics of Flow on a Submarine Ridge. Tellus 12, 418–426. 10.1111/j.2153-3490.1960.tb01328.x.

Bunke, D., Leipe, T., Moros, M., Morys, C., Tauber, F., Virtasalo, J.J., Forster, S., Arz, H.W., 2019. Natural and Anthropogenic Sediment Mixing Processes in the South-Western Baltic Sea. Frontiers in Marine Science 6, 677.

Christoffersen, P.L., Christiansen, C., Jensen, J.B., Leipe, T., Hille, S., 2007. Depositional conditions and organic matter distribution in the Bornholm Basin, Baltic Sea. Geo-Mar Lett 27, 325–338. 10.1007/s00367-007-0054-6.

EMODnet Bathymetry Consortium, 2020. EMODnet Digital Bathymetry (DTM). https://doi.org/10.12770/bb6a87dd-e579-4036-abe1-e649cea9881a.

Gingele, F.X., Leipe, T., 2001. Southwestern Baltic Sea—A sink for suspended matter from the North Sea? Geology 29, 215. 10.1130/0091-7613(2001)029<0215:SBSASF>2.0.CO;2.

Harris, P.T., Pattiaratchi, C.B., Cole, A.R., Keene, J.B., 1992. Evolution of subtidal sandbanks in Moreton Bay, eastern Australia. Marine Geology 103, 225–247. 10.1016/0025-3227(92)90018-D.

Hernández-Molina, F.J., Wåhlin, A., Bruno, M., Ercilla, G., Llave, E., Serra, N., Rosón, G., Puig, P., Rebesco, M., van Rooij, D., Roque, D., González-Pola, C., Sánchez, F., Gómez, M., Preu, B., Schwenk, T., Hanebuth, T.J., Sánchez Leal, R.F., García-Lafuente, J., Brackenridge, R.E., Juan, C., Stow, D.A.V., Sánchez-González, J.M., 2016. Oceanographic processes and morphosedimentary products along the Iberian margins: A new multidisciplinary approach. Marine Geology 378, 127–156. 10.1016/j.margeo.2015.12.008.

Jönsson, A., Danielsson, Å., Rahm, L., 2005. Bottom type distribution based on wave friction velocity in the Baltic Sea. Continental Shelf Research 25, 419–435. 10.1016/j.csr.2004.09.011.

Kunzendorf, H., Larsen, B., 2009. Environmental changes in the Bornholm Basin as deduced from the geochemistry of short and long sediment cores. Baltica 22, 101–110.

Laanaia, N., Wirth, A., Molines, J.M., Barnier, B., Verron, J., 2010. On the numerical resolution of the bottom layer in simulations of oceanic gravity currents. Ocean Sci 6, 563–572. 10.5194/os-6-563-2010.

Larsen, B., Kögler, F.-C., 1975. A submarine channel between the deepest parts of the Arkona and the Bornholm basins in the Baltic Sea. Deutsche Hydrographische Zeitschrift 28, 274–276. 10.1007/BF02225971.

Lass, H.U., Mohrholz, V., 2003. On dynamics and mixing of inflowing saltwater in the Arkona Sea. Journal of Geophysical Research: Oceans 108.

Leipe, T., Moros, M., Kotilainen, A.T., Vallius, H., Kabel, K., Endler, M., Kowalski, N., 2013. Mercury in Baltic Sea sediments—natural background and anthropogenic impact. Chemie der Erde-Geochemistry 73, 249–259.

Meier, H.E.M., 2007. Modeling the pathways and ages of inflowing salt- and freshwater in the Baltic Sea. Timescale- and tracer-based methods for understanding the results of complex marine models 74, 610–627. 10.1016/j.ecss.2007.05.019.

Mulder, T., Hassan, R., Ducassou, E., Zaragosi, S., Gonthier, E., Hanquiez, V., Marchès, E., Toucanne, S., 2013. Contourites in the Gulf of Cadiz: a cautionary note on potentially ambiguous indicators of bottom current velocity. Geo-Marine Letters 33, 357–367. 10.1007/s00367-013-0332-4.

Pattiaratchi, C., Collins, M., 1987. Mechanisms for linear sandbank formation and maintenance in relation to dynamical oceanographic observations. Progress in Oceanography 19, 117–176. 10.1016/0079-6611(87)90006-1.

Piechura, J., Beszczynska-Möller, A., 2004. Inflow waters in the deep regions of the southern Baltic Sea-transport and transformations. Oceanologia 46.

Pinto, L., Fortunato, A.B., Zhang, Y.J., Oliveira, A., Sancho, F.E., 2012. Development and validation of a three-dimensional morphodynamic modelling system for non-cohesive sediments. Ocean Modelling 57, 1–14.

Porz, L., Zhang, W., Schrum, C., 2021. Density-driven bottom currents control development of muddy basins in the southwestern Baltic Sea. Marine Geology. 10.1016/j.margeo.2021.106523.

Poulos, S., 2001. The contribution of near-bed currents to modern sedimentation processes in the deep waters of the Hellenic Arc-Trench system, eastern Mediterranean. Geo-Marine Letters 20, 201–208. 10.1007/s003670000057.

Ramster, J.W., Hughes, D.G., Furnes, G.K., 1978. A ‘steadiness’ factor for estimating the variability of residual drift in current meter records. Deutsche Hydrografische Zeitschrift 31, 230–236.

Rebesco, M., Hernández-Molina, F.J., van Rooij, D., Wåhlin, A., 2014. Contourites and associated sediments controlled by deep-water circulation processes: State-of-the-art and future considerations. Marine Geology 352, 111–154. 10.1016/j.margeo.2014.03.011.

Sayin, E., Krauss, W., 1996. A numerical study of the water exchange through the Danish Straits. Tellus A 48, 324–341. 10.1034/j.1600-0870.1996.t01-1-00009.x.

Seifert, T., Tauber, F., Kayser, B., 2001. A high resolution spherical grid topography of the Baltic Sea–revised edition, In: Baltic Sea Science Congress, Stockholm 25-29. November 2001, Poster #147.

Shanmugam, G., 2017. Chapter 9 - The Contourite Problem, In: Mazumder, R. (Ed.), Sediment Provenance. Elsevier, pp. 183–254.

Sivkov, V., Gorbatskiy, V., Kuleshov, A., Zhurov, Y., 2002. Muddy contourites in the Baltic Sea: an example of a shallow-water contourite system. Geological Society, London, Memoirs 22, 121–136. 10.1144/GSL.MEM.2002.022.01.10.

Sivkov, V., Sviridov, N., 1994. The relation between erosional-accumulative forms of bottom relief and near-bottom currents in the Bornholm deep. Oceanologiya (English Translation), 266–270.

Stow, D.A.V., Faugères, J.-C., Howe, J.A., Pudsey, C.J., Viana, A.R., 2002. Bottom currents, contourites and deep-sea sediment drifts: Current state-of-the-art. Geological Society, London, Memoirs 22, 7–20. 10.1144/GSL.MEM.2002.022.01.02.

Stow, D.A.V., Smillie, Z., 2020. Distinguishing between Deep-Water Sediment Facies: Turbidites, Contourites and Hemipelagites. Geosciences 10. 10.3390/geosciences10020068.

Zhang, W., Hanebuth, T.J., Stöber, U., 2016a. Short-term sediment dynamics on a meso-scale contourite drift (off NW Iberia): Impacts of multi-scale oceanographic processes deduced from the analysis of mooring data and numerical modelling. Marine Geology 378, 81–100. 10.1016/j.margeo.2015.12.006.

Zhang, Y.J., Ye, F., Stanev, E.V., Grashorn, S., 2016b. Seamless cross-scale modeling with SCHISM. Ocean Modelling 102, 64–81. 10.1016/j.ocemod.2016.05.002.

5. Discussion and Perspectives

This thesis strongly reinforces the awareness that shelf mud sedimentation is not the quiescent, hemipelagic process entertained by some oceanographers and geologists. Porz et al. (2021a) identify physical drivers of shelf mud deposition, many of which turn out to be quite energetic, and discuss the problem of continuous versus episodic sedimentation. Porz et al. (2021b) offer a way forward by combining oceanographic modeling, observations, and geological data in order to discern sediment sources and sinks of fine-grained sediment in the southwestern Baltic Sea. Porz et al. (2021c) attempt to explain the different morphologies of the mud depocenters in that area, and develop a conceptual model of their recent development.

While a source-to-sink mentality has been widely adopted by environmental authorities for sediment management practices, it has only recently been re-discovered by the academic world (Walsh et al., 2016). The results presented in Porz et al. (2021b) demonstrate the utility of the source-to-sink approach. Notably, the straightforward mass budgeting method applied therein does not require elaborate mineralogical or geochemical provenance analysis, which is not to say that this study could not benefit from such methods. In fact, the notion that dense-water inflows serve as a sediment source for the Baltic Sea was in large part inspired by the mineralogical studies of Gingele and Leipe (1997; 2001). As a major result of this thesis, their hypothesis can now be considered confirmed. At the same time, some limitations of the budgeting approach are revealed through the high uncertainties of the sources compared to the sinks. One reason for this is that the mud depocenters can be assumed relatively homogenous in composition, owing to lateral mixing during transport processes, whereas the sources exhibit a comparatively high spatial and temporal heterogeneity. Flux estimates are only as good as the accuracy of the compiled data. Though the information on coastal erosion rates in the study area is probably more plentiful than in many other regions, uncertainties in the resulting mass estimates are on the same order of magnitude as the estimates themselves (Porz et al., 2021b, their Table 1). A technique for automatic estimation of coastal erosion rates with high spatial and temporal resolution from remote sensing data has recently been developed (Luijendijk et al., 2018), which would allow further verification of erosion fluxes. However, while this method can already detect changes in the lateral migration of the land-water-interface in the study area with reasonable accuracy

(EMODnet, 2021), it is not yet suitable for the detection of cliff retreat, because the cliff-face is usually located several meters behind the shoreline.

Some complexities of the study area's morphology shall be pointed out, which have not been explicitly addressed in the studies contained in this thesis. Although the Arkona Basin has been deemed decidedly non-contouritic, closer inspection does reveal a subtle, mounded feature at its southwestern edge (M. Endler, personal communication, May 28, 2019). When interpreted as a mounded drift, this could be explained by the high persistence of the cyclonic gyre at the basin's southern rim during inflow events shown in Porz et al. (2021c, their Figure 8). Anthropogenic activity occurs primarily in the Arkona Basin in the form of bottom trawling. The entire seafloor of the Arkona Basin is subjected to bottom trawling multiple times per year (HELCOM, 2015). According to Bunke et al. (2019), bottom trawling disturbs the sediment's geochemical signals down to a depth of 27 cm in the Arkona Basin. Notably, this influence is greater than that of natural bioturbation by benthic organisms, which live primarily in the upper 5-7 cm. The effect of direct resuspension by bottom trawling and subsequent advection by bottom currents on lateral sediment fluxes in the Arkona Basin deserves further investigation.

Another potential anthropogenic disturbance exists in the form of bridge and wind turbine foundations, which generate additional vertical mixing in the water column (Burchard et al., 2005). Little is known about the influence of these structures on bottom current and sediment dynamics in the study area. A modeling study by Rennau et al. (2012) concluded that wind farms lead to a minor decrease in average bottom salinity in the Arkona Sea (0.1-0.3 PSU), indicating a rather small overall mixing effect. Our understanding of hydrodynamics in the wake of structures is rapidly evolving (e.g. Cazenave et al., 2016; Jensen et al., 2018; Schultze et al., 2020), encouraging an evaluation of their influence on sediment dynamics during MBI events. In the Bornholm Basin, the situation is complicated by possible neo-tectonic activity as part of the Tornquist-Zone, a complex fault system crossing the Bornholm Island area (Jensen et al., 2017). Seismic data in Jensen et al. (2017) indicate slumping in Baltic Ice Lake sediments in the Bornholm Basin, which may be related to neo-tectonic events. Although no direct evidence of such effects on Post-Littorina sediments has been reported, the possibility that tectonic subsidence is partially responsible for creating accommodation space in the Bornholm Basin cannot be discounted, representing a second morphologic control mechanism along with shaping by bottom currents.

While this thesis has focused on the impacts of bottom current in the southwestern Baltic Sea, the inflows also propagate further into the Gotland Basin. Suspended matter transported through the Stolpe Channel is deposited and forms the “Stolpe Foredelta” where the channel merges with the Eastern Gotland Basin (Harff et al., 2011). Surprisingly, strong westerly winds that initialize inflow events are not conducive to transport from the Bornholm Basin further on over the Stolpe Sill. Instead, easterly or northerly winds trigger this exchange flow (Krauss and Brügge, 1991). An investigation of the development of this foredelta in relation to MBIs is intriguing, as it potentially records variations in inflow intensity (Emelyanov et al., 2011).

Although MBIs represent violent events in the context of the Baltic Sea, on a global scale these events must be considered minor in terms of current velocity and sediment flux. For example, at about 80 cm/s, peak near-bottom currents during the strongest MBIs are hardly stronger than the principal Lunar (M2) tidal currents in parts of the North Sea (Vindenes et al., 2018). In the Bay of Bengal, individual tropical cyclones generate dm-scale deposits (Kudrass et al., 2018), orders of magnitude thicker than deposits induced by an MBI. Bottom SPM concentrations reach the order of 10^3 mg/l during flood- and storm-related gravity-driven transport events on the Eel shelf, northern California (Ogston et al., 2000), compared to 10^0 mg/l in the southwestern Baltic Sea during MBIs (Lund-Hansen and Christiansen, 2008). In principal, the method of source-to-sink analysis in combination with numerical modeling and upscaling in time can be applied to such depocenters as well. This is especially intriguing because long hydrographical time-series from fixed observational platforms are quite common nowadays, whereas direct measurements of sediment dynamics remain strongly scattered in space and time. An additional challenge of open-shelf environments is that a considerable amount of sediment may bypass the shelf altogether. In these systems, a quantification of the preservation potential in addition to short-term fluxes would become crucial for any source-to-sink analyses.

On a technical level, this thesis highlights the efficacy of unstructured grid models, which allow local model grid refinements in areas of interest with manageable increase in computational expense. Recent developments in numerical modeling of sediment transport and morphodynamics include cohesive processes, consolidation, and early diagenesis (e.g. Sherwood et al., 2018; Radtke et al., 2019). The sediment model used in this study is rather basic by comparison. However, the number of parameters to be calibrated increases with model complexity, and when data for validation of SPM dynamics is insufficient, as is the case for MBIs, there is little benefit in introducing additional non-tunable parameters. Nevertheless, including such effects as biostabilization and -destabilization, flocculation, and bioturbation in the context of sensitivity analyses could further enhance our conceptual understanding of shelf mud morphodynamics. In this context, a realistic representation of the highly mobile fluff layer (see chapter 1.2) may be especially critical. Measurements of near-bottom SPM concentrations will be necessary for the validation of these dynamics.

The scientific community is beginning to recognize that shelf mud sedimentation is a considerably more dynamic process than previously thought. The potentially far-reaching implications of this fact on our understanding of carbon cycling, the spreading of contaminants in coastal seas, and the interpretation of the geological record remain to be determined

References

Ager, D.V., 1973. The nature of the stratigraphical record. Macmillan, London.

Almroth-Rosell, E., Eilola, K., Hordoir, R., Meier, H.E.M., Hall, P.O., 2011. Transport of fresh and resuspended particulate organic material in the Baltic Sea — a model study. J. Mar. Sys. 87, 1–12. 10.1016/j.jmarsys.2011.02.005.

Andrén, T., Björck, S., Andrén, E., Conley, D., Zillén, L., Anjar, J., 2011. The development of the Baltic Sea Basin during the last 130 ka, In: Harff, J., Björck, S., Hoth, P. (Eds.), The Baltic Sea Basin. Springer Berlin Heidelberg, Berlin, Heidelberg, pp. 75–97.

Baltic Marine Environment Protection Commission, 2015. Maps on pressure from fishing activity in the HELCOM area 2009-2013.

Bentley, S.J., Nittrouer, C.A., 2003. Emplacement, modification, and preservation of event strata on a flood-dominated continental shelf: Eel shelf, Northern California. Continental Shelf Research 23, 1465–1493. 10.1016/j.csr.2003.08.005.

Bobertz, B., Harff, J., 2004. Sediment facies and hydrodynamic setting: a study in the south western Baltic Sea. Ocean Dynamics 54, 39–48. 10.1007/s10236-003-0061-8.

Bobertz, B., Harff, J., Bohling, B., 2009. Parameterisation of clastic sediments including benthic structures. J. Mar. Sys. 75, 371–381. 10.1016/j.jmarsys.2007.06.010.

Bonacker, P., 1996. Massenbilanzmodell holozäner Ostseesedimente [Research Report]. Institut für Ostseeforschung Warnemünde.

Bundesamt für Seeschifffahrt und Hydrographie, 2020. Marine Environmental Monitoring Network in the North Sea and Baltic Sea. https://www.bsh.de/EN/TOPICS/Monitoring_systems/MARNET_monitoring_network/marnet_monitoring_network_node.html. Accessed 11 November 2020.

Bunke, D., Leipe, T., Moros, M., Morys, C., Tauber, F., Virtasalo, J.J., Forster, S., Arz, H.W., 2019. Natural and Anthropogenic Sediment Mixing Processes in the South-Western Baltic Sea. Frontiers in Marine Science 6, 677.

Burchard, H., Lass, H.U., Mohrholz, V., Umlauf, L., Sellschopp, J., Fiekas, V., Bolding, K., Arneborg, L., 2005. Dynamics of medium-intensity dense water plumes in the Arkona Basin, Western Baltic Sea. Ocean Dynamics 55, 391–402.

Catuneanu, O., 2019. Scale in sequence stratigraphy. Marine and Petroleum Geology 106, 128–159. 10.1016/j.marpetgeo.2019.04.026.

Cazenave, P.W., Torres, R., Allen, J.I., 2016. Unstructured grid modelling of offshore wind farm impacts on seasonally stratified shelf seas. Progress in Oceanography 145, 25–41. 10.1016/j.pocean.2016.04.004.

Cheriton, O.M., McPhee-Shaw, E.E., Shaw, W.J., Stanton, T.P., Bellingham, J.G., Storlazzi, C.D., 2014. Suspended particulate layers and internal waves over the southern Monterey Bay continental shelf: An important control on shelf mud belts? J. Geophys. Res. Oceans 119, 428–444. 10.1002/2013JC009360.

Christiansen, C., Edelvang, K., Emeis, K., Graf, G., Jähmlich, S., Kozuch, J., Laima, M., Leipe, T., Löffler, A., Lund-Hansen, L., Miltner, A., Pazdro, K., Pempkowiak, J., Shimmield, G., Shimmield, T., Smith, J., Voss, M., Witt, G., 2002. Material transport from the nearshore to the basinal environment in the southern Baltic Sea: I. Processes and mass estimates. Journal of Marine Systems 35, 133–150. 10.1016/S0924-7963(02)00126-4.

Cong, J., Hu, G., Jonell, T.N., Zhang, Y., Li, Y., Bi, S., 2021. Source-to-sink and evolutionary processes of the East China Sea inner-shelf mud belt and its response to environmental changes since the Holocene: New evidence from the distal mud belt. The Holocene. 10.1177/09596836211003202.

Deltares, 2020. Delft3D-Flow: Simulation of Multi-Dimensional Hydrodynamic Flows and Transport Phenomena, Including Sediments. User Manual. Version 3.15, Delft. https://content.oss.deltares.nl/delft3d/manuals/Delft3D-FLOW_User_Manual.pdf. Accessed 21 September 2020.

Diaz, M., Grasso, F., Le Hir, P., Sottolichio, A., Caillaud, M., Thouvenin, B., 2020. Modeling Mud and Sand Transfers Between a Macrotidal Estuary and the Continental Shelf: Influence of the Sediment Transport Parameterization. J. Geophys. Res. Oceans 125, e2019JC015643. 10.1029/2019JC015643.

Dott, R.H., 1983. Episodic sedimentation - how normal is average? How rare is rare? Does it matter? 1982 SEPM presidential address. Journal of Sedimentary Petrology 53, 5–23.

Dott, R.H., 1996. Episodic event deposits versus stratigraphic sequences—shall the twain never meet? Sedimentary Geology 104, 243–247. 10.1016/0037-0738(95)00131-X.

Edelvang, K., Lund-Hansen, L.C., Christiansen, C., Petersen, O.S., Uhrenholdt, T., Laima, M., Berastegui, D.A., 2002. Modelling of suspended matter transport from the Oder River. Journal of Coastal Research, 62–74.

Emeis, K.-C., Christiansen, C., Edelvang, K., Jähmlich, S., Kozuch, J., Laima, M., Leipe, T., Löffler, A., Lund-Hansen, L.C., Miltner, A., Pazdro, K., Pempkowiak, J., Pollehne, F., Shimmield, T., Voss, M., Witt, G., 2002. Material transport from the near shore to the basinal environment in the southern Baltic Sea: II: Synthesis of data on origin and properties of material. J. Mar. Sys. 35, 151–168. 10.1016/S0924-7963(02)00127-6.

Emelyanov, E.M., Trimonis, E., Slobodyanik, V., Nielsen, O., 1995. Quaternary sediments and deposits, In: Emelyanov, E.M., Christiansen, C., Michelsen, O. (Eds.), Geology of the Bornholm Basin. Aarhus Geosci 5.

Emelyanov, E.M., Trimonis, E.S., Vaikutiéné, G., Harff, J., 2011. Reference sediment core and paleogeography of the underwater Slupsk river foredelta in the Baltic Sea. Oceanology 51, 836. 10.1134/S0001437011050055.

European Marine Observation and Data network, 2021. European coastal migration analysis from field data. https://www.emodnet-geology.eu/. Accessed 10 June 2021.

Farnsworth, K.L., Warrick, J.A., 2007. Sources, dispersal, and fate of fine sediment supplied to coastal California. Scientific Investigations Report 2007-5254. U.S. Geological Survey, Reston, VA, 86 pp.

Faugères, J.-C., Stow, D.A.V., 1993. Bottom-current-controlled sedimentation: a synthesis of the contourite problem. Sedimentary Geology 82, 287–297. 10.1016/0037-0738(93)90127-Q.

Fringer, O.B., Dawson, C.N., He, R., Ralston, D.K., Zhang, Y.J., 2019. The future of coastal and estuarine modeling: Findings from a workshop. Ocean Modelling 143, 101458. 10.1016/j.ocemod.2019.101458.

Gingele, F.X., Leipe, T., 1997. Clay mineral assemblages in the western Baltic Sea: recent distribution and relation to sedimentary units. Marine Geology 140, 97–115. 10.1016/S0025-3227(97)00023-6.

Gingele, F.X., Leipe, T., 2001. Southwestern Baltic Sea—A sink for suspended matter from the North Sea? Geology 29, 215. 10.1130/0091-7613(2001)029<0215:SBSASF>2.0.CO;2.

Gonthier, E.G., Faugères, J.-C., Stow, D.A.V., 1984. Contourite facies of the Faro Drift, Gulf of Cadiz. Geological Society, London, Special Publications 15, 275. 10.1144/GSL.SP.1984.015.01.18.

Gräwe, U., Naumann, M., Mohrholz, V., Burchard, H., 2015. Anatomizing one of the largest saltwater inflows into the Baltic Sea in December 2014. J. Geophys. Res. Oceans 120, 7676–7697. 10.1002/2015JC011269.

Hanebuth, T.J., Lantzsch, H., Nizou, J., 2015. Mud depocenters on continental shelves—appearance, initiation times, and growth dynamics. Geo-Mar Lett 35, 487–503. 10.1007/s00367-015-0422-6.

Harff, J., Endler, R., Emelyanov, E.M., Kotov, S., Leipe, T., Moros, M., Olea, R., Tomczak, M., Witkowski, A., 2011. Late Quaternary Climate Variations Reflected in Baltic Sea Sediments, In: Harff, J., Björck, S., Hoth, P. (Eds.), The Baltic Sea Basin. Springer Berlin Heidelberg, Berlin, Heidelberg, pp. 99–132.

Heezen, B.C., Hollister, C.D., Ruddiman, W.F., 1966. Shaping of the Continental Rise by Deep Geostrophic Contour Currents. Science 152, 502. 10.1126/science.152.3721.502.

Helland-Hansen, W., Sømme, T.O., Martinsen, O.J., Lunt, I., Thurmond, J., 2016. Deciphering Earth's Natural Hourglasses: Perspectives On Source-To-Sink Analysis. Journal of Sedimentary Research 86, 1008–1033. 10.2110/jsr.2016.56.

Hofmeister, R., Beckers, J.-M., Burchard, H., 2011. Realistic modelling of the exceptional inflows into the central Baltic Sea in 2003 using terrain-following coordinates. Ocean Modelling 39, 233–247. 10.1016/j.ocemod.2011.04.007.

International Council for the Exploration of the Sea, 2021. Baltic Sea (HELCOM) Monitoring data. https://ocean.ices.dk/helcom/.

Jähmlich, S., Lund-Hansen, L.C., Leipe, T., 2002. Enhanced settling velocities and vertical transport of particulate matter by aggregation in the benthic boundary layer. Geografisk Tidsskrift-Danish Journal of Geography 102, 37–49.

Jensen, B., Carstensen, S., Christensen, D.E., 2018. Mixing of Stratified Flow around Bridge Piers in Steady Current. Journal of Hydraulic Engineering 144, 4018041. 10.1061/(ASCE)HY.1943-7900.0001481.

Jensen, J.B., Moros, M., Endler, R., IODP Expedition 347 Members, 2017. The Bornholm Basin, southern Scandinavia: a complex history from Late Cretaceous structural developments to recent sedimentation. Boreas 46, 3–17. 10.1111/bor.12194.

Krauss, W., Brügge, B., 1991. Wind-Produced Water Exchange between the Deep Basins of the Baltic Sea. Journal of Physical Oceanography 21, 373–384.

Kudrass, H., Machalett, B., Palamenghi, L., Meyer, I., Zhang, W., 2018. Sediment transport by tropical cyclones recorded in a submarine canyon off Bangladesh. Geo-Marine Letters. 10.1007/s00367-018-0550-x.

Kuehl, S.A., Alexander, C.R., Blair, N.E., Harris, C.K., Marsaglia, K.M., Ogston, A.S., Orpin, A.R., Roering, J.J., Bever, A.J., Bilderback, E.L., Carter, L., Cerovski-Darriau, C., Childress, L.B., Reide Corbett, D., Hale, R.P., Leithold, E.L., Litchfield, N., Moriarty, J.M., Page, M.J., Pierce, L.E., Upton, P., Walsh, J.P., 2016. A source-to-sink perspective of the Waipaoa River margin. Earth-Science Reviews 153, 301–334. 10.1016/j.earscirev.2015.10.001.

Kuhrts, C., Fennel, W., Seifert, T., 2004. Model studies of transport of sedimentary material in the western Baltic. J. Mar. Sys. 52, 167–190. 10.1016/j.jmarsys.2004.03.005.

Leipe, T., Löffler, A., Emeis, K.-C., Jaehmlich, S., Bahlo, R., Ziervogel, K., 2000. Vertical Patterns of Suspended Matter Characteristics Along a Coastal-basin Transect in the Western Baltic Sea. Estuarine, Coastal and Shelf Science 51, 789–804. 10.1006/ecss.2000.0715.

Lemke, W., 1998. Sedimentation und paläogeographische Entwicklung im westlichen Ostseeraum (Mecklenburger Bucht bis Arkonabecken) vom Ende der Weichselvereisung bis zur Litorinatransgression. Marine Science Reports, Institut für Ostseeforschung Warnemünde 31.

Liu, Z., Zhao, Y., Colin, C., Stattegger, K., Wiesner, M.G., Huh, C.-A., Zhang, Y., Li, X., Sompongchaiyakul, P., You, C.-F., Huang, C.-Y., Liu, J.T., Siringan, F.P., Le, K.P., Sathiamurthy, E., Hantoro, W.S., Liu, J., Tuo, S., Zhao, S., Zhou, S., He, Z., Wang, Y., Bunsomboonsakul, S., Li, Y., 2016. Source-to-sink transport processes of fluvial sediments in the South China Sea. Earth-Science Reviews 153, 238–273. 10.1016/j.earscirev.2015.08.005.

Luijendijk, A., Hagenaars, G., Ranasinghe, R., Baart, F., Donchyts, G., Aarninkhof, S., 2018. The State of the World's Beaches. Scientific reports 8, 6641. 10.1038/s41598-018-24630-6.

Lund-Hansen, L.C., Christiansen, C., 2008. Suspended particulate matter (SPM) in the North Sea-Baltic Sea transition: Distributions, inventories, and the autumn 2002 inflows. Geografisk Tidsskrift-Danish Journal of Geography 108, 37–47. 10.1080/00167223.2008.10649587.

Miall, A.D., 2015. Updating uniformitarianism: Stratigraphy as just a set of 'frozen accidents'. Geological Society, London, Special Publications 404, 11–36. 10.1144/SP404.4.

Oberle, F.K.J., Swarzenski, P.W., Reddy, C.M., Nelson, R.K., Baasch, B., Hanebuth, T.J., 2016. Deciphering the lithological consequences of bottom trawling to sedimentary habitats on the shelf. J. Mar. Sys. 159, 120–131. 10.1016/j.jmarsys.2015.12.008.

Ogston, A.S., Cacchione, D.A., Sternberg, R.W., Kineke, G.C., 2000. Observations of storm and river flood-driven sediment transport on the northern California continental shelf. Continental Shelf Research 20, 2141–2162. 10.1016/S0278-4343(00)00065-0.

Osinski, R.D., Enders, K., Gräwe, U., Klingbeil, K., Radtke, H., 2020. Model uncertainties of a storm and their influence on microplastics and sediment transport in the Baltic Sea. Ocean Sci 16, 1491–1507. 10.5194/os-16-1491-2020.

Paola, C., Ganti, V., Mohrig, D., Runkel, A.C., Straub, K.M., 2018. Time Not Our Time: Physical Controls on the Preservation and Measurement of Geologic Time. Annu. Rev. Earth Planet. Sci. 46, 409–438. 10.1146/annurev-earth-082517-010129.

Pinto, L., Fortunato, A.B., Zhang, Y.J., Oliveira, A., Sancho, F.E., 2012. Development and validation of a three-dimensional morphodynamic modelling system for non-cohesive sediments. Ocean Modelling 57, 1–14.

Porz, L., Zhang, W., Hanebuth, T.J., Schrum, C., 2021a. Physical processes controlling mud depocenter development on continental shelves – Geological, oceanographic, and modeling concepts. Marine Geology 432, 106402. 10.1016/j.margeo.2020.106402.

Porz, L., Zhang, W., Schrum, C., 2021b. Density-driven bottom currents control development of muddy basins in the southwestern Baltic Sea. Marine Geology. 10.1016/j.margeo.2021.106523.

Porz, L., Zhang, W., Schrum, C., 2021c. On the development of two mud depocenters in the southwestern Baltic Sea.

Radtke, H., Lipka, M., Bunke, D., Morys, C., Woelfel, J., Cahill, B., Böttcher, M.E., Forster, S., Leipe, T., Rehder, G., Neumann, T., 2019. Ecological ReGional Ocean Model with vertically resolved sediments (ERGOM SED 1.0): coupling benthic and pelagic biogeochemistry of the south-western Baltic Sea. Geosci. Model Dev. 12, 275–320. 10.5194/gmd-12-275-2019.

Rebesco, M., 2005. Contourites, In: Selley, R.C., Cocks, L.R.M., Plimer, I.R. (Eds.), Encyclopedia of Geology. Elsevier, Oxford, pp. 513–527.

Rebesco, M., Hernández-Molina, F.J., van Rooij, D., Wåhlin, A., 2014. Contourites and associated sediments controlled by deep-water circulation processes: State-of-the-art and future considerations. Marine Geology 352, 111–154. 10.1016/j.margeo.2014.03.011.

Rennau, H., Schimmels, S., Burchard, H., 2012. On the effect of structure-induced resistance and mixing on inflows into the Baltic Sea: A numerical model study. Coastal Engineering 60, 53–68. 10.1016/j.coastaleng.2011.08.002.

Sadler, P.M., 1981. Sediment accumulation rates and the completeness of stratigraphic sections. The Journal of Geology 89, 569–584.

Schultze, L.K.P., Merckelbach, L.M., Horstmann, J., Raasch, S., Carpenter, J.R., 2020. Increased Mixing and Turbulence in the Wake of Offshore Wind Farm Foundations. J. Geophys. Res. Oceans 125, e2019JC015858. 10.1029/2019JC015858.

Seibold, E., 1965. The role of the Great Belt for the recent sedimentation in the Baltic Sea. Baltica 26, 139–166.

Seifert, T., Fennel, W., Kuhrts, C., 2009. High resolution model studies of transport of sedimentary material in the south-western Baltic. J. Mar. Sys. 75, 382–396. 10.1016/j.jmarsys.2007.01.017.

Sherwood, C.R., Aretxabaleta, A.L., Harris, C.K., Rinehimer, J.P., Verney, R., Ferré, B., 2018. Cohesive and mixed sediment in the Regional Ocean Modeling System (ROMS v3.6) implemented in the Coupled Ocean–Atmosphere–Wave–Sediment Transport Modeling System (COAWST r1234). Geosci. Model Dev. 11, 1849–1871. 10.5194/gmd-11-1849-2018.

Sivkov, V., Gorbatskiy, V., Kuleshov, A., Zhurov, Y., 2002. Muddy contourites in the Baltic Sea: an example of a shallow-water contourite system. Geological Society, London, Memoirs 22, 121–136. 10.1144/GSL.MEM.2002.022.01.10.

Sivkov, V., Skyum, P., Christiansen, C., 1995. The distribution of the suspended matter in relation to the hydrographical conditions. Aarhus Geoscience 5, 111–117.

Sivkov, V., Sviridov, N., 1994. The relation between erosional-accumulative forms of bottom relief and near-bottom currents in the Bornholm deep. Oceanologiya (English Translation), 266–270.

Sommerfield, C.K., 2006. On sediment accumulation rates and stratigraphic completeness: Lessons from Holocene ocean margins. Continental Shelf Research 26, 2225–2240.

Stanev, E.V., Pein, J., Grashorn, S., Zhang, Y.J., Schrum, C., 2018. Dynamics of the Baltic Sea straits via numerical simulation of exchange flows. Ocean Modelling 131, 40–58. 10.1016/j.ocemod.2018.08.009.

Stow, D.A.V., Faugères, J.-C., 2008. Contourite Facies and the Facies Model, In: Rebesco, M., Camerlenghi, A. (Eds.), Developments in Sedimentology : Contourites, vol. 60. Elsevier, pp. 223–256.

Stow, D.A.V., Faugères, J.-C., Howe, J.A., Pudsey, C.J., Viana, A.R., 2002. Bottom currents, contourites and deep-sea sediment drifts: Current state-of-the-art. Geological Society, London, Memoirs 22, 7–20. 10.1144/GSL.MEM.2002.022.01.02.

Thorne, J.A., Swift, D.J.P., 1991. Sedimentation on continental margins, II: application of the regime concept, In: Swift, D.J.P., Oertel, G.F., Tillman, R.W., Thorne, J.A. (Eds.), Shelf sand and sandstone bodies: geometry, facies and sequence stratigraphy. International Association of Sedimentologists, pp. 33–58.

Vindenes, H., Orvik, K.A., Søiland, H., Wehde, H., 2018. Analysis of tidal currents in the North Sea from shipboard acoustic Doppler current profiler data. Continental Shelf Research 162, 1–12. 10.1016/j.csr.2018.04.001.

Virtasalo, J.J., Endler, M., Moros, M., Jokinen, S.A., Hämäläinen, J., Kotilainen, A.T., 2016. Base of brackish-water mud as key regional stratigraphic marker of mid-Holocene marine flooding of the Baltic Sea Basin. Geo-Mar Lett 36, 445–456. 10.1007/s00367-016-0464-4.

Walsh, J.P., Wiberg, P.L., Aalto, R., Nittrouer, C.A., Kuehl, S.A., 2016. Source-to-sink research: economy of the Earth's surface and its strata. Earth-Science Reviews 153, 1–6. 10.1016/j.earscirev.2015.11.010.

Warner, J.C., Sherwood, C.R., Signell, R.P., Harris, C.K., Arango, H.G., 2008. Development of a three-dimensional, regional, coupled wave, current, and sediment-transport model. Computers & Geosciences 34, 1284–1306. 10.1016/j.cageo.2008.02.012.

Wheatcroft, R.A., Drake, D.E., 2003. Post-depositional alteration and preservation of sedimentary event layers on continental margins, I. The role of episodic sedimentation. Marine Geology 199, 123–137. 10.1016/S0025-3227(03)00146-4.

Witt, G., Leipe, T., Emeis, K.-C., 2001. Using Fluffy Layer Material To Study the Fate of Particle-Bound Organic Pollutants in the Southern Baltic Sea. Environ. Sci. Technol. 35, 1567–1573. 10.1021/es000187u.

Woodroffe, C.D., Murray-Wallace, C.V., 2012. Sea-level rise and coastal change: the past as a guide to the future. Quaternary Science Reviews 54, 4–11. 10.1016/j.quascirev.2012.05.009.

Wright, L.D., Friedrichs, C.T., 2006. Gravity-driven sediment transport on continental shelves: A status report. Continental Shelf Research 26, 2092–2107. 10.1016/j.csr.2006.07.008.

Zhang, W., Cui, Y., Santos, A.I., Hanebuth, T.J., 2016. Storm-driven bottom sediment transport on a high-energy narrow shelf (NW Iberia) and development of mud depocenters. J. Geophys. Res. Oceans 121, 5751–5772. 10.1002/2015JC011526.

Zhang, W., Didenkulova, I., Kurkina, O., Cui, Y., Haberkern, J., Aepfler, R., Santos, A.I., Zhang, H., Hanebuth, T.J., 2019. Internal solitary waves control offshore extension of mud depocenters on the NW Iberian shelf. Marine Geology 409, 15–30. 10.1016/j.margeo.2018.12.008.

Zhurbas, V., Väli, G., Golenko, M., Paka, V., 2018. Variability of bottom friction velocity along the inflow water pathway in the Baltic Sea. Journal of Marine Systems 184, 50–58. 10.1016/j.jmarsys.2018.04.008.

Ziervogel, K., Bohling, B., 2003. Sedimentological parameters and erosion behaviour of submarine coastal sediments in the south-western Baltic Sea. Geo-Marine Letters 23, 43–52. 10.1007/s00367-003-0123-4.

Ziervogel, K., Forster, S., 2005. Aggregation and sinking behaviour of resuspended fluffy layer material. Continental Shelf Research 25, 1853–1863. 10.1016/j.csr.2005.06.008.

Versicherung an Eides statt – Affirmation on Oath

Hiermit erkläre ich an Eides statt, dass ich die vorliegende Dissertationsschrift selbst verfasst und keine anderen als die angegebenen Quellen und Hilfsmittel benutzt habe.

I hereby declare upon oath that I have written the present dissertation independently and have not used further resources and aids than those stated.

Hamburg, 30.06.2021

Acknowledgements

Foremost, I would like to thank my principal advisor Prof. Corinna Schrum, whose perpetual positive and optimistic attitude always motivated me to go on. Her vast experience, not only in physical oceanography, but also in the organizational aspects of scientific work, were always a great source of support, which I value highly. I am equally grateful to my co-advisor Dr. Wenyan Zhang, who acquainted me with the field of morphodynamics with great patience and dedication. His drive, determination and capacity to isolate the essentials from complex matters continue to astound me. Furthermore, he has introduced me to several inspiring scientists whom I otherwise would not have had the pleasure of meeting: Prof. Volkhard Spieß of the University of Bremen, who invited me to his annual geophysical research cruise on RV Alkor in the autumn of 2017 and whose immense knowledge of Baltic Sea geology made a great impression on me; Prof. Helge Arz and Dr. Peter Feldens of the Institute of Baltic Sea Research, Warnemünde (IOW), who generously granted me access to their research reports and geo-acoustic database; Prof. Till Hanebuth of Coastal Carolina University, who familiarized me with the geological perspective of sediment dynamics and hosted me in South Carolina during the autumn of 2018.

Thanks are due to my colleagues at the Department of Sediment Transport and Morphodynamics: Peter Arlinghaus, with whom I regularly had fruitful discussions related to numerical modeling, among other things; Mengyao Ma and Carolyn Chercham for the many helpful comments on my second manuscript. I am indebted to Philippa Schindler, who graciously gave me regular lifts during the commute between Hamburg and Geesthacht, of which I have fond memories. I am grateful to my officemate Elena Mikheeva who, along with a myriad of potted plants, made ours the nicest office in the building. I appreciate the help of Dr. Richard Hofmeister in getting me acquainted with the numerical model and of Dr. Johannes Pein for offering advice along the way. The cheerful and reliable Sabine Billerbeck is thanked for always keeping her door open in case of administrative questions. I wish to also thank the remaining colleagues at the Department of Matter Transport and Ecosystem Dynamics, whose members have grown too numerous over the years to list, and each of whom made the time at the institute so enjoyable. Special thanks go to other PhD students, both current and former, at the Institute of Coastal Systems: Anne, Changjin, David, Enpei, Fabian, Ina, Jan, Nils, Pascal, and Seyed. Their camaraderie outweighed any doubts and frustrations of everyday scientific work.

I could not have completed this thesis without the continuous support of my parents and the unending encouragement, motivation and cheering-up by Lea.